Role and Relevance of PEPT1 in Intestinal Absorption and Pharmacokinetics of 5-Aminolevulinic Acid

by

Yehua Xie

A dissertation submitted in partial fulfillment
of the requirements for the degree of
Doctor of Philosophy
(Pharmaceutical Sciences)
in The University of Michigan
2015

Doctoral Committee:

Professor David E. Smith, Chair
Professor Richard F. Keep
Professor Steven P. Schwendeman
Professor Duxin Sun

DEDICATION

To my dearest father Xie, Yubiao (谢毓标) and mother Ye, Jinlan (叶金兰)

ACKNOWLEDGEMENTS

First of all, I would like to express my deepest gratitude to my advisor Professor David E. Smith for the tremendous help, support and encouragement he always gave me during the past five years. Without his guidance and mentorship, this dissertation project would not have been possible. I feel privileged to be one of his students and have opportunities to learn both scientific knowledge and critical thinking from him.

I want to thank all of my committee members: Professor Richard F. Keep, Professor Steven P. Schwendeman and Professor Duxin Sun for their constructive advice, insightful comments and constant supports on my thesis research. I am also very grateful to Dr. Meihua Rose Feng for teaching me population pharmacokinetic modeling and mentoring on my modeling side projects.

I want to thank all the past and present members in Smith group: Yongjun Hu, Shu-Pei Wu, Naoki Nishio, Bei Yang, Maria M. Posada, Yeamin Huh, Xiaomei Chen, Xiaoxing Wang and Yuqing Wang for their help and friendship. I would especially like to thank Yongjun and Shu-Pei for teaching me experimental techniques and their support work in the laboratory.

I am deeply thankful for the faculty members and staff in the College of Pharmacy: Dr. Wei Cheng, Dr. Gregory Amidon, Dr. Gordon Amidon, Maria Herbel,

Jeanne Getty, Gail Benninghoff, Mark Nelson, Antoinette Hopper, Patrina Hardy and Pat Greeley for all of their help during my doctoral study.

I also want to thank all my friends and fellow students in the College of Pharmacy for their friendship and help including, but not limited to, Yajun Liu, Hao Xu, Xu Ran, Jingyu Jerry Yu, Kefeng Sun, Yiqun Jiang, Tao Zhang, Peng Zou, Nan Zheng, Oluseyi Adeniyi, Brittany Bailey, Joseph Burnett, Brian Krieg, Maya Lipert, Hanna Song, Arjang Talattof, Hayley Paholak, Karthik Pisupati and Rui Kuai.

I would like to thank my colleagues and mentors during my internship at Merck, especially Dr. Paul Statkevich and Dr. Daniel Tatosian.

Last, but not least, I would like to thank my parents for their endless love, encouragement and support that make me fulfill power on this journey.

TABLE OF CONTENTS

DEDICATION ..... **ii**

ACKNOWLEDGEMENTS ..... **iii**

LIST OF FIGURES ..... **vii**

LIST OF TABLES ..... **xi**

LIST OF APPENDICES ..... **xiii**

ABSTRACT ..... **xiv**

CHAPTER 1 RESEARCH OBJECTIVE **1**

CHAPTER 2 BACKGROUND AND LITERATURE REVIEW **4**

PROTON-COUPLED OLIGOPEPTIDE TRANSPORTERS 4

PROTON-COUPLED OLIGOPEPTIDE TRANSPORTER 1 (PEPT1) 8

5-AMINOLEVULINIC ACID 19

FIGURES AND TABLES 28

REFERENCES 36

CHAPTER 3 SIGNIFICANCE OF PEPT1 IN THE IN SITU INTESTINAL PERMEABILITY OF 5-AMINOLEVULINIC ACID IN WILDTYPE AND PEPT1 KNOCKOUT MICE **54**

ABSTRACT 54

INTRODUCTION 56

MATERIALS AND METHODS 59

RESULTS 65

DISCUSSION 68

FIGURES 73

REFERENCES 79

CHAPTER 4 ROLE OF PEPT1 ON THE IN VIVO PHARMACOKINETICS OF 5-AMINOLEVULINIC ACID IN WILD-TYPE AND PEPT1 KNOCKOUT MICE 85

ABSTRACT 85

INTRODUCTION 87

MATERIALS AND METHODS 90

RESULTS 95

DISCUSSION 98

FIGURES AND TABLES 103

REFERENCES 114

CHAPTER 5 FUTURE DIRECTION 119

APPENDICES 122

LIST OF FIGURES

Figure 2.1 Overview of protein digestion and absorption in the gastrointestinal tract. (1) Brush-border peptidases; (2) brush-border amino-acid transport systems; (3) brush-border peptide transport system; (4) cytoplasmic peptidases; (5) basolateral amino acid transport systems; (6) basolateral peptide transport system(s). GI, gastrointestinal. (Adopted from Ganapathy et al. Protein digestion and absorption. Chapter 65, Physiology of the gastrointestinal tract, fourth edition.) 28

Figure 2.2 Schematic model of PEPT1-mediated cellular transport in intestinal epithelial cells (Adopted from Daniel 1996). 29

Figure 2.3 Chemical structures of 5-Aminolaevulinic acid (5-ALA) and protoporphyrin IX (PpIX). 30

Figure 2.4 Overview of photodynamic therapy mechanism. (Adopted from Wachowska, Muchowicz et al. 2011) 31

Figure 2.5 5-ALA in the major route of heme biosynthesis pathway. (Adopted from Wachowska, Muchowicz et al. 2011) 32

Figure 3.1 HPLC chromatogram of (A) blank perfusion buffer (B) 5-ALA in perfusate before and after perfusion from (C) duodenum (D) jejunum (E) ileum and (F) colon segments in wildtype mouse. The chromatographic peak at 4.1 min represents 5-ALA. 73

Figure 3.2 HPLC chromatogram of 5-ALA in perfusate after perfusion from (A) duodenum (B) jejunum (C) ileum and (D) colon segments in PepT1 knockout mouse. The chromatographic peak at 4.1 min represents 5-ALA. 74

Figure 3.3 Concentration dependency of 5-ALA flux in the jejunum of wildtype mice (mean ± SE, n=4). C_{in} was referenced to the inlet concentration of 5-ALA. ... 75

Figure 3.4 Concentration dependency of 5-ALA flux in the jejunum of wildtype mice (mean ± SE, n=4). C_w was referenced to the estimated intestinal wall concentration of 5-ALA. ... 76

Figure 3.5 Effect of potential inhibitors (25 mM) on the effective permeability of 10 μM 5-ALA during jejunal perfusion in wildtype mice. Data are presented as mean ± SE (n=4). Statistical analyses were performed by one-way ANOVA and Dunnett's test. ***$p < 0.001$ as compared to control. ... 77

Figure 3.6 Effective permeability of 10 μM 5-ALA in the duodenum, jejunum, ileum, and colon of wildtype and PEPT1 knockout (KO) mice. Data are presented as mean ± SE (n=4). Groups with different letters are statistically different as determined by one-way ANOVA and Tukey's test. ... 78

Figure 4.1 Plasma concentration-time curves of 5-ALA in wildtype and PepT1 knockout (KO) mice after oral administration of 0.2 μmol/g [^{14}C]5-ALA. The y-axis is displayed as a linear scale (A) or a logarithmic scale (B). Data are presented as mean ± SE (n=4-5). ... 103

Figure 4.2 Plasma concentration-time curves of 5-ALA in wildtype and PepT1 knockout (KO) mice after oral administration of 2 μmol/g [^{14}C]5-ALA. The y-axis is displayed as a linear scale (A) or a logarithmic scale (B). Data are presented as mean ± SE (n=4). ... 104

Figure 4.3 Tissue concentrations of 5-ALA 180 min after oral administration of 0.2 μmol/g [^{14}C] 5-ALA in wildtype and PepT1 knockout (KO) mice: (A) non-gastrointestinal tissues; (B) gastrointestinal segments. Data are expressed as mean ± SE (n= 4-5). ** $p<0.01$, compared with wildtype mice. ... 105

Figure 4.4 Tissue-to-blood concentration ratios of 5-ALA 180 min after oral administration of 0.2 μmol/g [^{14}C] 5-ALA in wildtype and PepT1 knockout (KO) mice: (A) non-gastrointestinal tissues; (B) gastrointestinal segments. Data are expressed as mean ± SE (n= 4-5). ** $p<0.01$, compared with wildtype mice. 106

Figure 4.5 Plasma concentration-time curves of 5-ALA in wildtype and PepT1 knockout (KO) mice after intravenous dosing of 0.01 μmol/g [^{14}C] 5-ALA. The y-axis is displayed as a linear scale (A) or a logarithmic scale (B). Data are presented as mean ± SE (n=7). 107

Figure A.1 Individual predicted and observed plasma concentration-time profiles at 0.2 μmol/g oral dose in wildtype (WT) mcie. 129

Figure A.2 Individual predicted and observed plasma concentration-time profiles at 0.2 μmol/g oral dose in PepT1 knockout (P1) mcie. 130

Figure A.3 Individual predicted and observed plasma concentration-time profiles at 2 μmol/g oral dose in wildtype (WT) mcie. 131

Figure A.4 Individual predicted and observed plasma concentration-time profiles at 2 μmol/g oral dose in PepT1 knockout (P1) mcie. 132

Figure A.5 Individual predicted and observed plasma concentration-time profiles at 0.01 μmol/g intravenous dose in wildtype (WT) mcie. 133

Figure A.6 Individual predicted and observed plasma concentration-time profiles at 0.01 μmol/g intravenous dose in PepT1 knockout (P1) mcie. 134

Figure B.1 Schematic two-compartment models of cefadroxil after intravenous bolus administration in PepT2 knockout (A) and wildtype (B) mice. 154

Figure B.2 Plasma concentration-time profiles of cefadroxil after intravenous bolus administrations of 1, 12.5, 50 and 100 nmol/g in PepT2 knockout (A) and wildtype (B) mice. The figures were adapted from a previous publication (Shen, Ocheltree et al. 2007). 155

Figure B.3 Goodness-of-fit plots for the final pharmacokinetic model of cefadroxil in PepT2 knockout mice. Solid lines represent the line of identity. 156

Figure B.4 Goodness-of-fit plots for the final pharmacokinetic model of cefadroxil in wildtype mice. Solid lines represent the line of identity..... 157

Figure B.5 Prediction corrected visual predictive check plots in PepT2 knockout (A) and wildtype (B) mice. Plasma concentration-time profiles are displayed in which the circles represent prediction corrected observed data. Dashed lines depict the 5^{th} and 95^{th} percentiles, and solid lines represent the median values of 1,000 simulated data sets. 158

LIST OF TABLES

Table 2.1 The proton-coupled oligopeptide transporter family (SLC15) 33

Table 2.2 Approved 5-ALA products and their application 34

Table 2.3 Transporters involved in the transport of 5-ALA 35

Table 4.1 Noncompartmental analysis of 5-ALA after oral administration of 0.2 μmol/g [^{14}C] 5-ALA in wildtype (WT) and PepT1 knockout (KO) mice 108

Table 4.2 Compartmental analysis of 5-ALA after oral administration of 0.2 μmol/g [^{14}C] 5-ALA in wildtype (WT) and PepT1 knockout (KO) mice..... 109

Table 4.3 Noncompartmental analysis of 5-ALA after oral administration of 2 μmol/g [^{14}C] 5-ALA in wildtype (WT) and PepT1 knockout (KO) mice..... 110

Table 4.4 Compartmental analysis of 5-ALA after oral administration of 2 μmol/g [^{14}C] 5-ALA in wildtype (WT) and PepT1 knockout (KO) mice..... 111

Table 4.5 Noncompartmental analysis of 5-ALA after intravenous bolus administration of 0.01 μmol/g [^{14}C] 5-ALA in wildtype (WT) and PepT1 knockout (KO) mice 112

Table 4.6 Compartmental analysis of 5-ALA after intravenous bolus administration of 0.01 μmol/g [^{14}C] 5-ALA in wildtype (WT) and PepT1 knockout (KO) mice 113

Table A.1 Individual PK parameters of 5-ALA after 0.2 μmol/g oral dose in wildtype (WT) and PepT1 knockout (P1) mice (two-compartmental model)..... 123

Table A.2 Individual PK parameters of 5-ALA after 0.2 μmol/g oral dose in wildtype (WT) and PepT1 knockout (P1) mice (non-compartmental analysis)..... 124

Table A.3 Individual PK parameters of 5-ALA after 2 μmol/g oral dose in wildtype (WT) and PepT1 knockout (P1) mice (two-compartmental model)..... 125

Table A.4 Individual PK parameters of 5-ALA after 2 μmol/g oral dose in wildtype (WT) and PepT1 knockout (P1) mice (non-compartmental analysis)..... 126

Table A.5 Individual PK parameters of 5-ALA after 0.01 μmol/g intravenous dose in wildtype (WT) and PepT1 knockout (P1) mice (two-compartmental model) 127

Table A.6 Individual PK parameters of 5-ALA after 0.01 μmol/g intravenous dose in wildtype (WT) and PepT1 knockout (P1) mice (non-compartmental analysis) 128

Table B.1 Noncompartmental analysis of cefadroxil pharmacokinetics in PepT2 knockout (KO) and wildtype mice after intravenous bolus administration[a]... 159

Table B.2 Parameter estimates of the final population pharmacokinetic model of cefadroxil in PepT2 knockout (KO) and wildtype mice after intravenous bolus administration 160

Table B.3 Comparison of parameter estimates of the final population pharmacokinetic model of cefadroxil in PepT2 knockout (KO) and wildtype mice based on the original data set and from 1,000 bootstrap replicates 161

LIST OF APPENDICES

APPENDIX A INDIVIDUAL DATA FROM CHAPTER 4 123

APPENDIX B POPULATION PHARMACOKINETIC MODELING OF CEFADROXIL RENAL TRANSPORT IN WILDTYPE AND PEPT2 KNOCKOUT MICE 135

ABSTRACT

Peptide transporter 1 (PepT1), a member of the proton-coupled oligopeptide transporter family, is known to transport di-/tri-peptides and peptidomimetic therapeutic agents across biological membranes. Due to its abundant expression in small intestine, broad substrate specificity and high transport capacity, PepT1 is considered an ideal oral drug delivery target and plays a pivotal role in transporting numerous pharmacological compounds. The therapeutic agent 5-aminolevulinic acid (5-ALA) is widely applied in photodynamic therapy and fluorescence diagnosis for the treatment of various cancers and non-malignant diseases. PepT1 knockout mice, available in our laboratory, provide a novel tool to investigate the role and quantitative significance of PepT1 in the intestinal absorption and pharmacokinetics of 5-ALA. In this project, experimental results from *in situ* perfusion and *in vivo* pharmacokinetic studies offer a deeper understanding of the PepT1-mediated intestinal absorption of 5-ALA.

The effective permeability of 5-ALA was evaluated as a function of drug concentration, potential inhibitors and regional segments of the intestines using *in situ* perfusions in wildtype and PepT1 knockout mice. The results from *in situ* perfusions indicated that PepT1 accounted for approximately 90% of 5-ALA permeability in mouse small intestine. In wildtype mice, 5-ALA intestinal uptake was shown to be concentration dependent with an apparent K_m of 13.4 mM, based on bulk

concentrations of substrate. The differential segmental permeability of 5-ALA was consistent with PepT1 expression along the intestinal segments, in which high permeabilities of 1-2 x 10^{-4} cm/s were observed in the duodenum, jejunum and ileum of wildtype mice with little permeability in colon. In contrast, the residual permeability of 5-ALA in the duodenum, jejunum, and ileum of PepT1 knockout mice was only about 10% of that in wildtype mice and similar to that of colon permeability. The contribution of other transporters, including the amino acid transporter PAT1, in mediating the intestinal permeability of 5-ALA was minor at best. After oral administration (0.2 and 2 μmol/g) of 5-ALA, the maximum plasma concentration (C_{max}) and area under the plasma concentration-time curve (AUC) of 5-ALA were decreased approximately 2-fold in PepT1 knockout mice as compared to wildtype mice. The tissue distribution results after 0.2 μmol/g 5-ALA oral dose and intravenous pharmacokinetic study (0.01 μmol/g) revealed that PepT1 had marginal, if any, effect on the *in vivo* disposition of 5-ALA. In conclusion, research in this dissertation project offered solid evidence in defining the significant role of PepT1 on the intestinal absorption and systemic exposure of 5-ALA after oral dosing.

CHAPTER 1

RESEARCH OBJECTIVE

Proton-coupled oligopeptide transporter 1 (PepT1), a transmembrane protein with predominant expression at the intestinal epithelium, is responsible for the uptake of dipeptides and tripeptides, and break down products from dietary protein ingestion across the apical membrane into enterocytes. Due to its broad substrate specificity, high transport capacity and abundant expression in the small intestine, PepT1 is considered to play a pivotal role in the oral absorption of numerous peptidomimetic compounds. Besides di/tripeptides, PepT1 can transport a variety of therapeutic agents with different structural and chemical characteristics, including β-lactam antibiotics (e.g., cefadroxil), angiotensin converting enzyme inhibitors (e.g., enalapril) and antiviral prodrugs (e.g., valacyclovir). Recently, prodrug strategies that combine rational drug design and PepT1 targeted drug delivery have been employed to improve the intestinal bioavailability of poorly absorbed drugs after oral administration.

5-Aminolevulinic acid (5-ALA), a photosensitizer agent, is widely applied in photodynamic therapy and fluorescence diagnosis for the treatment of various cancers and non-malignant diseases. Although 5-ALA is a non-peptide mimetic small molecule, previous research has indicated that PepT1 may play an important

role in facilitating 5-ALA intestinal absorption and its good oral bioavailability based on *in vitro* results. However, the transport mechanism of 5-ALA from the gastrointestinal tract lumen into the systemic circulation system is still poorly understood. Moreover, the relative contribution of intestinal transporter PepT1 in this process is unclear, as compared to other potential intestinal transporters such as the amino acid transporter PAT1.

Genetically modified mice, with targeted disruption of the PEPT1 gene, have been established and characterized recently in our laboratory. Compared to *in vitro* experimental systems with exogenously expressed transporters, the availability of PepT1 knockout mice provides a powerful animal model to thoroughly examine the functional role of PepT1 in the transport of nutritional and pharmacological substrates (e.g., glycylsarcosine, cefadroxil, valacyclovir, fMet-Leu-Phe) under physiological conditions.

The research objective of this project is to unravel the transport mechanism of 5-ALA intestinal absorption and characterize the quantitative contribution of PepT1 to the oral absorption and systemic exposure of 5-ALA after oral dosing. The two specific aims of this project are presented below as:

(1) To characterize the role and relative contribution of PepT1 in the intestinal absorption of 5-ALA in wildtype and PepT1 knockout mice via *in situ* single-pass perfusion studies.

(2) To determine the impact of PepT1 on the *in vivo* intestinal absorption of 5-ALA and pharmacokinetic profiles after oral dosing in wildtype and PepT1 knockout mice.

CHAPTER 2

BACKGROUND AND LITERATURE REVIEW

PROTON-COUPLED OLIGOPEPTIDE TRANSPORTERS

Proton-coupled Oligopeptide Transporters (POTs) are a family of transporter proteins that translocate various di-/tri-peptides and peptidomimetics across the biological membrane (Herrera-Ruiz and Knipp 2003; Daniel and Kottra 2004; Smith, Clemencon et al. 2013). According to the HUGO Gene Nomenclature Committee (HGNC) system, this transporter family is also known as solute carrier family 15 (SLC15).

To date four members in POT family have been identified in mammals, denoted as PEPT1 (SLC15A1), PEPT2 (SLC15A2), PHT1 (SLC15A4), and PHT2 (SLC15A3). In virtue of expression cloning techniques applied in the 1990s, encoding genes of these four transporters were identified in succession. PEPT1 was the first member cloned from a rabbit intestinal cDNA library (Fei, Kanai et al. 1994) and soon followed by PEPT2 which was cloned from a human renal cDNA library (Liu, Liang et al. 1995). The other two oligopeptide transporters, PHT1 and PHT2, were then isolated from a rat brain cDNA library (Yamashita, Shimada et al. 1997; Sakata, Yamashita et al. 2001). Dissimilar to their paralogs PEPT1 and PEPT2, the latter two transporters were demonstrated to recognize the

amino acid L-histidine as their substrate in addition to di- and tri-peptides. Few studies have been focused on the peptide/histidine transporters PHT1 and PHT2 after their identification, therefore, little is known about their pharmaceutical and pharmacological relevance (Brandsch, Knutter et al. 2008).

POT proteins vary in size from 572-729 amino acids across species (Table 2.1) and they share sequence and structural similarities. PEPT1 and PEPT2 share high homology in amino acids sequence between species (i.e., 80-90% amino acid identity between human, rat, mouse, and rabbit). However, sequence similarity between different POT transporters within a given species is relatively low. The human PEPT1 protein consists of 708 amino acid residues and shares overall a 50% sequence identity and 70% similarity with hPEPT2, whereas PHT1 and PHT2 proteins share much less sequence identity to PEPT1 and PEPT2 (i.e., approximately 20 % ~ 25%) (Botka, Wittig et al. 2000).

It has been shown that POT transporters are proton driven symporters, using an inwardly direct proton electrochemical gradient and the negative membrane potential to drive the uptake of peptides across the cell membrane (Adibi 1997; Nussberger, Steel et al. 1997; Nussberger, Steel et al. 1997). Such a proton gradient is generally provided and maintained by exchange of proton and sodium in opposite direction. This feature of POT transporters differs from many other known membrane transporters that are dependent on ATP hydrolysis or Na^+ concentration gradient.

The unique tissue distribution and expression patterns for the different POTs have been elucidated. First, PEPT1 mRNA and protein were found to express in a variety of tissues with primary expression in the small intestine (Liang, Fei et al. 1995; Lu and Klaassen 2006; Jappar, Wu et al. 2010). Specifically, PEPT1 protein is localized at the brush-border membrane of intestinal epithelial cells (Ogihara, Saito et al. 1996; Thwaites, Ford et al. 1999). Lower expression of PEPT1 was detected in other tissues such as kidney, bile duct, liver, placenta, monocyte, and pancreas (Daniel and Kottra 2004; Smith, Clemencon et al. 2013). PEPT2 has a quite different tissue distribution pattern, compared to PEPT1, with a predominant expression in kidney and brain. Moreover, relative low expression of PEPT2 was also shown in lung, liver, heart, mammary gland, eyes, spleen, testis, prostate, ovary, and uterus (Lu and Klaassen 2006; Kamal, Keep et al. 2008). Regarding to PHT1 and PHT2, much less information is available about the expression and tissue distribution. PHT1 transcripts were found in the brain and eye (Yamashita, Shimada et al. 1997) and PHT2 transcripts were expressed primarily in the lung, thymus and spleen (Sakata, Yamashita et al. 2001). Recently, significant expression of PhT1 protein was detected in adult rodents (Hu, Xie et al. 2014).

Due to their broad substrate specificity and differential tissue distribution, PEPT1 and PEPT2 have been extensively studied for their significant physiological and pharmacological roles in the absorption and disposition of peptide nutrients as well as peptidomimetic drugs (Daniel and Kottra 2004; Brandsch, Knutter et al. 2008; Rubio-Aliaga and Daniel 2008; Smith, Clemencon

et al. 2013). PEPT1 (low affinity and high capacity) as well as PEPT2 (high affinity and low capacity) were believed to recognize and transport a number of peptide-like therapeutic agents with different conformation, size, polarity, and charges. These peptide-like drugs include, but not limit to, some β-lactam antibiotics (e.g., cefadroxil), antitumor drugs (e.g., bestatin), angiotensin converting enzyme inhibitors (e.g., enalapril) and antiviral prodrugs (e.g., valacyclovir). Overall, PEPT1 is pharmaceutically relevant and considered as a promising target for rational drug design or prodrug strategy in the hope of enhancing the oral bioavailability of certain drugs. In my thesis project, PEPT1 is the topic of research interest, thus more detailed discussion with respect to PEPT1 will be present in the next section.

PROTON-COUPLED OLIGOPEPTIDE TRANSPORTER 1 (PEPT1)

Introduction

Nutritional needs for nitrogen and amino acids in mammalian animals are met by absorption of free amino acids (~ 20%) and small peptides (~ 80%) derived from dietary proteins in the digestive tract (Matthews 1975; Webb, Matthews et al. 1992; Ganapathy, Gupta et al. 2006). Carrier-mediated transport systems have been identified to play a pivotal role in this process that deliver di- and tri-peptides from the intestinal lumen into the enterocytes (Figure 2.1). Specifically, this process was generally believed to be attributable to the activity of proton-coupled oligopeptide transporter 1 (PEPT1).

The proton-coupled oligopeptide transporter 1 (PEPT1), the most widely studied member of the POT superfamily, was first isolated from a rabbit intestinal cDNA library in 1994 (Fei, Kanai et al. 1994). The successful cloning of rPEPT1 was achieved by mRNA isolation from rabbit small intestinal mucosa, functional expression of the carrier protein in *Xenopus laevis* oocytes and followed by its transport activity assessment. To date, PEPT1 has been cloned across different species such as human, mouse, rat, sheep, chicken, pig and monkey (Liang, Fei et al. 1995; Saito, Okuda et al. 1995; Fei, Sugawara et al. 2000; Pan, Wong et al. 2001; Chen, Pan et al. 2002; Zhang, Emerick et al. 2004; Klang, Burnworth et al. 2005). Indeed, PEPT1 gene is conserved and highly homologous across species, since human PEPT1 shares at least more than 80% amino acid sequence identity with any other mammalian species listed above. Whereas, hPEPT2, the paralog of

hPEPT1, shares about 50% identity and 70% similarity with hPEPT1 in terms of amino acid sequence.

Mammalian PEPT1 consists of 707-710 amino acid residues depending on species. Human PEPT1 is composed of 708 amino acid residues with a molecular weight of 78 kDa, and the gene is mapped on chromosome 13q33-34 with 23 exons (Liang, Fei et al. 1995). Since the mammalian PEPT1 protein crystal structure has not been characterized yet, it was predicted by computational modeling to consist of 12 putative transmembrane spanning domains (TMDs) with a large extracellular loop between the ninth and tenth TMDs, two putative protein kinase C-dependent phosphorylation sites and both the C- and N-termini face to the cytosol (Daniel and Kottra 2004; Rubio-Aliaga and Daniel 2008). The first 4 and 7-9 transmembrane domains were revealed to determine the substrate affinity and binding characteristics (Doring, Will et al. 1998; Terada, Saito et al. 2000; Doring, Martini et al. 2002; Rubio-Aliaga and Daniel 2008).

Pharmacogenomics of PEPT1

Over 40 coding single nucleotide polymorphisms (SNPs) and about 100 haplotypes of human PEPT1 gene have been identified (Zair, Eloranta et al. 2008; Sugiura, Umeda et al. 2013). Nine nonsynonymous and four synonymous coding-region SNPs were first reported by Zhang and coworkers and followed by functional analysis in heterologously transfected HeLa cells (Zhang, Fu et al. 2004). They found all PEPT1 nonsynonymous variants identified have conserved

substrate recognition, when compared with the reference PEPT1, although one rare variant P586L (i.e., SNP 1758C>T) showed significantly reduced GlySar uptake and may affect PEPT1 expression as demonstrated by protein analysis *in vitro*. In another study, 350G>A (S117N) and 1256G>C (G419A) were found to be the most common PEPT1 SNPs (Anderle, Nielsen et al. 2006). These two SNPs along with other six genetic variants were also tested for the transport of several PEPT1 substrates but no significant alternation was observed except for the SNP 83T>A (F28Y). This variant displayed significantly reduced uptake of cephalexin attributable to lower substrate affinity (i.e., increased K_m). As to the pharmaceutical and pharmacokinetic relevance of PEPT1 SNPs, little is known currently and further studies are still needed. Collectively, a low level of PEPT1 genetic polymorphisms has been found in human.

Tissue Distribution and Cellular Localization of PEPT1

PEPT1 was found to be expressed in a variety of tissues with primary expression in small intestine in mammals. Specifically, PEPT1 is localized at the brush border membrane of intestinal epithelial cells in villi tips, but not other cells in the crypts (Ogihara, Saito et al. 1996; Walker, Thwaites et al. 1998; Groneberg, Doring et al. 2001). The abundant mRNA expression of PEPT1 has been detected in small intestine of several mammalian species including human (Liang, Fei et al. 1995; Herrera-Ruiz, Wang et al. 2001; Englund, Rorsman et al. 2006; Meier, Eloranta et al. 2007), rabbit (Fei, Kanai et al. 1994), rat (Miyamoto, Shiraga et al.

1996; Shen, Smith et al. 1999; Howard, Goodlad et al. 2004; Lu and Klaassen 2006) and mouse (Lu and Klaassen 2006; Jappar, Wu et al. 2010). The predominant protein expression of PEPT1 was also detected and in agreement with its mRNA levels in small intestine (Ogihara, Saito et al. 1996; Shen, Smith et al. 1999; Jappar, Wu et al. 2010). However, the colonic expression of PEPT1 is still under debate since some contradictory studies have been published. Some researchers have observed PEPT1 protein expression in normal mouse, rat and human colon (Ziegler, Fernandez-Estivariz et al. 2002; Ford, Howard et al. 2003; Wuensch, Schulz et al. 2013), whereas others could not detect PEPT1 protein in normal colon (Ogihara, Saito et al. 1996; Shen, Smith et al. 1999; Groneberg, Doring et al. 2001; Merlin, Si-Tahar et al. 2001; Jappar, Wu et al. 2010).

Apart from the intestine, PEPT1 was also detected in S1 segments of renal proximal tubule in the kidney and localized on the apical membrane of renal epithelial cells (Fei, Kanai et al. 1994; Liang, Fei et al. 1995; Saito, Okuda et al. 1995; Miyamoto, Shiraga et al. 1996; Smith, Pavlova et al. 1998; Shen, Smith et al. 1999; Daniel and Kottra 2004; Lu and Klaassen 2006). The functional activity of PEPT1 in kidney was studied due to its renal expression. Studies using Pept2 knockout mice indicated that PEPT1 was less important than PEPT2 in terms of renal reabsorption of the peptide-bound amino nitrogen and peptidomimetic drugs (Ocheltree, Shen et al. 2005; Shen, Ocheltree et al. 2007).

Other tissues including liver, pancreas, lung, bile duct, ovary, placenta, testis, prostate, mammary gland, nasal epithelium, and placenta, have been reported to express modest or low level of PEPT1 mRNA (Herrera-Ruiz, Wang et

al. 2001; Knutter, Rubio-Aliaga et al. 2002; Lu and Klaassen 2006; Agu, Cowley et al. 2011; Sun, Tan et al. 2013). However, the functional role of PEPT1 in these tissues was little known and lack of investigation.

Transport mechanism of PEPT1

The fundamental cellular transport mechanism of PEPT1 has been delineated by numerous functional experimental studies as well as computational modeling for the last decades (Fei, Kanai et al. 1994; Mackenzie, Fei et al. 1996; Mackenzie, Loo et al. 1996; Amasheh, Wenzel et al. 1997; Nussberger, Steel et al. 1997; Kottra, Stamfort et al. 2002; Daniel 2004; Irie, Terada et al. 2005). In 1983, Ganapathy et al. offered the first evidence that indicate intestinal dipeptide uptake is driven by an inwardly directed proton gradient (Ganapathy and Leibach 1983). Now it has been demonstrated that PEPT1 uses a proton electrochemical gradient and negative membrane potential as its driving force to mediate the cellular uptake of peptides/peptidomimetics (Boll, Markovich et al. 1994; Fei, Kanai et al. 1994; Daniel 1996; Nussberger, Steel et al. 1997; Daniel 2004). By employing two-microelectrode voltage-clamp in cRNA-injected oocytes with dipeptide glycyl-sarcosine (GlySar) as the characterizing substrate, an ordered and simultaneous transport model has been suggested to describe the transport features of PEPT1 (Mackenzie, Loo et al. 1996), in which the transporter was first bound to proton under outward facing conformation with change of substrate-binding affinity. Then, PEPT1 started to translocate the substrate through a

conformational change once binding to the substrate molecule. Similar models were proposed including a symmetry proton binding intra- and extracellular model with focus on intracellular binding event (Nussberger, Steel et al. 1997). Based on their experimental results and previous studies, Irie *et al.* have developed a computational model to illustrate the proton-coupled transport mechanism of PEPT1 with two key hypotheses: (1) H^+ binds to both the H^+-binding site and the substrate-binding site; and (2) H^+ at the substrate binding site is essential for the interaction of anionic substrates, but could inhibit that of neutral and cationic substrates (Irie, Terada et al. 2005).

In mammalian cells, the proton gradient driving force was found to be generally provided and maintained by the activity of electro-neutral proton-cation exchangers (i.e., Na^+/H^+ antiporters) (Daniel 1996; Adibi 1997; Nussberger, Steel et al. 1997). For example, Thwaites has demonstrated that the activity of Na^+/H^+ exchanger (NHE3) on the apical membrane, but not basolateral membrane (NHE1), increased after GlySar was added in Caco-2 cells (Thwaites, Ford et al. 1999). Other evidence also showed that when NHE3 activity was blocked, the transport activity of PEPT1 was significantly influenced (Kennedy, Leibach et al. 2002; Thwaites, Kennedy et al. 2002; Watanabe, Kato et al. 2005). The Na^+-K^+-ATPase at the basolateral membrane of epithelial cells is identified to generate inwardly directed sodium gradient and maintain the intracellular sodium balance with apical Na^+/H^+ antiporter. Figure 2.2 (adopted from Daniel 1996) provides a schematic model of the proposed translocation mechanism for PEPT1.

Regard to the electrogenic transport of PEPT1, the neutral substrates are preferred by PEPT1 and translocated with a 1:1 stoichiometry in proton to substrate flux. Generally, PEPT1 will have higher activity when transporting anionic substrates at more acidic microclimate and when transporting cationic substrates at more neutral or slightly alkaline extracellular pH (Amasheh, Wenzel et al. 1997; Steel, Nussberger et al. 1997).

Substrate Specificity

It has been accepted that PEPT1 has exceptionally broad substrate specificity that covers hundreds of di-/tri-peptides and peptide-like drugs (Rubio-Aliaga and Daniel 2002; Daniel and Kottra 2004; Terada and Inui 2004). First of all, as a nutrient transporter, PEPT1 is capable to transport up to 400 dipeptides and 8000 tripeptides that are naturally occurring oligopeptides derived from dietary protein breakdown products (Daniel 2004; Daniel and Kottra 2004). However, not all the di-/tri-peptides are substrates of PEPT1 that have to meet certain criteria. For example, PEPT1 has preferences to transport peptides with L-α-amino acid residues to its D-isomers (Daniel, Morse et al. 1992). Another typical structure requirement for PEPT1 substrate is summarized as two oppositely charged head groups separated with a distance between 500 to 635 pm (Rubio-Aliaga and Daniel 2008). Based on numerous uptake and inhibition experiments, Rubio-Aliaga et al. summarized a few structure features that a typical di-/tri-peptide substrate of PEPT1 and PEPT2 should possess:1) L-amino

acids, 2) an acidic or hydrophobic group at C-terminus, 3) a weakly basic group in α-position at N-terminus, 4) a ketomethylene or acid amide bond, and 5) a *trans* conformation of peptide bonds (Rubio-Aliaga and Daniel 2008).

Aside from a wide array of di-/tri-peptides, PEPT1 is also capable of transporting many peptidomimetic drugs with variety in structure, molecular size, polarity, net charge, and stereochemistry. These pharmacological active compounds, which were demonstrated as PEPT1 substrates, include β-lactam antibiotics (e.g., ceftibuten, cephalexin, cefixime and cefadroxil), angiotensin converting enzyme inhibitors (e.g., captopril, enalapril, and fosinopril), antitumor drug bestatin, antiviral nucleoside prodrugs (e.g., valacyclovir, valganciclovir) and the photodynamic therapy agent 5-aminolevulinic acid.

Therefore, PEPT1 was viewed as an excellent oral drug delivery target due to its broad substrate specificity, high transport capacity and abundant expression in the small intestine. It should be noted that, with further research, the number of pharmacologically relevant compounds transported by PEPT1 will increase given that prodrug strategies which aim at PEPT1 have been employed to improve oral bioavailability of poorly absorbed drugs. Novel compounds such as zanamivir, oseltamivir and didanosine prodrugs have been developed recently that target PEPT1 as a drug transporter (Gupta, Gupta et al. 2011; Yan, Sun et al. 2011; Brandsch 2013; Gupta, Varghese Gupta et al. 2013).

Regulation of PEPT1

The expression or functional activity of PEPT1 has been shown to be regulated via a variety of mechanisms under varying conditions. Understanding the underlying mechanisms of PEPT1 regulation is essential to comprehending its role as mediator of nutritional and pharmacological substrate absorption. Factors such as diet, hormone, pathological conditions, and other exogenous stimuli have been demonstrated to affect the PEPT1 expression or transport activity. The mechanisms responsible for these regulations could be specified as transcriptional, translational, post-translational regulation of PEPT1 gene, or other unknown mechanisms.

Hormones such as insulin, leptin, growth hormone, and thyroid hormone are able to regulate PEPT1 abundance and activity in epithelial cells (Thamotharan, Bawani et al. 1999; Buyse, Berlioz et al. 2001; Ashida, Katsura et al. 2002; Sun, Zhao et al. 2003; Sun, Zhao et al. 2003). These hormones appear to increase the PEPT1 protein density on the apical membrane by recruitment of preformed transporters, therefore increasing the V_{max} (but not K_m) of PEPT1-mediated transport. As an acute regulation, PEPT1 activity was also found to be inhibited by protein kinase A (PKA) and protein kinase C (PKC), as well as their upstream molecules such as cAMP (Muller, Brandsch et al. 1996; Berlioz, Julien et al. 1999).

The PEPT1 promoter has been analyzed and several transcription factors were identified to be responsible for the transcriptional regulation of PEPT1. Sp1

was found to work on PEPT1 promoter through direct binding to the GC-rich region (Shimakura, Terada et al. 2005). Further studies revealed another specific transcription factor, caudal-related homeobox protein 2 (Cdx 2), is responsible for activating intestine-specific PEPT1 expression through cooperation with Sp1 and binding to the Cdx 2 responsive element (Shimakura, Terada et al. 2006). Dalmasso et al. also provided an evidence, for first time, that PEPT1 expression was regulated at a posttranscriptional level by miRNAs in intestinal epithelial cells (Dalmasso, Hang et al. 2011).

Several studies have demonstrated that the expression level of PEPT1 and its function is affected by dietary treatments. The mRNA and protein expressions of PEPT1 could be induced by several folds when incubating dipeptide GlySar in in Caco-2 cells (Thamotharan, Bawani et al. 1998). In rat, either fasting or feeding with dietary protein as well as peptides has been shown to increase the expression level of PEPT1 and its transport activity (Shiraga, Miyamoto et al. 1999; Thamotharan, Bawani et al. 1999). Ma et al. also demonstrated that 16 h of fasting can cause significant upregulation of PEPT1 protein expression in the murine small intestine and translating into a significant increase in oral absorption of GlySar (Ma, Hu et al. 2012).

Many physiological factors such as disease state, diurnal rhythm and development were also proved to be associated with PEPT1 expression and its functional activity. For example, PEPT1 is expressed throughout the small intestine but virtually absent in the colon under normal physiological conditions. However, under inflammatory conditions (e.g., short-bowel syndrome, chronic

ulcerative colitis and Crohn’s disease), PEPT1 is aberrantly expressed in colon tissues (Merlin, Si-Tahar et al. 2001; Dalmasso, Garg et al. 2007; Zucchelli, Torkvist et al. 2009).

5-AMINOLEVULINIC ACID

Introduction

5-Aminolevulinic acid (5-ALA or δ-Aminolevulinic acid or ALA) is a naturally occurring intermediate compound that normally formed in the mitochondria in the early stage of heme biosynthetic pathway. Through several metabolism steps, eight 5-ALA molecules can conjugate together to yield protoporphyrin IX (PpIX) and finally converts into heme. Protoporphyrin IX, the precursor of heme, is a potent photosensitizer that is widely applied in the photodynamic therapy (PDT) and fluorescence diagnosis (FD) in dermatology, urology, neurosurgery, Otorhinolaryngology, gynecology and gastroenterology. For the last two decades a substantial amount of studies have been focused on the clinical application of 5-ALA as a prodrug in PDT and elucidation of the mechanism of ALA-PDT.(Peng, Berg et al. 1997; Peng, Warloe et al. 1997; Kelty, Brown et al. 2002; Krammer and Plaetzer 2008)

The chemical structures of 5-ALA and its metabolite PpIX were shown in Figure 2.3. 5-ALA is a small polar molecule with molecular weight of 131.1. At physiological pH it exists mainly as a charged zwitterion, which accounts for its low lipid solubility. The pKa_1 and pKa_2 are 4.1 and 8.7, respectively (Uehlinger, Zellweger et al. 2000).

In the following section, current knowledge about pharmacokinetics, transport mechanism of 5-ALA and its application in photodynamic therapy were discussed.

Application of 5-ALA in Photodynamic Therapy

Photodynamic therapy (PDT) is a promising and minimally invasive therapeutic treatment for various cancers and non-malignant diseases. One of the major advantages of PDT over other anticancer treatment modalities is its high degree of selectivity. This is typically accomplished via the systemic administration of a non-toxic photosensitizing agent, which can accumulate in target tumor tissues, and subsequent illumination of the tumor site with visible light for photo-activation (Figure 2.4). The excited photosensitizer contributes to the generation of intracellular singlet oxygen and other reactive oxygen species, which results in the tumor cell damage (Cox, Krieg et al. 1982; Cox and Whitten 1982; Dickson and Pottier 1995; Peng, Berg et al. 1997; Peng, Warloe et al. 1997). Besides oxidative cytotoxicity induced in PDT, the vascular shutdown and local inflammatory reaction also are recognized to contribute to the overall PDT effect (Dougherty, Gomer et al. 1998; Castano, Mroz et al. 2008; Garg, Nowis et al. 2010; Firczuk, Winiarska et al. 2011).

There are many types of photosensitizers available and several routes (topical, oral, or intravenous) by which they can be delivered to the patient. Additional selectivity of PDT may be achieved by the administration of a photosensitizer precursor. One clinically approved example of such a compound is 5-ALA, a precursor of the natural photosensitizer PpIX. As a photosensitizer prodrug for PDT, 5-ALA has no intrinsic photochemical properties, but its metabolite PpIX is an ideal photosensitizing agent which is non-toxic, biologically stable, photodynamically active and selectively retained in the target

tissue. Once exogenous 5-ALA is administered topically or systemically, it will be quickly converted into active photosensitizer PpIX through several biochemical reactions in the heme biosynthesis pathway. It has been found that differential enzymes activity and limited availability of iron in tumor cells compared to normal tissues finally leads to a higher accumulation of PpIX within tumor cells. When PpIX concentration reaches the therapeutic level in the target tissue, subsequent exposure to visible light will activates PpIX and consequently triggers the oxidative cytotoxicity (Peng, Berg et al. 1997; Peng, Warloe et al. 1997; Krammer and Plaetzer 2008; Wachowska, Muchowicz et al. 2011).

5-ALA also serves as a photodynamic agent for fluorescence diagnosis (FD) and fluorescence-guided resection of malignant and non-malignant diseases in clinical practice. Many clinical studies using ALA for FD have suggested "this technique is more efficient than white cystoscopy as the contrast is enhanced" (Jichlinski, Wagnieres et al. 1997; Jichlinski, Wagnieres et al. 1997; Datta, Loh et al. 1998; Kelty, Brown et al. 2002; Krammer and Plaetzer 2008). The distinct wavelength chosen for irradiation causes different outcome (i.e., near 400 nm can induce fluorescence for FD and 635 nm can produce physic-chemical reaction for PDT).

During the last two decades numerous researches have been focused on the 5-ALA and its therapeutic application in ALA-PDT and ALA-FD. In 1987, 5-ALA was employed, for the first time, in photodynamic therapy of erythroleukaemic cells as a photosensitizing agent (Malik and Lugaci 1987). In the same year Qian et al. showed the results of the porphyrin accumulation and

fluorescence in tumors and other tissues 24h post intraperitoneal injection of ALA in mice (Qian, Evensen et al. 1987). In 1990 Kennedy and Pottier reported the earliest clinical trial with ALA-PDT for superficial basal cell carcinomas (Kennedy and Pottier 1992). Thereafter, the systematic and topical application of ALA in clinical practice was growing rapidly and attracted a large body of research in this field. Currently, ALA and its esters has been approved by US FDA as a promising treatment of several malignant and premalignant conditions such as actinic keratosis, basal cell carcinoma, Bowen's disease, bladder cancer and others. In Europe, 5-ALA has been approved for intraoperative photodynamic diagnosis of residual malignant glioma while methyl-ester and hexyl-ester derivatives of 5-ALA have been approved for treatment of basal cell carcinoma and actinic keratosis and diagnostic application of bladder cancer, respectively (Dolmans, Fukumura et al. 2003; Fotinos, Campo et al. 2006; Krammer and Plaetzer 2008; Nokes, Apel et al. 2013). In summary, information about currently approved 5-ALA products and their application was provided in Table 2.2.

Heme Biosynthesis Pathway

5-ALA is an endogenous compound that can be found in the body naturally. As we know, there are a number of substrates and enzymes involved in the heme biosynthesis pathway (Figure 2.5). The initial and rate-limiting step in this pathway is the synthesis of 5-ALA. ALA is normally synthesized by the condensation of glycine and succinyl-CoA in mitochondria that is catalyzed by

ALA synthase (ALAS) and affiliated by pyridoxal-5-phosphate (PLP) as a cofactor (Ajioka, Phillips et al. 2006). After transferring from inside of the mitochondria to cytosol, two molecules of ALA are condensed to yield porphobilinogen (PBG) with the aid of zinc-dependent enzyme-aminolevulinate dehydratase (ALAD). After a series of intermediate biochemical reaction, four molecules of PBG can form a linear and unstable tetrapyrolle called hydroxymethylbilane (HMB) in a head-to-tail manner. This reaction is a rate-limiting step which is catalyzed by uroporphyrin I synthase. Hydroxymethylbilane can then convert into uroporphyrinogen III using uroporphyrinogen III synthase (URO3S) as a major route, as well as undergo spontaneous cyclization that leads to the formation of uroporphyrinogen III. Uroporphyrinogen decarboxylase (UROD) catalyzes decarboxylation of uroporphyrinogen III to yield coproporphyrinogen III which is transported back to the inter-membrane space of mitochondria. The next intermediate in this pathway, protoporporphyrinogen IX, is synthesized from coproporphyrinogen III under catalyzation of Coproporphyrinogen oxidase (CPO) and soon oxidized into protoporphyrin IX (PpIX) by removal of six hydrogens. The final product, heme, is formed via the insertion of an iron into the center of PpIX (Fukuda, Casas et al. 2005; Ishizuka, Abe et al. 2011; Wachowska, Muchowicz et al. 2011).

Pharmacokinetics of 5-ALA

The endogenous 5-ALA level in the body has been determined by several studies. Fauteck et al. reported the endogenous 5-ALA plasma concentration in

human was 11.2 μg/L (Fauteck, Ackermann et al. 2008). Similarly, Dalton et al. also reported the endogenous 5-ALA plasma concentrations were 28 ± 18 μg/L (mean ± S.D.) in a clinical pharmacokinetic study (Dalton, Yates et al. 2002). The endogenous plasma concentrations of 5-ALA were around 1.5 μg/L and 25 μg/L in rat and dog, respectively (Dalton, Meyer et al. 1999; Tahara, Tanaka et al. 2007). 5-ALA was also detected by Gorchen et al in cerebrospinal fluid with a range from 6 to 36 nmol/L (Gorchein and Webber 1987).

5-ALA has been shown to be rapidly eliminated from the human body, with a plasma half-life of 50 min when given intravenously and 45 min when given orally (Dalton, Yates et al. 2002). Systemic administration of 5-ALA was followed by clearance via the liver, bile and kidney. The small volume of distribution of 9.3 L indicates that a large portion was excreted unchanged in the urine and eliminated by first-pass metabolism (Dalton, Yates et al. 2002). Good oral bioavailability (> 50%) of 5-ALA was shown in human and dog (van den Boogert, van Hillegersberg et al. 1998; Dalton, Meyer et al. 1999; Dalton, Yates et al. 2002). A study on the plasma protein binding of 5-ALA showed that protein binding was 12% in human in the range of 500 to 5000 μg/L. The fluorescence microscopy of tissue samples revealed peak concentration of PpIX was achieved at 4 to 6 h after oral administration of 5-ALA (Loh, MacRobert et al. 1993). And intracellular PpIX returns to background levels within 24 to 48 hours post application.

Transport mechanism of 5-ALA

The mechanism of 5-ALA transport into the cells and its disposition in normal as well as malignant tissues has intrigued research interests and been investigated for a long time since 5-ALA was applied as a photosensitizer in photodynamic therapy. Numerous uptake and transport studies have identified several distinct carrier-mediated transport systems which are involved in the translocation of 5-ALA.

In 1998, Daniel group demonstrated, for first time, that 5-ALA uses the peptide transporters PepT1 and PepT2 for entering into epithelial cells through uptake studies in *Xenopus laevis* oocytes and yeast cells (Doring, Walter et al. 1998). Although it does not possess a typical peptide bond in the narrower sense but a ketomethylene group, 5-ALA shares similar structure with a dipeptide GlySar which is a substrate for PepT1 and PepT2. Having shown earlier that PepT1 is also expressed in the extra hepatic biliary duct, Neumann et al. characterized the transport of 5-ALA in bile duct tumor cells and discussed that 5-ALA could be accumulated in such cells via PepT1 before photodynamic tumor therapy (Neumann and Brandsch 2003). In 2013, Chung et al. confirmed both the expression of PepT1 in cholangiocyte cell lines derived from bile duct carcinoma and the transport of 5-ALA via PepT1 in these cells (Chung, Kim et al. 2013). Moreover, Hagiya et al. found that high expression of PepT1 and low expression of the ATP-binding cassette transporter ABCG2 (a porphyrin efflux transporter) together determined the 5-ALA-induced protoporphyrin IX production and the effective photocytotoxicity in gastric and bladder cancer cells. Evaluation of the

expression levels of PepT1 and ABCG2 genes could be useful to predict the efficacy of 5-ALA-based photodynamic therapy (Hagiya, Endo et al. 2012; Hagiya, Fukuhara et al. 2013).

5-ALA was also reported to be a substrate of peptide transporter PepT2 (Doring, Walter et al. 1998; Novotny, Xiang et al. 2000; Ennis, Novotny et al. 2003). Recently Smith group explored the pivot role of PepT2 in modulating 5-ALA concentrations in CNS and found PepT2 can significantly influence 5-ALA pharmacokinetics and pharmacodynamics with genetically-modified mouse model (Ocheltree, Shen et al. 2004; Hu, Shen et al. 2007; Kamal, Keep et al. 2008).

Besides PepT1 and PepT2, the results of certain *in vitro* studies also supported the involvement of other transporters in facilitating 5-ALA entering into cells. Rud et al. showed that γ-aminobutyric acid (GABA) and several amino acids inhibited 5-ALA uptake in several cell lines, and the uptake increased in a Na^+- and Cl^--dependent manner (Rud, Gederaas et al. 2000). Similar observations from Bermudez et al. also suggested that Na^+- and Cl^--dependent neurotransmitter transporters (or BETA transporters) may take up 5-ALA into murine mammary adenocarcinoma cells (Bermudez Moretti, Correa Garcia et al. 2002). A recent study found specifically that the expression of SLC6A6 and SLC6A13, members of BETA transporters, increased the 5-ALA uptake, resulting in enhanced 5-ALA-induced photodamage in cancerous cells (Tran, Mu et al. 2014). In addition to neurotransmitter transporters, other investigators have shown that proton-coupled amino acid transporter PAT1 (SLC36A1) was able to recognize and transport 5-ALA in PAT1-expressing *Xenopus laevis* oocytes and Cos-7 cells (Anderson,

Jevons et al. 2010; Frolund, Marquez et al. 2010). In conclusion, several carrier-mediated transport systems of 5-ALA identified and investigated in mammals were summarized in Table 2.3.

FIGURES AND TABLES

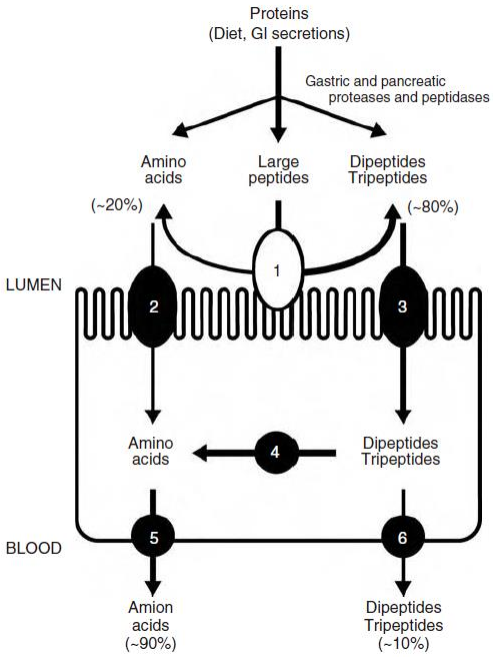

Figure 2.1 Overview of protein digestion and absorption in the gastrointestinal tract. (1) Brush-border peptidases; (2) brush-border amino-acid transport systems; (3) brush-border peptide transport system; (4) cytoplasmic peptidases; (5) basolateral amino acid transport systems; (6) basolateral peptide transport system(s). GI, gastrointestinal. (Adopted from Ganapathy et al. Protein digestion and absorption. Chapter 65, Physiology of the gastrointestinal tract, fourth edition.)

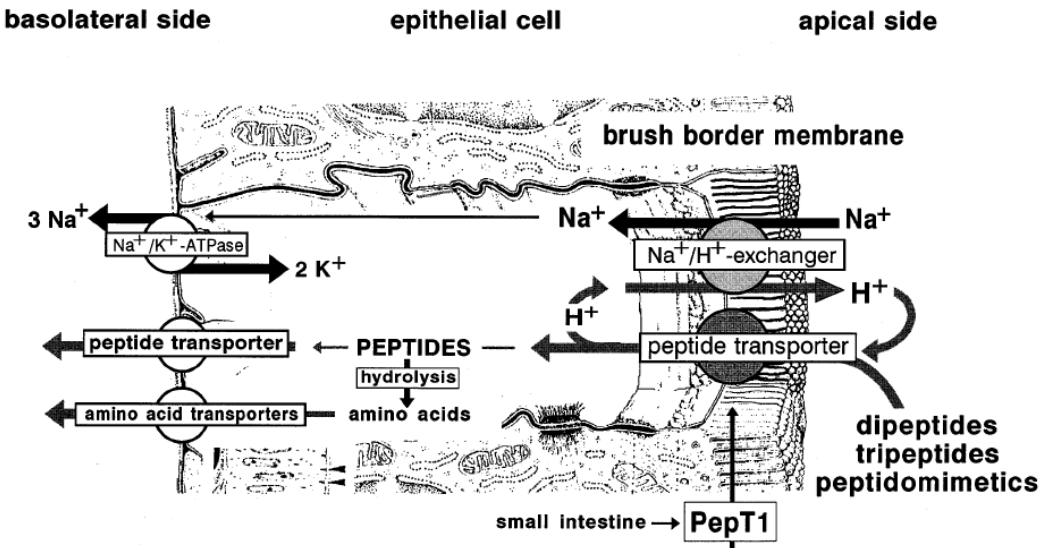

Figure 2.2 Schematic model of PEPT1-mediated cellular transport in intestinal epithelial cells (Adopted from Daniel 1996).

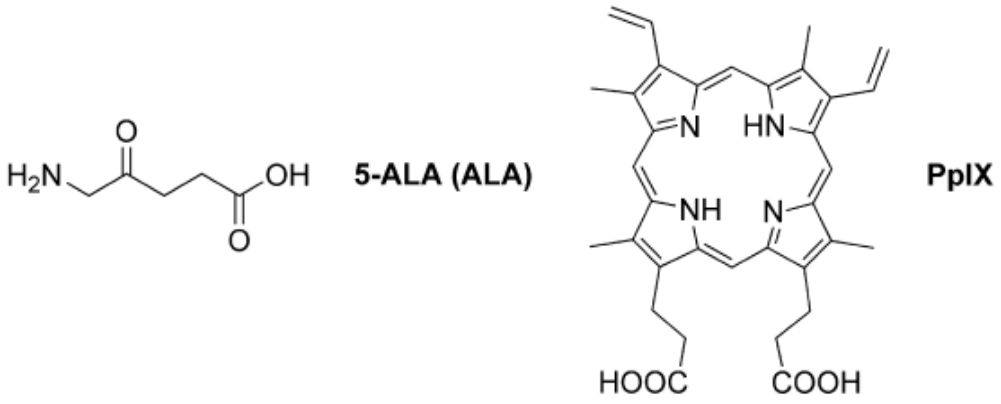

Figure 2.3 Chemical structures of 5-Aminolaevulinic acid (5-ALA) and protoporphyrin IX (PpIX).

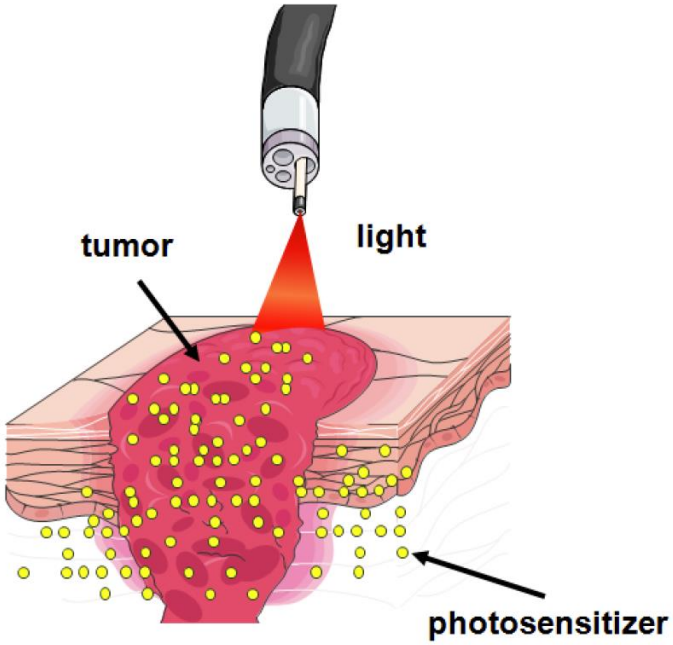

Figure 2.4 Overview of photodynamic therapy mechanism. (Adopted from Wachowska, Muchowicz et al. 2011)

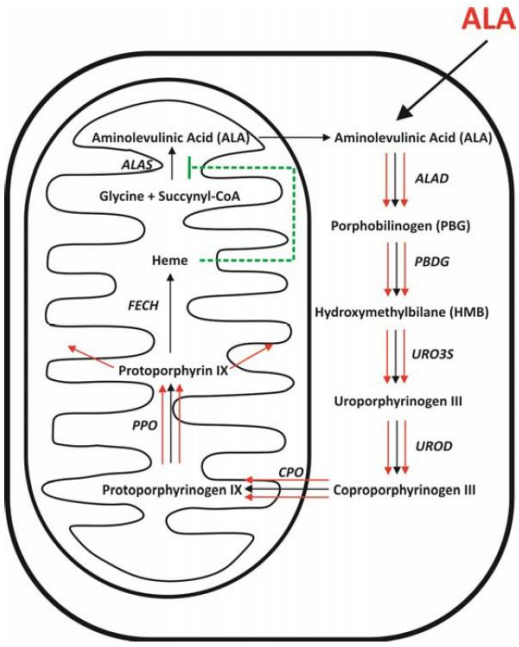

Figure 2.5 5-ALA in the major route of heme biosynthesis pathway. (Adopted from Wachowska, Muchowicz et al. 2011)

Table 2.1 The proton-coupled oligopeptide transporter family (SLC15)

Human gene name	Protein name	Aliases	Predominant substrates	Transport type/ coupling ions	Tissue distribution and cellular/ subcellular expression	Human gene locus	Protein length (a.a.)
SLC15A1	PepT1	Oligopeptide transporter 1, H+-peptide transporter 1	Di- and tripeptides, protons, beta-lactam antibiotics	C/H+	Apical surface of epithelial cells from small intestine and kidney; pancreas, bile duct and liver	13q32.3	Human 708 Mouse 709 Rat 710
SLC15A2	PepT2	Oligopeptide transporter 2, H+-peptide transporter 2	Di- and tripeptides, protons, beta-lactam antibiotics	C/H+	Apical surface of epithelial cells from kidney and choroid plexus; neurons, astrocytes (neonates), lung, mammary gland, spleen, enteric nervous system	3q21.1	Human 729 Mouse 729 Rat 729
SLC15A3	PhT2	Peptide/ histidine transporter 2, PTR3	Di- and tripeptides, protons, histidine	C/H+	Lung, spleen, thymus, intestine (faintly in brain, liver, adrenal gland, heart)	11q12.2	Human 577 Mouse 574 Rat 572
SLC15A4	PhT1	Peptide/ histidine transporter 1, PTR4	Di- and tripeptides, protons, histidine	C/H+	Brain, eye, intestine (faintly in lung and spleen)	12q24.32	Human 581 Mouse 578 Rat 582

References:

(Herrera-Ruiz and Knipp 2003; Daniel and Kottra 2004; Smith, Clemencon et al. 2013)

Table 2.2 Approved 5-ALA products and their application

Generic name	Chemical name	Approval	Applications	Activation wavelength
Levulan	5-Aminolevulinic acid	EU, USA	Actinic keratosis, basal-cell carcinoma, head and neck, and gynaecological tumors	635 nm
			Diagnosis of brain, head and neck, and bladder tumors	375–400 nm
Gilolan	5-Aminolevulinic acid	EU	Intraoperative photodynamic diagnosis of residual glioma	400–410 nm
Metvix	Methyl 5-Aminolevulinic acid	EU, Australia	Actinic keratoses, basal-cell carcinoma	635 nm
Hexvix	Hexyl 5-Aminolevulinic acid	EU	Diagnosis of bladder tumors	375–400 nm
Benzvix	Benzyl 5-Aminolevulinic acid	n clinical trials	Gastrointestinal cancer	635 nm

References:

(Dolmans, Fukumura et al. 2003)

(Krammer and Plaetzer 2008)

Table 2.3 Transporters involved in the transport of 5-ALA

Transporter	Alias	Animal species	Experimental system	Reference
PEPT1 (SLC15A1)	Solute Carrier Family 15 Oligopeptide Transporter Member 1	Human	cRNA-injected XLO, cDNA-transfected yeast cells, bile duct tumor cells, gastric and bladder tumor cells, cDNA-transfected MDCK cells, Caco-2 cells	(Doring, Walter et al. 1998; Neumann and Brandsch 2003; Anderson, Jevons et al. 2010; Frolund, Marquez et al. 2010; Hagiya, Endo et al. 2012; Chung, Kim et al. 2013; Hagiya, Fukuhara et al. 2013)
PEPT2 (SLC15A2)	Solute Carrier Family 15 Oligopeptide Transporter Member 2	Human, Mouse, Rat	cRNA-injected XLO, cDNA-transfected yeast cells, rat CP epithelial cells, PepT2 knockout mice	(Doring, Walter et al. 1998; Novotny, Xiang et al. 2000; Ennis, Novotny et al. 2003; Ocheltree, Shen et al. 2004; Hu, Shen et al. 2007)
PAT1 (SLC36A1)	Proton-coupled Amino Acid Transporter 1	Human	cRNA-injected XLO, cDNA-transfected COS-7 cells, Caco-2 cells	(Anderson, Jevons et al. 2010; Frolund, Marquez et al. 2010)
TAUT (SLC6A6)	Sodium- and Chloride-Dependent Taurine Transporter	Human, Mouse	murine mammary adenocarcinoma cells, human colon cancer cells, human cervical cancer HeLa cells	(Rud, Gederaas et al. 2000; Bermudez Moretti, Correa Garcia et al. 2002; Tran, Mu et al. 2014)
GAT2 (SLC6A13)	Sodium- and Chloride-Dependent GABA Transporter 2			

XLO, Xenopus laevis oocytes

MDCK, Madin-Darby canine kidney

CP, choroid plexus

REFERENCES

Adibi, S. A. (1997). "The oligopeptide transporter (Pept-1) in human intestine: biology and function." Gastroenterology **113**(1): 332-340.

Agu, R., E. Cowley, et al. (2011). "Proton-coupled oligopeptide transporter (POT) family expression in human nasal epithelium and their drug transport potential." Mol Pharm **8**(3): 664-672.

Ajioka, R. S., J. D. Phillips, et al. (2006). "Biosynthesis of heme in mammals." Biochim Biophys Acta **1763**(7): 723-736.

Amasheh, S., U. Wenzel, et al. (1997). "Transport of charged dipeptides by the intestinal H+/peptide symporter PepT1 expressed in Xenopus laevis oocytes." J Membr Biol **155**(3): 247-256.

Anderle, P., C. U. Nielsen, et al. (2006). "Genetic variants of the human dipeptide transporter PEPT1." J Pharmacol Exp Ther **316**(2): 636-646.

Anderson, C. M., M. Jevons, et al. (2010). "Transport of the photodynamic therapy agent 5-aminolevulinic acid by distinct H+-coupled nutrient carriers coexpressed in the small intestine." J Pharmacol Exp Ther **332**(1): 220-228.

Ashida, K., T. Katsura, et al. (2002). "Thyroid hormone regulates the activity and expression of the peptide transporter PEPT1 in Caco-2 cells." American Journal of Physiology-Gastrointestinal and Liver Physiology **282**(4): G617-G623.

Berlioz, F., S. Julien, et al. (1999). "Neural modulation of cephalexin intestinal absorption through the di- and tripeptide brush border transporter of rat jejunum

in vivo." Journal of Pharmacology and Experimental Therapeutics **288**(3): 1037-1044.

Bermudez Moretti, M., S. Correa Garcia, et al. (2002). "Delta-Aminolevulinic acid transport in murine mammary adenocarcinoma cells is mediated by beta transporters." Br J Cancer **87**(4): 471-474.

Boll, M., D. Markovich, et al. (1994). "Expression cloning of a cDNA from rabbit small intestine related to proton-coupled transport of peptides, beta-lactam antibiotics and ACE-inhibitors." Pflugers Arch **429**(1): 146-149.

Botka, C. W., T. W. Wittig, et al. (2000). "Human proton/oligopeptide transporter (POT) genes: identification of putative human genes using bioinformatics." Aaps Pharmsci **2**(2): E16.

Brandsch, M. (2013). "Drug transport via the intestinal peptide transporter PepT1." Curr Opin Pharmacol **13**(6): 881-887.

Brandsch, M., I. Knutter, et al. (2008). "Pharmaceutical and pharmacological importance of peptide transporters." J Pharm Pharmacol **60**(5): 543-585.

Buyse, M., F. Berlioz, et al. (2001). "PepT1-mediated epithelial transport of dipeptides and cephalexin is enhanced by luminal leptin in the small intestine." Journal of Clinical Investigation **108**(10): 1483-1494.

Castano, A. P., P. Mroz, et al. (2008). "Photodynamic therapy plus low-dose cyclophosphamide generates antitumor immunity in a mouse model." Proc Natl Acad Sci U S A **105**(14): 5495-5500.

Chen, H., Y. X. Pan, et al. (2002). "Molecular cloning and functional expression of a chicken intestinal peptide transporter (cPepT1) in Xenopus oocytes and Chinese hamster ovary cells." Journal of Nutrition **132**(3): 387-393.

Chung, C. W., C. H. Kim, et al. (2013). "Aminolevulinic acid derivatives-based photodynamic therapy in human intra- and extrahepatic cholangiocarcinoma cells." Eur J Pharm Biopharm **85**(3 Pt A): 503-510.

Cox, G. S., M. Krieg, et al. (1982). "Photochemical reactivity in organized assemblies. 30. Self-sensitized photooxidation of protoporphyrin IX derivatives in aqueous surfactant solutions; product and mechanistic studies." Journal of the American Chemical Society **104**(25): 6930-6937.

Cox, G. S. and D. G. Whitten (1982). "Mechanisms for the photooxidation of protoporphyrin IX in solution." Journal of the American Chemical Society **104**(2): 516-521.

Dalmasso, G., P. Garg, et al. (2007). "PepT1-mediated anti-inflammatory tri-peptide (KPV) transport reduces intestinal inflammation." Faseb Journal **21**(5): A586-A586.

Dalmasso, G., T. T. N. Hang, et al. (2011). "MicroRNA-92b regulates expression of the oligopeptide transporter PepT1 in intestinal epithelial cells." American Journal of Physiology-Gastrointestinal and Liver Physiology **300**(1): G52-G59.

Dalton, J. T., M. C. Meyer, et al. (1999). "Pharmacokinetics of aminolevulinic acid after oral and intravenous administration in dogs." Drug Metab Dispos **27**(4): 432-435.

Dalton, J. T., C. R. Yates, et al. (2002). "Clinical pharmacokinetics of 5-aminolevulinic acid in healthy volunteers and patients at high risk for recurrent bladder cancer." J Pharmacol Exp Ther **301**(2): 507-512.

Daniel, H. (1996). "Function and molecular structure of brush border membrane peptide/H+ symporters." J Membr Biol **154**(3): 197-203.

Daniel, H. (2004). "Molecular and integrative physiology of intestinal peptide transport." Annu Rev Physiol **66**: 361-384.

Daniel, H. and G. Kottra (2004). "The proton oligopeptide cotransporter family SLC15 in physiology and pharmacology." Pflugers Arch **447**(5): 610-618.

Daniel, H., E. L. Morse, et al. (1992). "Determinants of substrate affinity for the oligopeptide/H+ symporter in the renal brush border membrane." J Biol Chem **267**(14): 9565-9573.

Datta, S. N., C. S. Loh, et al. (1998). "Quantitative studies of the kinetics of 5-aminolaevulinic acid induced fluorescence in bladder transitional cell carcinoma." British Journal of Cancer **78**(8): 1113-1118.

Dickson, E. F. G. and R. H. Pottier (1995). "On the role of protoporphyrin IX photoproducts in photodynamic therapy." Journal of Photochemistry and Photobiology B: Biology **29**(1): 91-93.

Dolmans, D. E., D. Fukumura, et al. (2003). "Photodynamic therapy for cancer." Nat Rev Cancer **3**(5): 380-387.

Doring, F., C. Martini, et al. (2002). "Importance of a small N-terminal region in mammalian peptide transporters for substrate affinity and function." Journal of Membrane Biology **186**(2): 55-62.

Doring, F., J. Walter, et al. (1998). "Delta-aminolevulinic acid transport by intestinal and renal peptide transporters and its physiological and clinical implications." J Clin Invest **101**(12): 2761-2767.

Doring, F., J. Will, et al. (1998). "Minimal molecular determinants of substrates for recognition by the intestinal peptide transporter." Journal of Biological Chemistry **273**(36): 23211-23218.

Dougherty, T. J., C. J. Gomer, et al. (1998). "Photodynamic therapy." J Natl Cancer Inst **90**(12): 889-905.

Englund, G., F. Rorsman, et al. (2006). "Regional levels of drug transporters along the human intestinal tract: Co-expression of ABC and SLC transporters and comparison with Caco-2 cells." European Journal of Pharmaceutical Sciences **29**(3-4): 269-277.

Ennis, S. R., A. Novotny, et al. (2003). "Transport of 5-aminolevulinic acid between blood and brain." Brain Res **959**(2): 226-234.

Fauteck, J. D., G. Ackermann, et al. (2008). "Fluorescence characteristics and pharmacokinetic properties of a novel self-adhesive 5-ALA patch for photodynamic therapy of actinic keratoses." Arch Dermatol Res **300**(2): 53-60.

Fei, Y. J., Y. Kanai, et al. (1994). "Expression cloning of a mammalian proton-coupled oligopeptide transporter." Nature **368**(6471): 563-566.

Fei, Y. J., M. Sugawara, et al. (2000). "cDNA structure, genomic organization, and promoter analysis of the mouse intestinal peptide transporter PEPT1." Biochimica Et Biophysica Acta-Gene Structure and Expression **1492**(1): 145-154.

Firczuk, M., M. Winiarska, et al. (2011). "Approaches to improve photodynamic therapy of cancer." Frontiers in Bioscience **16**: 208-224.

Ford, D., A. Howard, et al. (2003). "Expression of the peptide transporter hPepT1 in human colon: a potential route for colonic protein nitrogen and drug absorption." Histochem Cell Biol **119**(1): 37-43.

Fotinos, N., M. A. Campo, et al. (2006). "5-Aminolevulinic acid derivatives in photomedicine: Characteristics, application and perspectives." Photochemistry and Photobiology **82**(4): 994-1015.

Frolund, S., O. C. Marquez, et al. (2010). "Delta-aminolevulinic acid is a substrate for the amino acid transporter SLC36A1 (hPAT1)." Br J Pharmacol **159**(6): 1339-1353.

Fukuda, H., A. Casas, et al. (2005). "Aminolevulinic acid: from its unique biological function to its star role in photodynamic therapy." Int J Biochem Cell Biol **37**(2): 272-276.

Ganapathy, V., N. Gupta, et al. (2006). Chapter 65 - Protein Digestion and Absorption. Physiology of the Gastrointestinal Tract (Fourth Edition). L. R. Johnson, K. E. Barret, F. K. Gishanet al. Burlington, Academic Press**:** 1667-1692.

Ganapathy, V. and F. H. Leibach (1983). "Role of pH gradient and membrane potential in dipeptide transport in intestinal and renal brush-border membrane

vesicles from the rabbit. Studies with L-carnosine and glycyl-L-proline." Journal of Biological Chemistry **258**(23): 14189-14192.

Garg, A. D., D. Nowis, et al. (2010). "Photodynamic therapy: illuminating the road from cell death towards anti-tumour immunity." Apoptosis **15**(9): 1050-1071.

Gorchein, A. and R. Webber (1987). "delta-Aminolaevulinic acid in plasma, cerebrospinal fluid, saliva and erythrocytes: studies in normal, uraemic and porphyric subjects." Clin Sci (Lond) **72**(1): 103-112.

Groneberg, D. A., F. Doring, et al. (2001). "Intestinal peptide transport: ex vivo uptake studies and localization of peptide carrier PEPT1." Am J Physiol Gastrointest Liver Physiol **281**(3): G697-704.

Gupta, D., S. Varghese Gupta, et al. (2013). "Increasing oral absorption of polar neuraminidase inhibitors: a prodrug transporter approach applied to oseltamivir analogue." Mol Pharm **10**(2): 512-522.

Gupta, S. V., D. Gupta, et al. (2011). "Enhancing the intestinal membrane permeability of zanamivir: a carrier mediated prodrug approach." Mol Pharm **8**(6): 2358-2367.

Hagiya, Y., Y. Endo, et al. (2012). "Pivotal roles of peptide transporter PEPT1 and ATP-binding cassette (ABC) transporter ABCG2 in 5-aminolevulinic acid (ALA)-based photocytotoxicity of gastric cancer cells in vitro." Photodiagnosis Photodyn Ther **9**(3): 204-214.

Hagiya, Y., H. Fukuhara, et al. (2013). "Expression levels of PEPT1 and ABCG2 play key roles in 5-aminolevulinic acid (ALA)-induced tumor-specific

protoporphyrin IX (PpIX) accumulation in bladder cancer." Photodiagnosis Photodyn Ther **10**(3): 288-295.

Herrera-Ruiz, D. and G. T. Knipp (2003). "Current perspectives on established and putative mammalian oligopeptide transporters." J Pharm Sci **92**(4): 691-714.

Herrera-Ruiz, D., Q. Wang, et al. (2001). "Spatial expression patterns of peptide transporters in the human and rat gastrointestinal tracts, Caco-2 in vitro cell culture model, and multiple human tissues." Aaps Pharmsci **3**(1): art. no.-9.

Howard, A., R. A. Goodlad, et al. (2004). "Increased expression of specific intestinal amino acid and peptide transporter mRNA in rats fed by TPN is reversed by GLP-2." Journal of Nutrition **134**(11): 2957-2964.

Hu, Y., H. Shen, et al. (2007). "Peptide transporter 2 (PEPT2) expression in brain protects against 5-aminolevulinic acid neurotoxicity." J Neurochem **103**(5): 2058-2065.

Hu, Y., Y. Xie, et al. (2014). "Divergent developmental expression and function of the proton-coupled oligopeptide transporters PepT2 and PhT1 in regional brain slices of mouse and rat." Journal of Neurochemistry **129**(6): 955-965.

Irie, M., T. Terada, et al. (2005). "Computational modelling of H+-coupled peptide transport via human PEPT1." J Physiol **565**(Pt 2): 429-439.

Ishizuka, M., F. Abe, et al. (2011). "Novel development of 5-aminolevurinic acid (ALA) in cancer diagnoses and therapy." Int Immunopharmacol **11**(3): 358-365.

Jappar, D., S. P. Wu, et al. (2010). "Significance and regional dependency of peptide transporter (PEPT) 1 in the intestinal permeability of glycylsarcosine: in

situ single-pass perfusion studies in wild-type and Pept1 knockout mice." Drug Metab Dispos **38**(10): 1740-1746.

Jichlinski, P., G. Wagnieres, et al. (1997). "Clinical assessment of fluorescence cystoscopy during transurethral bladder resection in superficial bladder cancer." Urological Research **25**: S3-S6.

Jichlinski, P., G. Wagnieres, et al. (1997). "Clinical value of fluorescence cystoscopy in the detection of superficial transitional cell carcinomas of the bladder." Annales D Urologie **31**(1): 43-48.

Kamal, M. A., R. F. Keep, et al. (2008). "Role and relevance of PEPT2 in drug disposition, dynamics, and toxicity." Drug Metab Pharmacokinet **23**(4): 236-242.

Kelty, C. J., N. J. Brown, et al. (2002). "The use of 5-aminolaevulinic acid as a photosensitiser in photodynamic therapy and photodiagnosis." Photochemical & Photobiological Sciences **1**(3): 158-168.

Kennedy, D. J., F. H. Leibach, et al. (2002). "Optimal absorptive transport of the dipeptide glycylsarcosine is dependent on functional Na+/H+ exchange activity." Pflugers Arch **445**(1): 139-146.

Kennedy, J. C. and R. H. Pottier (1992). "Endogenous protoporphyrin IX, a clinically useful photosensitizer for photodynamic therapy." J Photochem Photobiol B **14**(4): 275-292.

Klang, J. E., L. A. Burnworth, et al. (2005). "Functional characterization of a cloned pig intestinal peptide transporter (pPepT1)." J Anim Sci **83**(1): 172-181.

Knutter, I., I. Rubio-Aliaga, et al. (2002). "H+-peptide cotransport in the human bile duct epithelium cell line SK-ChA-1." Am J Physiol Gastrointest Liver Physiol **283**(1): G222-229.

Kottra, G., A. Stamfort, et al. (2002). "PEPT1 as a Paradigm for Membrane Carriers That Mediate Electrogenic Bidirectional Transport of Anionic, Cationic, and Neutral Substrates." Journal of Biological Chemistry **277**(36): 32683-32691.

Krammer, B. and K. Plaetzer (2008). "ALA and its clinical impact, from bench to bedside." Photochem Photobiol Sci **7**(3): 283-289.

Krammer, B. and K. Plaetzer (2008). "ALA and its clinical impact, from bench to bedside." Photochemical & Photobiological Sciences **7**(3): 283-289.

Liang, R., Y. J. Fei, et al. (1995). "Human intestinal H+/peptide cotransporter. Cloning, functional expression, and chromosomal localization." Journal of Biological Chemistry **270**(12): 6456-6463.

Liu, W., R. Liang, et al. (1995). "Molecular cloning of PEPT 2, a new member of the H+/peptide cotransporter family, from human kidney." Biochim Biophys Acta **1235**(2): 461-466.

Loh, C. S., A. J. MacRobert, et al. (1993). "Oral versus intravenous administration of 5-aminolaevulinic acid for photodynamic therapy." Br J Cancer **68**(1): 41-51.

Lu, H. and C. Klaassen (2006). "Tissue distribution and thyroid hormone regulation of Pept1 and Pept2 mRNA in rodents." Peptides **27**(4): 850-857.

Ma, K., Y. Hu, et al. (2012). "Influence of fed-fasted state on intestinal PEPT1 expression and in vivo pharmacokinetics of glycylsarcosine in wild-type and Pept1 knockout mice." Pharm Res **29**(2): 535-545.

Mackenzie, B., Y. J. Fei, et al. (1996). "The human intestinal H+/oligopeptide cotransporter hPEPT1 transports differently-charged dipeptides with identical electrogenic properties." Biochim Biophys Acta **1284**(2): 125-128.

Mackenzie, B., D. D. Loo, et al. (1996). "Mechanisms of the human intestinal H+-coupled oligopeptide transporter hPEPT1." J Biol Chem **271**(10): 5430-5437.

Malik, Z. and H. Lugaci (1987). "Destruction of erythroleukaemic cells by photoactivation of endogenous porphyrins." Br J Cancer **56**(5): 589-595.

Matthews, D. M. (1975). "Intestinal absorption of peptides." Physiol Rev **55**(4): 537-608.

Meier, Y., J. J. Eloranta, et al. (2007). "Regional distribution of solute carrier mRNA expression along the human intestinal tract." Drug Metabolism and Disposition **35**(4): 590-594.

Merlin, D., M. Si-Tahar, et al. (2001). "Colonic epithelial hPepT1 expression occurs in inflammatory bowel disease: Transport of bacterial peptides influences expression of MHC class 1 molecules." Gastroenterology **120**(7): 1666-1679.

Miyamoto, K., T. Shiraga, et al. (1996). "Sequence, tissue distribution and developmental changes in rat intestinal oligopeptide transporter." Biochimica Et Biophysica Acta-Gene Structure and Expression **1305**(1-2): 34-38.

Muller, U., M. Brandsch, et al. (1996). "Inhibition of the H+/peptide cotransporter in the human intestinal cell line Caco-2 by cyclic AMP." Biochem Biophys Res Commun **218**(2): 461-465.

Neumann, J. and M. Brandsch (2003). "Delta-aminolevulinic acid transport in cancer cells of the human extrahepatic biliary duct." J Pharmacol Exp Ther **305**(1): 219-224.

Nokes, B., M. Apel, et al. (2013). "Aminolevulinic acid (ALA): photodynamic detection and potential therapeutic applications." J Surg Res **181**(2): 262-271.

Novotny, A., J. Xiang, et al. (2000). "Mechanisms of 5-aminolevulinic acid uptake at the choroid plexus." J Neurochem **75**(1): 321-328.

Nussberger, S., A. Steel, et al. (1997). "Structure and pharmacology of proton-linked peptide transporters." Journal of Controlled Release **46**(1–2): 31-38.

Nussberger, S., A. Steel, et al. (1997). "Symmetry of H+ binding to the intra- and extracellular side of the H+-coupled oligopeptide cotransporter PepT1." J Biol Chem **272**(12): 7777-7785.

Ocheltree, S. M., H. Shen, et al. (2005). "Role and relevance of peptide transporter 2 (PEPT2) in the kidney and choroid plexus: in vivo studies with glycylsarcosine in wild-type and PEPT2 knockout mice." J Pharmacol Exp Ther **315**(1): 240-247.

Ocheltree, S. M., H. Shen, et al. (2004). "Role of PEPT2 in the choroid plexus uptake of glycylsarcosine and 5-aminolevulinic acid: studies in wild-type and null mice." Pharm Res **21**(9): 1680-1685.

Ogihara, H., H. Saito, et al. (1996). "Immuno-localization of H+/peptide cotransporter in rat digestive tract." Biochem Biophys Res Commun **220**(3): 848-852.

Pan, Y. X., E. A. Wong, et al. (2001). "Expression of a cloned ovine gastrointestinal peptide transporter (oPepT1) in Xenopus oocytes induces uptake of oligopeptides in vitro." Journal of Nutrition **131**(4): 1264-1270.

Peng, Q., K. Berg, et al. (1997). "5-aminolevulinic acid-based photodynamic therapy: Principles and experimental research." Photochemistry and Photobiology **65**(2): 235-251.

Peng, Q., T. Warloe, et al. (1997). "5-aminolevulinic acid-based photodynamic therapy - Clinical research and future challenges." Cancer **79**(12): 2282-2308.

Qian, P., J. F. Evensen, et al. (1987). "A comparison of different photosensitizing dyes with respect to uptake C3H-tumors and tissues of mice." Cancer Letters **36**(1): 1-10.

Rubio-Aliaga, I. and H. Daniel (2002). "Mammalian peptide transporters as targets for drug delivery." Trends in Pharmacological Sciences **23**(9): 434-440.

Rubio-Aliaga, I. and H. Daniel (2008). "Peptide transporters and their roles in physiological processes and drug disposition." Xenobiotica **38**(7-8): 1022-1042.

Rud, E., O. Gederaas, et al. (2000). "5-aminolevulinic acid, but not 5-aminolevulinic acid esters, is transported into adenocarcinoma cells by system BETA transporters." Photochemistry and Photobiology **71**(5): 640-647.

Saito, H., M. Okuda, et al. (1995). "Cloning and characterization of a rat H+/peptide cotransporter mediating absorption of beta-lactam antibiotics in the intestine and kidney." J Pharmacol Exp Ther **275**(3): 1631-1637.

Sakata, K., T. Yamashita, et al. (2001). "Cloning of a lymphatic peptide/histidine transporter." Biochem J **356**(Pt 1): 53-60.

Shen, H., S. M. Ocheltree, et al. (2007). "Impact of genetic knockout of PEPT2 on cefadroxil pharmacokinetics, renal tubular reabsorption, and brain penetration in mice." Drug Metab Dispos **35**(7): 1209-1216.

Shen, H., D. E. Smith, et al. (1999). "Localization of PEPT1 and PEPT2 proton-coupled oligopeptide transporter mRNA and protein in rat kidney." American Journal of Physiology-Renal Physiology **276**(5): F658-F665.

Shimakura, J., T. Terada, et al. (2005). "Characterization of the human peptide transporter PEPT1 promoter: Sp1 functions as a basal transcriptional regulator of human PEPT1." American Journal of Physiology-Gastrointestinal and Liver Physiology **289**(3): G471-G477.

Shimakura, J., T. Terada, et al. (2006). "The transcription factor Cdx2 regulates the intestine-specific expression of human peptide transporter 1 through functional interaction with Sp1." Biochemical Pharmacology **71**(11): 1581-1588.

Shiraga, T., K. Miyamoto, et al. (1999). "Cellular and molecular mechanisms of dietary regulation on rat intestinal H+/peptide transporter PepT1." Gastroenterology **116**(4): A578-A578.

Smith, D. E., B. Clemencon, et al. (2013). "Proton-coupled oligopeptide transporter family SLC15: physiological, pharmacological and pathological implications." Mol Aspects Med **34**(2-3): 323-336.

Smith, D. E., A. Pavlova, et al. (1998). "Tubular localization and tissue distribution of peptide transporters in rat kidney." Pharm Res **15**(8): 1244-1249.

Steel, A., S. Nussberger, et al. (1997). "Stoichiometry and pH dependence of the rabbit proton-dependent oligopeptide transporter PepT1." J Physiol **498 (Pt 3)**: 563-569.

Sugiura, T., S. Umeda, et al. (2013). PEPT (SLC15A) Family. Pharmacogenomics of Human Drug Transporters, John Wiley & Sons, Inc.**:** 223-242.

Sun, B. W., X. C. Zhao, et al. (2003). "Changes of biological functions of dipeptide transporter (PepT1) and hormonal regulation in severe scald rats." World Journal of Gastroenterology **9**(12): 2782-2785.

Sun, B. W., X. C. Zhao, et al. (2003). "Hormonal regulation of dipeptide transporter (PepT1) in Caco-2 cells with normal and anoxia/reoxygenation management." World Journal of Gastroenterology **9**(4): 808-812.

Sun, D., F. Tan, et al. (2013). "Expression of proton-coupled oligopeptide transporter (POTs) in prostate of mice and patients with benign prostatic hyperplasia (BPH) and prostate cancer (PCa)." Prostate **73**(3): 287-295.

Tahara, T., M. Tanaka, et al. (2007). "Decrease of hepatic [delta]-aminolevulinate dehydratase activity in an animal model of fatigue." Biochemical and Biophysical Research Communications **353**(4): 1068-1073.

Terada, T. and K. Inui (2004). "Peptide transporters: structure, function, regulation and application for drug delivery." Curr Drug Metab **5**(1): 85-94.

Terada, T., H. Saito, et al. (2000). "N-terminal Halves of Rat H+/Peptide Transporters Are Responsible for Their Substrate Recognition." Pharmaceutical Research **17**(1): 15-20.

Thamotharan, M., S. Z. Bawani, et al. (1998). "Mechanism of dipeptide stimulation of its own transport in a human intestinal cell line." Proc Assoc Am Physicians **110**(4): 361-368.

Thamotharan, M., S. Z. Bawani, et al. (1999). "Functional and molecular expression of intestinal oligopeptide transporter (Pept-1) after a brief fast." Metabolism **48**(6): 681-684.

Thamotharan, M., S. Z. Bawani, et al. (1999). "Hormonal regulation of oligopeptide transporter pept-1 in a human intestinal cell line." Am J Physiol **276**(4 Pt 1): C821-826.

Thwaites, D. T., D. Ford, et al. (1999). "H+/solute-induced intracellular acidification leads to selective activation of apical Na+/H+ exchange in human intestinal epithelial cells." The Journal of Clinical Investigation **104**(5): 629-635.

Thwaites, D. T., D. J. Kennedy, et al. (2002). "H+/dipeptide absorption across the human intestinal epithelium is controlled indirectly via a functional Na+/H+ exchanger." Gastroenterology **122**(5): 1322-1333.

Tran, T. T., A. Mu, et al. (2014). "Neurotransmitter Transporter Family Including SLC6A6 and SLC6A13 Contributes to the 5-Aminolevulinic Acid (ALA)-

Induced Accumulation of Protoporphyrin IX and Photodamage, through Uptake of ALA by Cancerous Cells." Photochemistry and Photobiology.

Uehlinger, P., M. Zellweger, et al. (2000). "5-Aminolevulinic acid and its derivatives: physical chemical properties and protoporphyrin IX formation in cultured cells." Journal of Photochemistry and Photobiology B-Biology **54**(1): 72-80.

van den Boogert, J., R. van Hillegersberg, et al. (1998). "5-Aminolaevulinic acid-induced protoporphyrin IX accumulation in tissues: pharmacokinetics after oral or intravenous administration." J Photochem Photobiol B **44**(1): 29-38.

Wachowska, M., A. Muchowicz, et al. (2011). "Aminolevulinic Acid (ALA) as a Prodrug in Photodynamic Therapy of Cancer." Molecules **16**(5): 4140-4164.

Walker, D., D. T. Thwaites, et al. (1998). "Substrate upregulation of the human small intestinal peptide transporter, hPepT1." J Physiol **507 (Pt 3)**: 697-706.

Watanabe, C., Y. Kato, et al. (2005). "Na+/H+ exchanger 3 affects transport property of H+/oligopeptide transporter 1." Drug Metab Pharmacokinet **20**(6): 443-451.

Webb, K. E., Jr., J. C. Matthews, et al. (1992). "Peptide absorption: a review of current concepts and future perspectives." J Anim Sci **70**(10): 3248-3257.

Wuensch, T., S. Schulz, et al. (2013). "The peptide transporter PEPT1 is expressed in distal colon in rodents and humans and contributes to water absorption." American Journal of Physiology-Gastrointestinal and Liver Physiology **305**(1): G66-G73.

Yamashita, T., S. Shimada, et al. (1997). "Cloning and functional expression of a brain peptide/histidine transporter." Journal of Biological Chemistry **272**(15): 10205-10211.

Yan, Z., J. Sun, et al. (2011). "Bifunctional peptidomimetic prodrugs of didanosine for improved intestinal permeability and enhanced acidic stability: synthesis, transepithelial transport, chemical stability and pharmacokinetics." Mol Pharm **8**(2): 319-329.

Zair, Z. M., J. J. Eloranta, et al. (2008). "Pharmacogenetics of OATP (SLC21/SLCO), OAT and OCT (SLC22) and PEPT (SLC15) transporters in the intestine, liver and kidney." Pharmacogenomics **9**(5): 597-624.

Zhang, E. Y., R. M. Emerick, et al. (2004). "Comparison of human and monkey peptide transporters: PEPT1 and PEPT2." Mol Pharm **1**(3): 201-210.

Zhang, E. Y., D. J. Fu, et al. (2004). "Genetic polymorphisms in human proton-dependent dipeptide transporter PEPT1: implications for the functional role of Pro586." J Pharmacol Exp Ther **310**(2): 437-445.

Ziegler, T. R., C. Fernandez-Estivariz, et al. (2002). "Distribution of the H+/peptide transporter PepT1 in human intestine: up-regulated expression in the colonic mucosa of patients with short-bowel syndrome." Am J Clin Nutr **75**(5): 922-930.

Zucchelli, M., L. Torkvist, et al. (2009). "PepT1 Oligopeptide Transporter (SLC15A1) Gene Polymorphism in Inflammatory Bowel Disease." Inflammatory Bowel Diseases **15**(10): 1562-1569.

CHAPTER 3

SIGNIFICANCE OF PEPT1 IN THE IN SITU INTESTINAL PERMEABILITY OF 5-AMINOLEVULINIC ACID IN WILDTYPE AND PEPT1 KNOCKOUT MICE

ABSTRACT

PURPOSE: To determine the role of peptide transporter PepT1 in the intestinal absorption of the photodynamic therapy agent 5-aminolevulinic acid (5-ALA) in wildtype and PepT1 knockout mice.

METHODS: *In situ* single-pass intestinal perfusions were performed in the duodenum, jejunum, ileum and colon of wildtype and PepT1 knockout mice at 10 µM [^{14}C]5-ALA. 5-ALA effective permeability (P_{eff}) was evaluated at steady-state in pH 6.5 buffer for 90 min using inulin as a marker for water flux corrections. Inhibition studies were performed in the jejunum of wildtype mice with radiolabeled 5-ALA and 25 mM of the potential inhibitors glycylsarcosine (GlySar), cefadroxil, L-histidine, L-proline, β-alanine, tetraethylammonium (TEA) and p-aminohippuric acid (PAH). Concentration-dependent studies were also performed in the jejunum of wildtype mice using 0.01-50 mM of radiolabeled 5-ALA.

RESULTS: The P_{eff} of 5-ALA in wildtype mice was determined as 1.65×10^{-4} cm/s in duodenum, 1.91×10^{-4} cm/s in jejunum, 1.20×10^{-4} cm/s in ileum and 0.14×10^{-4} cm/s in colon. The P_{eff} of 5-ALA in the duodenum, jejunum, and ileum of PepT1 knockout mice was only about 10% of that in wildtype animals. Colonic P_{eff} values were very small and not different between the two genotypes. 5-ALA jejunal permeability was substantially reduced in the presence of GlySar (residual of 31%) and cefadroxil (residual of 16%). In contrast, the P_{eff} of 5-ALA was not altered when co-perfused with L-histidine, L-proline, β-alanine, TEA or PAH. The jejunal uptake of 5-ALA exhibited a saturable profile that was best described by Michaelis-Menten kinetics, where V_{max}' = 2.30 nmol/cm^2/sec and K_m' = 13.4 mM when referenced to inlet perfusate concentrations. When referenced to intestinal wall concentrations, the intrinsic absorption parameters were estimated as V_{max} = 1.89 nmol/cm^2/sec and K_m = 3.74 mM.

CONCLUSION: These findings indicate that the intestinal uptake of 5-ALA is primarily mediated by PepT1, which accounts for about 90% of its permeability in mouse small intestine. The different segmental permeability of 5-ALA was consistent with PepT1 expression along the intestinal segments. The contribution of other transporters, including PAT1, in mediating the intestinal permeability of 5-ALA is minor at best.

INTRODUCTION

Photodynamic therapy (PDT) is a promising and minimally invasive therapeutic modality for the treatment of various cancers and non-malignant diseases (Nokes, Apel et al. 2013). PDT involves two critical components (i.e., a certain wavelength of light and a photosensitive molecule) that combine to trigger oxidative cytotoxicity in target cells and/or tissues (Dolmans, Fukumura et al. 2003). 5-Aminolevulinic acid (5-ALA), a naturally occurring intermediate in the heme biosynthesis pathway, is widely applied as a prodrug in photodynamic therapy and photodynamic detection (Peng, Berg et al. 1997; Peng, Warloe et al. 1997; Kelty, Brown et al. 2002; Krammer and Plaetzer 2008). Although 5-ALA itself has no intrinsic photochemical properties, its metabolite protoporphyrin IX (PpIX) is an ideal photosensitizer which is non-toxic, biologically stable, photodynamically active and selectively retained in the target tissue. The mechanism of 5-ALA based PDT has been elucidated and applied in clinical practice (Wachowska, Muchowicz et al. 2011; Colditz and Jeffree 2012; Colditz, Leyen et al. 2012). Briefly, after exogenous 5-ALA is administered topically or systemically, it will be quickly converted into active photosensitizer PpIX through several enzymatic reactions in the heme biosynthesis pathway. The selective accumulation of PpIX within tumor cells, which reduces nonspecific tissue toxicity, is a unique advantage in the PDT and fluorescence diagnosis of solid tumors (e.g., malignant glioma, bladder cancer, etc.). It has been found that the differential enzyme activity and limited availability of iron in tumor cells, compared to normal tissues, contribute to the relatively specific accumulation of

PpIX within tumor cells (Navone, Polo et al. 1990; Stout and Becker 1990). However, the transport mechanism of 5-ALA into cells, which may partially explain the tumor selectivity of ALA-PDT, is poorly studied and unclear. In clinical practice, a high background accumulation after oral administration of 5-ALA has been reported in normal enterocytes (Loh, MacRobert et al. 1993; Regula, MacRobert et al. 1995). In addition, a remaining question concerns how the hydrophilic 5-ALA is absorbed from the gastrointestinal tract lumen into the systemic circulation system given good oral bioavailability of 5-ALA shown in several experimental and clinical studies (van den Boogert, van Hillegersberg et al. 1998; Dalton, Meyer et al. 1999; Dalton, Yates et al. 2002).

Proton coupled oligopeptide transporters (POTs) are an integral plasma membrane protein family that transport a broad spectrum of di/tripeptides and a variety of peptidomimetic substrates across the membrane. To date, four mammalian members in the POT superfamily, PepT1 (SLC15A1), PepT2 (SLC15A2), PhT1 (SLC15A4), and PhT2 (SLC15A3), have been identified and characterized functionally, each with both diverse and similar substrate specificities, capacities and affinities (Fei, Kanai et al. 1994; Brandsch 2009; Brandsch 2013; Smith, Clemencon et al. 2013). PepT1, the most widely studied transporter among the POT family, is considered to play a pivotal role in the oral absorption of small peptides and peptidomimetic drugs due to its dominant expression along the small intestine. Besides di/tripeptides, PepT1 can transport and influence the pharmacokinetics of a variety of therapeutic drugs with different structural and chemical characteristics, including some β-lactam antibiotics (e.g.,

cefadroxil), angiotensin converting enzyme inhibitors (e.g., enalapril) and antiviral prodrugs (e.g., valacyclovir). Many studies have been conducted and focused on understanding the mechanism and contribution of PepT1 toward the absorption and disposition of these drugs.

Previous research suggested that transporter-mediated (e.g., PepT1, PAT1) active uptake may play an important role in facilitating 5-ALA intestinal absorption and its good oral bioavailability (Doring, Walter et al. 1998; Anderson, Jevons et al. 2010; Frolund, Marquez et al. 2010). However, the relative contribution of intestinal transporter PepT1 (Slc15a1) in this process is not clear, as compared to other potential intestinal transporters such as PAT1 (Slc36a1) and PhT1/2 (Slc15a4/ Slc15a3). The PepT1 knockout mouse generated in our laboratory provides us a powerful research tool to evaluate the relevance of PepT1 in the intestinal effective permeability and absorption of model compounds and drugs (e.g., glycylsarcosine, cefadroxil, valacyclovir, fMet-Leu-Phe) (Hu, Smith et al. 2008; Jappar, Wu et al. 2010; Posada and Smith 2013; Wu and Smith 2013; Yang and Smith 2013).

Given this background information, the primary aim of the present study was to determine the quantitative contribution of PepT1 on the intestinal permeability of 5-ALA, via *in situ* single-pass perfusions, in wildtype and PepT1 knockout mice. Specifically, the regional permeability, substrate specificity and concentration dependency of 5-ALA were studied in mice. The possible role of other potential transporters in the intestinal absorption of 5-ALA was also investigated.

MATERIALS AND METHODS

Animals

All experiments performed on mice were carried out in accordance with the Guide for the Care and Use of Laboratory Animals as adopted by the U.S. National Institutes of Health. Gender-matched wildtype and PepT1 knockout mice (>99% C57BL/6 genetic background, 8-10 week old) were used in all experiments (Hu, Smith et al. 2008). The mice were kept under a 12-hour light/dark cycle and in an ambient temperature-controlled environment, fed with standard diet and water ad libitum (Unit for Laboratory Animal Medicine, University of Michigan, Ann Arbor, MI).

Materials

[^{14}C]5-ALA (55 mCi/mmol) and [^{3}H]inulin (201 mCi/g) were purchased from American Radiolabeled Chemicals (St. Louis, MO). All other reagents were obtained from Sigma-Aldrich (St. Louis, MO).

Stability of 5-ALA in Intestinal Segments

In situ single-pass perfusions were performed in different intestinal segments, the outlet perfusate samples collected and subsequently analyzed by High Performance Liquid Chromatography (HPLC). The HPLC system consisted of a Waters 515 pump (Waters Inc., Milford, MA), a β-RAM 5 radiochemical detector and Laura (Version 4.1.8) data acquisition software (LabLogic Systems, Brandon, FL). A reversed-phase 250 × 4.6 mm C18 column (Discovery, Supelco,

Bellefonte, PA) was used for chromatographic separation. The mobile phase consisted of 5% acetonitrile plus 0.1% TFA, pumped isocratically at 1.0 mL/min under ambient conditions. All perfusate samples were centrifuged at 10,000 × g for 10 minutes and 20 μL aliquots of supernatant were injected manually into the HPLC. Under these conditions, the retention time of [^{14}C]5-ALA was 4.1 minutes.

In Situ Single-Pass Jejunal Perfusion Studies

Gender-matched wildtype and PepT1 knockout mice were fasted overnight (approximately 16 hours) with free access to water. Perfusion experiments were performed according to the methods described previously (Adachi, Suzuki et al. 2003; Jappar, Wu et al. 2010). Briefly, the mice were anesthetized with sodium pentobarbital (40-60 mg/kg i.p.) and placed on a heated pad to maintain normal body temperature after anesthesia. Prior to surgery, isopropyl alcohol was applied to wet and sterilize the abdominal area, and then the abdomen was opened through a 1.5-cm midline incision longitudinally to expose the small intestine. For jejunal perfusion, an 8 cm segment of proximal jejunum was isolated (i.e., ~2 cm distal to the ligament of Treitz) with incisions made at both proximal and distal ends. Glass cannulas (2 mm outer diameter) were inserted into both ends of the jejunum and secured in place with silk suture. Following cannulation, the isolated intestinal segment was rinsed with isotonic saline solution, and covered with saline-wetted gauze and parafilm to prevent dehydration. After the surgical procedure, the mice were transferred to a temperature-controlled chamber (31°C) to maintain the body temperature during the experiment. The inlet cannula was connected to a 30-mL syringe placed on a

perfusion pump (Model 22; Harvard Apparatus, South Natick, MA) and the outlet tubing was placed in a collection vial.

The perfusion buffer (pH 6.5), containing 135mM NaCl, 5mM KCl, 10 mM MES, 0.01 % (w/v) [^{3}H]inulin, and [^{14}C]5-ALA, was perfused through the intestinal segment at rate of 0.1 ml/min for 90 min. The exiting perfusate was collected every 10 min for 90 min. A 100 μl aliquot from each 10-min collection was added to a vial containing scintillation fluid (CytoScint®, MP Biomedicals, Solon, OH) and measured by a dual-channel liquid scintillation counter (Beckman LS 6000 SC, Beckman Coulter, Inc, Fullerton, CA). The permeability of 5-ALA uptake in jejunum was determined at steady-state, which was achieved after 30 minutes of perfusion. Water flux was corrected by the non-permeable marker [^{3}H]inulin. At the end of experiments, the length of intestinal segments was directly measured.

For concentration-dependent perfusion studies, the 5-ALA concentration in perfusate varied over a broad range (0.01 – 50 mM) to assess the saturable jejunal uptake kinetics of 5-ALA in wildtype mice.

To examine the specificity of PepT1-mediated uptake of 5-ALA, the jejunum of wildtype mice was co-perfused with 10 μM 5-ALA and 25 mM of potential inhibitors such as GlySar, cefadroxil, tetraethylammonium (TEA), *p*-aminohippurate (PAH), L-histidine, L-proline or β-alanine.

In Situ Single-Pass Segment-Dependent Perfusions

To characterize the effective permeability of 5-ALA in different intestinal regions, four major intestinal segments including duodenum, jejunum, ileum, and colon were isolated and perfused simultaneously in wildtype and PepT1 knockout mice. In addition to the jejunal segment, a 2-cm segment of duodenum (i.e. ~ 0.25 cm distal to the pyloric sphincter), a 6-cm segment of ileum (i.e., ~ 1 cm proximal to the cecum), and a 3-cm segment of colon (i.e., ~ 0.5 cm distal to the cecum) were isolated and perfused as previously described.

Data Analysis

The effective permeability of 5-ALA was calculated at steady-state (after 30 min perfusion) by using the following formula:(Johnson and Amidon 1988)

$$P_{eff} = -\frac{Q \ln(C_{out} / C_{in})}{2\pi RL} \qquad (1)$$

Where P_{eff} is the effective permeability, C_{out} and C_{in} are the outlet (corrected for water flux) and inlet concentrations of 5-ALA in perfusate, Q is the perfusate flow rate, R is the radius of intestinal segment, and L is the length of intestinal segment.

The steady-state flux (J) through the intestinal membrane was calculated as:

$$J = P_{eff} \times C_{in} \qquad (2)$$

The steady-state flux (J) across the intestinal membrane was then used to determine the kinetic parameters (V_{max}' and K_m') when referenced to inlet drug concentrations (C_{in}) as shown in eq. 3.

$$J = \frac{V_{max}' \times C_{in}}{K_m' + C_{in}} \quad (3)$$

V_{max} and K_m were also determined after factoring out the resistance across the unstirred water layer and the steady-state flux (J) was referenced to intestinal wall concentrations (C_w) as shown in eq. 4 (Johnson and Amidon 1988; Sinko and Amidon 1988).

$$J = \frac{V_{max} \times C_w}{K_m + C_w} \quad (4)$$

The relationship between intestinal wall and inlet drug concentrations is shown in eq. 5, where P_{aq} is the unstirred aqueous layer permeability.

$$C_w = C_{in} \times (1 - P_{eff} / P_{aq}) \quad (5)$$

The P_{aq} was calculated by:

$$P_{aq} = \left(\frac{ARGz^{1/3}}{D}\right)^{-1} \quad (6)$$

$$G_z = \frac{\pi DL}{2Q} \quad (7)$$

Where D is the aqueous diffusion coefficient ($6.596*10^{-4}$ cm^2/min), calculated according to the Hayduk-Laudie expression, Gz is the Graetz number (0.0829), and A is a unitless constant (1.332) estimated by A = 2.5Gz + 1.125.

Statistical Analysis

Data were reported as mean ± S.E. Unpaired two-tailed student's t tests were used to compare statistical differences between two groups. One-way ANOVA followed by Dunnett's or Tukey's post hoc test were performed to compare statistical differences between multiple groups (Prism version 5.0; GraphPad Software Inc., La Jolla, CA). The quality of the fitting of nonlinear regression was assessed by the coefficient of determination (r^2), by the variation of the parameter estimates, and by visual inspection of the residuals. For all the statistical significance tests, a p-value ≤ 0.05 was considered significant.

RESULTS

Stability of 5-ALA in Intestinal Segments

Stability of 5-ALA was assessed during the in situ single-pass intestinal perfusion studies. As shown in Fig. 3.1, there is no metabolism or degradation of 5-ALA in pre- and post-perfusion buffer (pH 6.5) for the small and large intestinal segments. Although 5-ALA is known to convert into its metabolite PpIX rapidly in the mitochondria under intracellular condition, our findings indicates 5-ALA is quite stable in the lumen of gastrointestinal tract during the perfusion procedure. This phenomenon is consistent and the same in the PepT1 knockout mice as well as wildtype mice (Fig. 3.2). These results suggest the 5-ALA effective permeability can be determined directly by loss of 5-ALA in perfusate and without concern on its stability during the following perfusion studies.

Concentration-Dependent Perfusion Studies

To evaluate whether the jejunal uptake kinetics of 5-ALA was saturable, *in situ* perfusion experiments were conducted over a wide range of 5-ALA concentrations in perfusate (0.01 – 50 mM) of wildtype mice. As depicted in Figure 3.3, the jejunal uptake of 5-ALA exhibited a saturable profile that was best described by Michaelis-Menten kinetics, where transport parameters were estimated as $V_{max}' = 2.30 \pm 0.16$ nmol/cm^2/sec and $K_m' = 13.4 \pm 2.44$ mM when referenced to inlet perfusate concentrations ($R^2 = 0.937$). When referenced to intestinal wall concentrations (Fig. 3.4), the intrinsic absorption parameters were

estimated as V_{max} = 1.89 ± 0.12 nmol/cm^2/sec and K_m = 3.74 ± 0.95 mM (R^2 = 0.857).

Substrate Specificity Studies

To probe the specificity of the PepT1-mediated jejunal transport of 5-ALA, the effective permeability of 10 μM 5-ALA was evaluated by co-perfusion with a variety of potential inhibitors (25 mM). As shown in Figure 3.5, 5-ALA jejunal permeability was substantially reduced in the presence of the typical PepT1 substrates GlySar (residual of 31%) or cefadroxil (residual of 16%). In contrast, the 5-ALA jejunal permeability was not altered when co-perfused with L-histidine (i.e., an amino acid substrate of PhT1/2), L-proline (i.e., an amino acid substrate of PAT1), β-alanine (i.e., an amino acid substrate of PAT1), TEA (an organic cation substrate of OCTs) or PAH (an organic anion substrate of OATs). These results demonstrated that the jejunal permeability of 5-ALA was primarily mediated by PEPT1. The contribution of other transporters, including PAT1, in mediating the intestinal permeability of 5-ALA is unlikely and minor at best.

Segment-Dependent Perfusion Studies

To investigate whether the 5-ALA permeability would be affected by the differential expression of PepT1 along the small and large intestines, the effective permeability of 10 μM 5-ALA was measured in four intestinal segments and the results compared between genotypes. As demonstrated in Figure 3.6, the mean effective permeability (P_{eff}) of 5-ALA in wildtype mice was determined as 1.65×10^{-4} cm/s in duodenum, 1.91×10^{-4} cm/s in jejunum, 1.20×10^{-4} cm/s in ileum

and 0.14×10^{-4} cm/s in colon. The P_{eff} of 5-ALA in the duodenum, jejunum, and ileum of PepT1 knockout mice was approximately 10% of that in wildtype animals. Colonic P_{eff} values were very small and not different between the two genotypes. Moreover, no statistical differences in the P_{eff} of 5-ALA were observed between any of the intestinal segments in PepT1 knockout mice.

DISCUSSION

Numerous studies have focused on investigating the function and relevance of PepT1 in the intestinal uptake of a variety of peptide-like drugs (Daniel and Kottra 2004; Brandsch 2009; Brandsch 2013; Smith, Clemencon et al. 2013). The photodynamic therapy agent 5-ALA has been shown to be a substrate of PepT1 in hPepT1-expressing yeast cells (Doring, Walter et al. 1998; Rodriguez, Batlle et al. 2006), human bile duct tumor cells (Neumann and Brandsch 2003; Chung, Kim et al. 2013), human gastric cancer cells (Hagiya, Endo et al. 2012), hPepT1-expressing Xenopus oocytes (Anderson, Jevons et al. 2010), stably transfected hPepT1-expressing Madin-Darby canine kidney (MDCK) cells (Frolund, Marquez et al. 2010) and hPepT1-expressing Caco-2 cells (Anderson, Jevons et al. 2010; Frolund, Marquez et al. 2010). However, these *in vitro* studies were inherently deficient in probing the precise contribution of PepT1 on 5-ALA intestinal absorption because they lacked an intact blood supply and, thus, a normal physiological environment. The recent development of genetically-modified mice has provided us a unique animal model to tackle this problem and characterize the functional activity of PepT1 under physiological conditions (Hu, Smith et al. 2008).

The present study has revealed several novel findings in determining the predominant role of transporter PepT1 on the intestinal absorption of 5-ALA via *in situ* single-pass perfusions in wildtype and PepT1 knockout mice. In particular, we found that (1) 5-ALA exhibited stability in the lumen of the gastrointestinal tract under perfusion conditions; (2) jejunal uptake of 5-ALA was carrier-

mediated and saturable with an intrinsic K_m value of 3.7 mM; (3) intestinal transport of 5-ALA was dependent on PepT1 while the potential contribution of other transporters (e.g., PAT1) was extremely low; (4) the permeability of 5-ALA in small intestine was approximately 10-fold higher in wildtype as compared to PepT1 knockout mice; (5) colonic permeability of 5-ALA was only about 10% of that observed in small intestine of wildtype animals and showed no difference between two genotypes.

The high capacity and low affinity nature of transporter PepT1, relative to PepT2, has been characterized in many studies (Brandsch, Knutter et al. 2008; Rubio-Aliaga and Daniel 2008; Smith, Clemencon et al. 2013). The apparent Michaelis–Menten affinity constant (K_m) for a typical substrate of PepT1 was usually reported in the mM range (i.e., 0.1-10 mM), depending upon the substrate specificity, species difference and type of experimental system. As shown in the literature, K_m values of 5-ALA were estimated under different experimental systems and reported as 0.4 mM in hPepT1-expressing yeast cells (Doring, Walter et al. 1998), 6.4 mM in transfected hPepT1-expressing MDCK cells (Frolund, Marquez et al. 2010) and 1.6 mM in hPepT1-expressing Xenopus oocytes (Anderson, Jevons et al. 2010). In this study, the transport properties of 5-ALA were evaluated with escalating concentrations (i.e., 0.01-50 mM) in jejunum of wildtype mice. The kinetic profile was best fitted by a Michaelis-Menten equation with an estimated intrinsic K_m value equal to 3.74 mM when referenced to intestinal wall concentrations of 5-ALA. Therefore, the K_m value obtained in our

studies was comparable with literature values reported previously and highly consistent with the low-affinity feature of PepT1-mediated transport.

In wildtype mice, the effective permeability values of 5-ALA in duodenum, jejunum and ileum were $1.65 \pm 0.07\times10^{-4}$ cm/s, $1.91 \pm 0.13\times10^{-4}$ cm/s and $1.20 \pm 0.05\times10^{-4}$ cm/s, respectively, while the colonic P_{eff} value was only $0.14 \pm 0.05\times10^{-4}$ cm/s, a value significantly lower than those observed in the small intestinal segments. These results which reflect PepT1 functional activity, were very similar to the PepT1 protein expression pattern along the small and large intestines as previous reported (i.e., abundant in small intestine but negligible in colon) (Jappar, Wu et al. 2010). In contrast, the residual P_{eff} of 5-ALA in the duodenum, jejunum, and ileum of PepT1 knockout mice was only about 10% of that in wildtype mice and similar to that of colon P_{eff}, indicating that PepT1 was responsible for approximately 90% of 5-ALA uptake in mouse small intestine. This conclusion was consistent with previous results for other PepT1 substrates (e.g., GlySar, valacyclovir, cefadroxil) in the same experimental platform (Jappar, Wu et al. 2010; Posada and Smith 2013; Yang and Smith 2013).

The potential contribution of other transporters in the jejunal uptake of 5-ALA was examined in the wildtype mice through inhibition studies. Specifically, excessive concentrations of known PepT1 substrates or non-substrates (25 mM) were added to the buffer during the *in situ* perfusion studies. Not surprisingly, two typical PepT1 substrates, the di-peptide GlySar and the aminocephalosporin drug cefadroxil, significantly reduced the intestinal permeability of 5-ALA. In contrast, other potential inhibitors including the amino acids L-histidine, L-proline, β-

alanine, the organic base TEA and the organic acid PAH, all failed to exhibit any inhibition activity when perfused concomitantly with 5-ALA. These results supported the dominant and probably exclusive role of PepT1 in the small intestinal uptake of 5-ALA. The residual permeability of 5-ALA in the small and large intestines after PEPT1 gene ablation would also argue against a significant role of other transporters in the uptake of 5-ALA. It is worth noting that this conclusion is contradictory to other studies regarding the role of the amino acid transporter PAT1 in transporting 5-ALA. In this regard, 5-ALA was reported to be a substrate of the transporter PAT1 as tested in Caco-2 cells, hPAT1-expressing COS-7 cells and hPAT1-expressing oocytes (Anderson, Jevons et al. 2010; Frolund, Marquez et al. 2010). Although several amino acid transporters for α-amino acids exist, PAT1 (SLC36A1) is the only proton-coupled amino acid transporter involved in the intestinal uptake of small zwitterionic α-amino acids such as proline, glycine and alanine (Thwaites, McEwan et al. 1995; Chen, Fei et al. 2003). Based on their *in vitro* uptake experiments, these authors argued that 5-ALA showed substrate overlap between PepT1 and PAT1 in mediating 5-ALA uptake at the intestinal brush border membrane. However, our inhibition studies using the α-amino acids L-proline and β-alanine clearly do not support this contention. In addition, the intestinal expression of PAT1 transcripts was substantially lower as compared to PEPT1 in wildtype mice (unpublished data in Smith group). Collectively, our *in situ* findings demonstrated that in mice the contribution of PAT1 is marginal at best in mediating 5-ALA intestinal uptake.

In conclusion, our *in situ* single-pass perfusion results in wildtype and PepT1 knockout mice provided strong evidence in defining the significant role of PepT1 in the intestinal permeability of 5-ALA. Moreover, these findings provided solid mechanistic basis for enhancing 5-ALA oral absorption via a PepT1 targeting strategy.

FIGURES

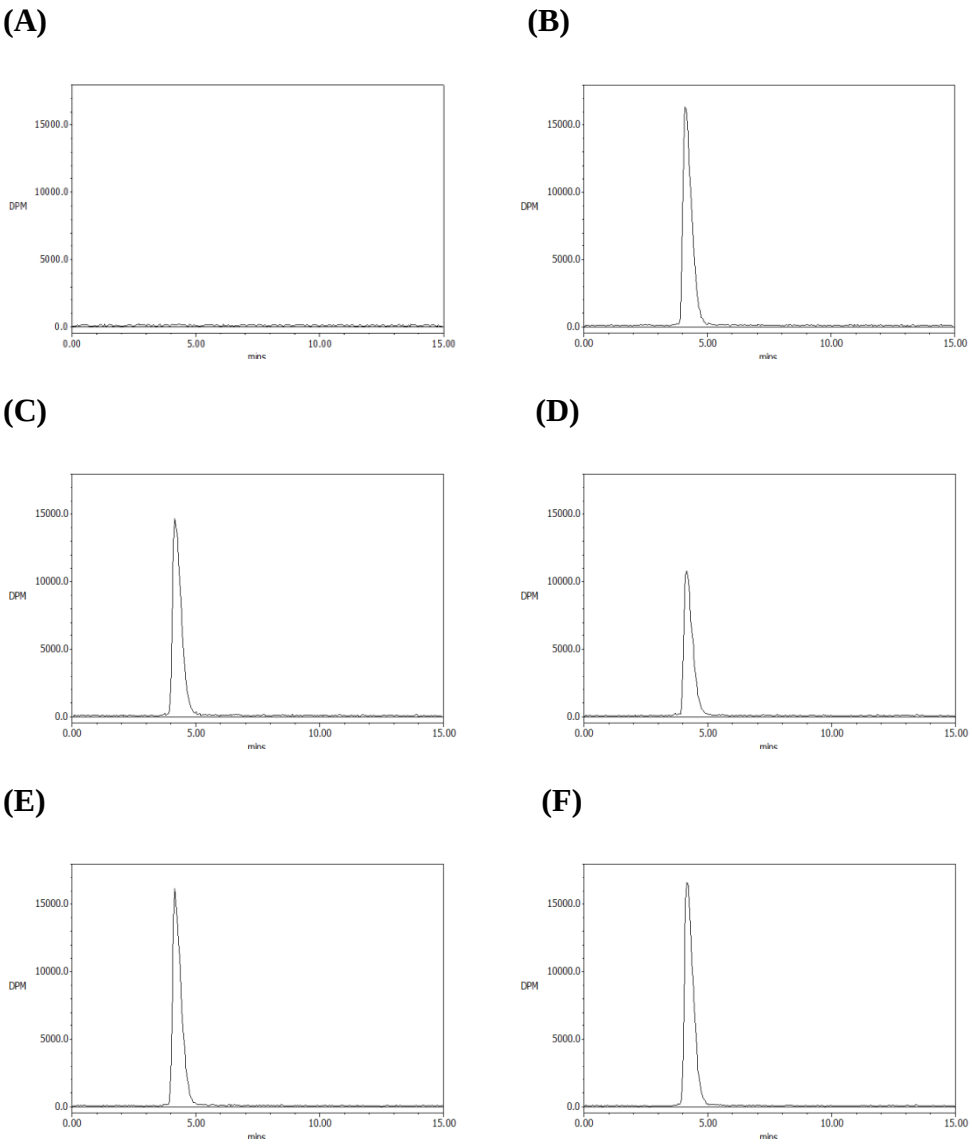

Figure 3.1 HPLC chromatogram of (A) blank perfusion buffer (B) 5-ALA in perfusate before and after perfusion from (C) duodenum (D) jejunum (E) ileum and (F) colon segments in wildtype mouse. The chromatographic peak at 4.1 min represents 5-ALA.

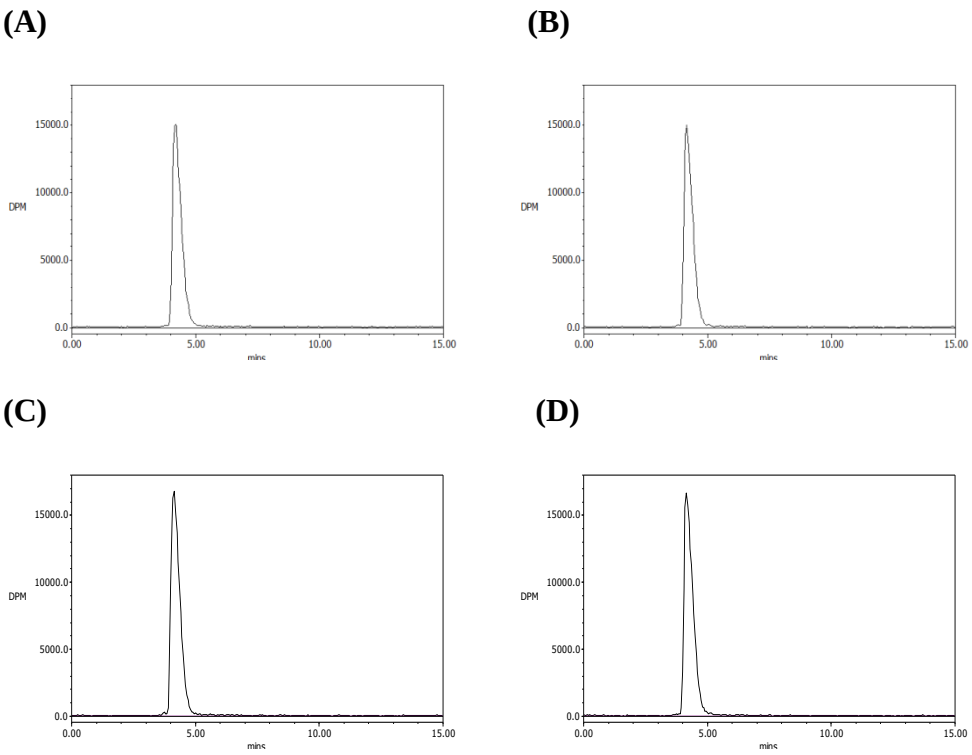

Figure 3.2 HPLC chromatogram of 5-ALA in perfusate after perfusion from (A) duodenum (B) jejunum (C) ileum and (D) colon segments in PepT1 knockout mouse. The chromatographic peak at 4.1 min represents 5-ALA.

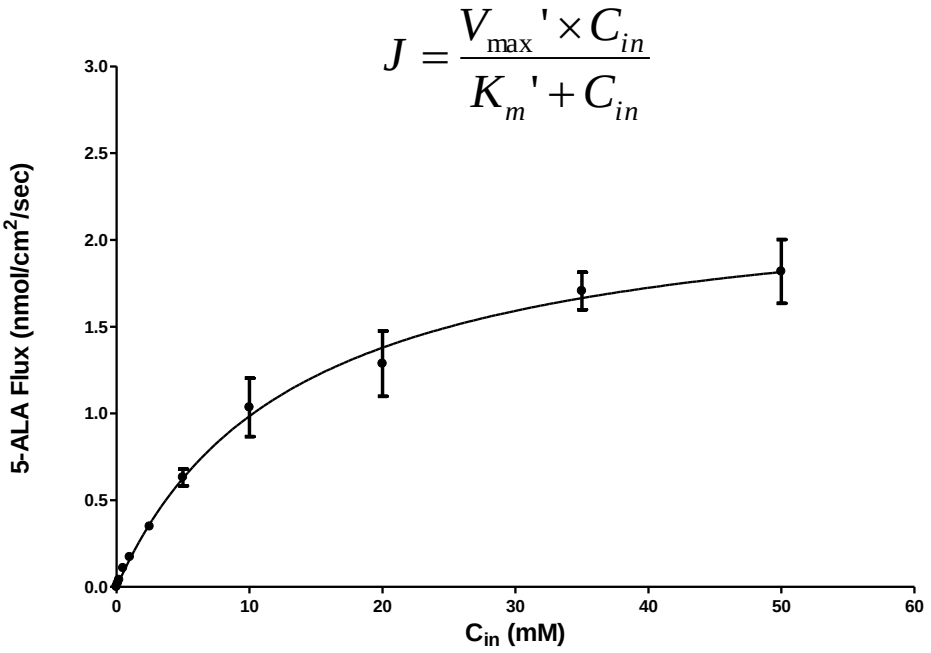

Figure 3.3 Concentration dependency of 5-ALA flux in the jejunum of wildtype mice (mean ± SE, n=4). C_{in} was referenced to the inlet concentration of 5-ALA.

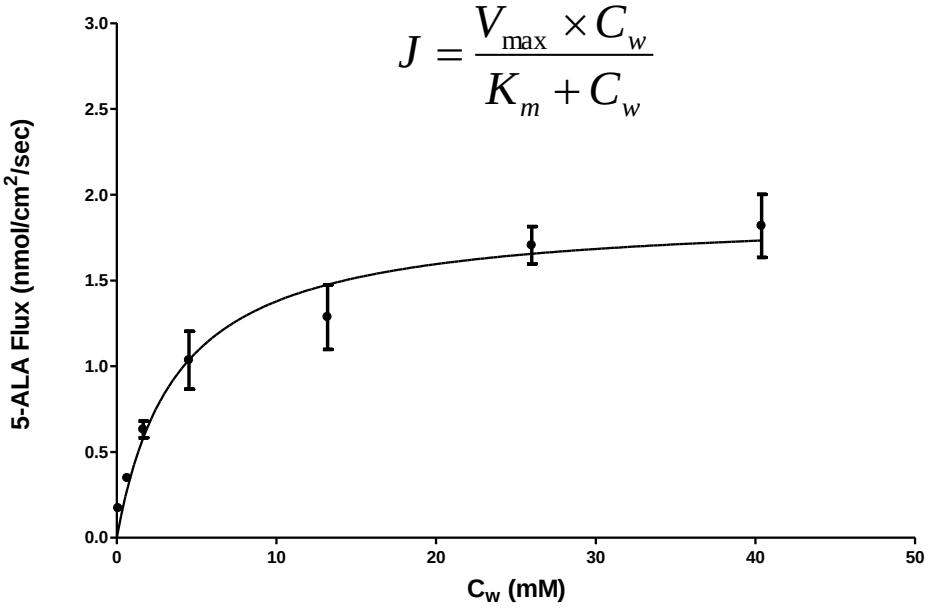

Figure 3.4 Concentration dependency of 5-ALA flux in the jejunum of wildtype mice (mean ± SE, n=4). C_w was referenced to the estimated intestinal wall concentration of 5-ALA.

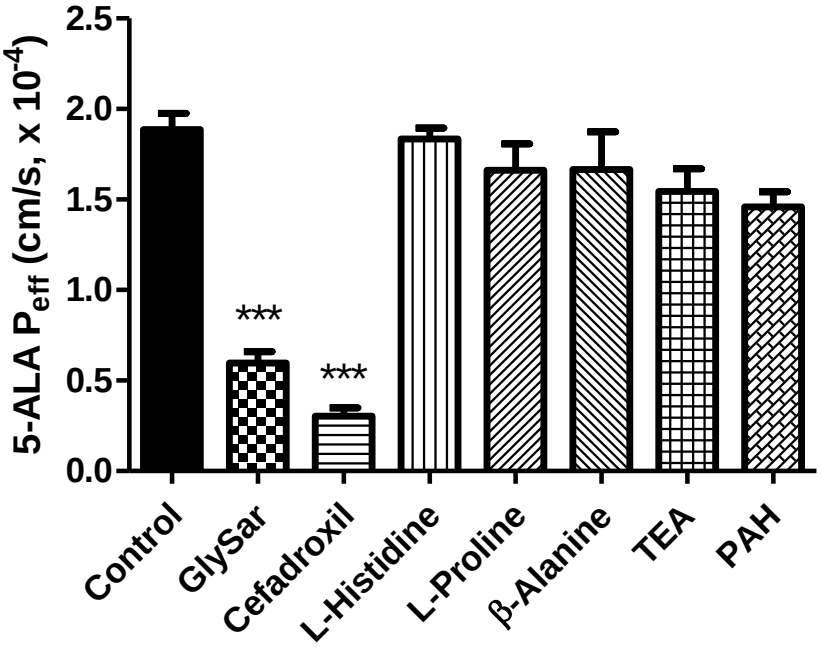

Figure 3.5 Effect of potential inhibitors (25 mM) on the effective permeability of 10 μM 5-ALA during jejunal perfusion in wildtype mice. Data are presented as mean ± SE (n=4). Statistical analyses were performed by one-way ANOVA and Dunnett's test. ***$p < 0.001$ as compared to control.

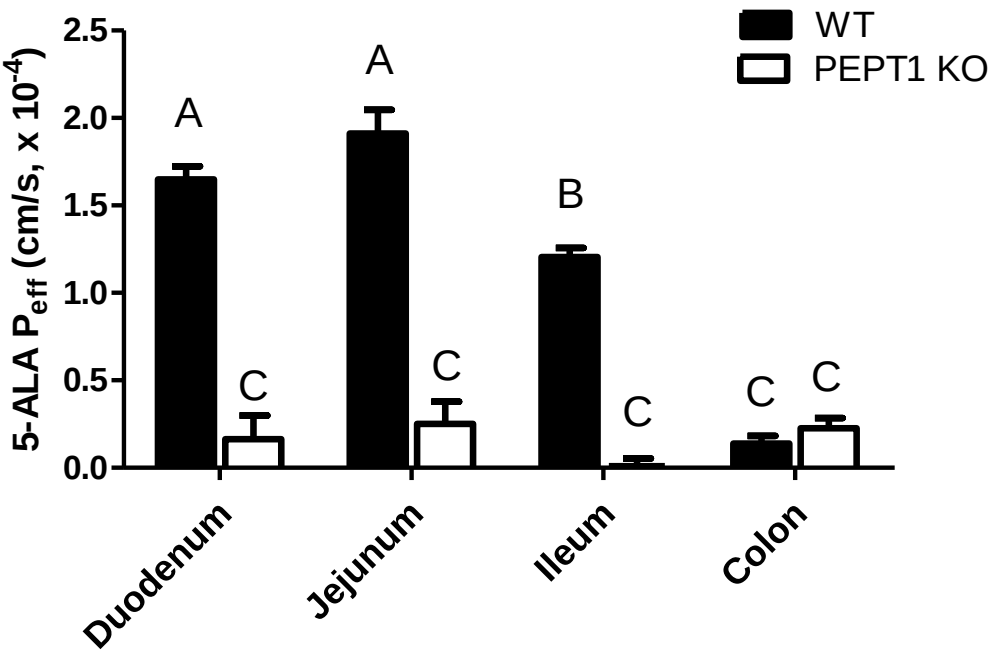

Figure 3.6 Effective permeability of 10 μM 5-ALA in the duodenum, jejunum, ileum, and colon of wildtype and PEPT1 knockout (KO) mice. Data are presented as mean ± SE (n=4). Groups with different letters are statistically different as determined by one-way ANOVA and Tukey's test.

REFERENCES

Adachi, Y., H. Suzuki, et al. (2003). "Quantitative evaluation of the function of small intestinal P-glycoprotein: comparative studies between in situ and in vitro." Pharm Res **20**(8): 1163-1169.

Anderson, C. M., M. Jevons, et al. (2010). "Transport of the photodynamic therapy agent 5-aminolevulinic acid by distinct H+-coupled nutrient carriers coexpressed in the small intestine." J Pharmacol Exp Ther **332**(1): 220-228.

Brandsch, M. (2009). "Transport of drugs by proton-coupled peptide transporters: pearls and pitfalls." Expert Opin Drug Metab Toxicol **5**(8): 887-905.

Brandsch, M. (2013). "Drug transport via the intestinal peptide transporter PepT1." Curr Opin Pharmacol **13**(6): 881-887.

Brandsch, M., I. Knutter, et al. (2008). "Pharmaceutical and pharmacological importance of peptide transporters." J Pharm Pharmacol **60**(5): 543-585.

Chen, Z., Y. J. Fei, et al. (2003). "Structure, function and immunolocalization of a proton-coupled amino acid transporter (hPAT1) in the human intestinal cell line Caco-2." J Physiol **546**(Pt 2): 349-361.

Chung, C. W., C. H. Kim, et al. (2013). "Aminolevulinic acid derivatives-based photodynamic therapy in human intra- and extrahepatic cholangiocarcinoma cells." Eur J Pharm Biopharm **85**(3 Pt A): 503-510.

Colditz, M. J. and R. L. Jeffree (2012). "Aminolevulinic acid (ALA)-protoporphyrin IX fluorescence guided tumour resection. Part 1: Clinical, radiological and pathological studies." J Clin Neurosci **19**(11): 1471-1474.

Colditz, M. J., K. Leyen, et al. (2012). "Aminolevulinic acid (ALA)-protoporphyrin IX fluorescence guided tumour resection. Part 2: theoretical, biochemical and practical aspects." J Clin Neurosci **19**(12): 1611-1616.

Dalton, J. T., M. C. Meyer, et al. (1999). "Pharmacokinetics of aminolevulinic acid after oral and intravenous administration in dogs." Drug Metab Dispos **27**(4): 432-435.

Dalton, J. T., C. R. Yates, et al. (2002). "Clinical pharmacokinetics of 5-aminolevulinic acid in healthy volunteers and patients at high risk for recurrent bladder cancer." J Pharmacol Exp Ther **301**(2): 507-512.

Daniel, H. and G. Kottra (2004). "The proton oligopeptide cotransporter family SLC15 in physiology and pharmacology." Pflugers Arch **447**(5): 610-618.

Dolmans, D. E., D. Fukumura, et al. (2003). "Photodynamic therapy for cancer." Nat Rev Cancer **3**(5): 380-387.

Doring, F., J. Walter, et al. (1998). "Delta-aminolevulinic acid transport by intestinal and renal peptide transporters and its physiological and clinical implications." J Clin Invest **101**(12): 2761-2767.

Fei, Y. J., Y. Kanai, et al. (1994). "Expression cloning of a mammalian proton-coupled oligopeptide transporter." Nature **368**(6471): 563-566.

Frolund, S., O. C. Marquez, et al. (2010). "Delta-aminolevulinic acid is a substrate for the amino acid transporter SLC36A1 (hPAT1)." Br J Pharmacol **159**(6): 1339-1353.

Hagiya, Y., Y. Endo, et al. (2012). "Pivotal roles of peptide transporter PEPT1 and ATP-binding cassette (ABC) transporter ABCG2 in 5-aminolevulinic acid (ALA)-based photocytotoxicity of gastric cancer cells in vitro." Photodiagnosis Photodyn Ther **9**(3): 204-214.

Hu, Y., D. E. Smith, et al. (2008). "Targeted disruption of peptide transporter Pept1 gene in mice significantly reduces dipeptide absorption in intestine." Mol Pharm **5**(6): 1122-1130.

Jappar, D., S. P. Wu, et al. (2010). "Significance and regional dependency of peptide transporter (PEPT) 1 in the intestinal permeability of glycylsarcosine: in situ single-pass perfusion studies in wild-type and Pept1 knockout mice." Drug Metab Dispos **38**(10): 1740-1746.

Johnson, D. A. and G. L. Amidon (1988). "Determination of intrinsic membrane transport parameters from perfused intestine experiments: a boundary layer approach to estimating the aqueous and unbiased membrane permeabilities." J Theor Biol **131**(1): 93-106.

Kelty, C. J., N. J. Brown, et al. (2002). "The use of 5-aminolaevulinic acid as a photosensitiser in photodynamic therapy and photodiagnosis." Photochem Photobiol Sci **1**(3): 158-168.

Krammer, B. and K. Plaetzer (2008). "ALA and its clinical impact, from bench to bedside." Photochem Photobiol Sci **7**(3): 283-289.

Loh, C. S., A. J. MacRobert, et al. (1993). "Oral versus intravenous administration of 5-aminolaevulinic acid for photodynamic therapy." Br J Cancer **68**(1): 41-51.

Navone, N. M., C. F. Polo, et al. (1990). "Heme biosynthesis in human breast cancer--mimetic "in vitro" studies and some heme enzymic activity levels." International Journal of Biochemistry **22**(12): 1407-1411.

Neumann, J. and M. Brandsch (2003). "Delta-aminolevulinic acid transport in cancer cells of the human extrahepatic biliary duct." J Pharmacol Exp Ther **305**(1): 219-224.

Nokes, B., M. Apel, et al. (2013). "Aminolevulinic acid (ALA): photodynamic detection and potential therapeutic applications." J Surg Res **181**(2): 262-271.

Peng, Q., K. Berg, et al. (1997). "5-Aminolevulinic acid-based photodynamic therapy: principles and experimental research." Photochem Photobiol **65**(2): 235-251.

Peng, Q., T. Warloe, et al. (1997). "5-aminolevulinic acid-based photodynamic therapy - Clinical research and future challenges." Cancer **79**(12): 2282-2308.

Posada, M. M. and D. E. Smith (2013). "Relevance of PepT1 in the intestinal permeability and oral absorption of cefadroxil." Pharm Res **30**(4): 1017-1025.

Regula, J., A. J. MacRobert, et al. (1995). "Photosensitisation and photodynamic therapy of oesophageal, duodenal, and colorectal tumours using 5 aminolaevulinic acid induced protoporphyrin IX--a pilot study." Gut **36**(1): 67-75.

Rodriguez, L., A. Batlle, et al. (2006). "Study of the mechanisms of uptake of 5-aminolevulinic acid derivatives by PEPT1 and PEPT2 transporters as a tool to

improve photodynamic therapy of tumours." Int J Biochem Cell Biol **38**(9): 1530-1539.

Rubio-Aliaga, I. and H. Daniel (2008). "Peptide transporters and their roles in physiological processes and drug disposition." Xenobiotica **38**(7-8): 1022-1042.

Sinko, P. J. and G. L. Amidon (1988). "Characterization of the oral absorption of beta-lactam antibiotics. I. Cephalosporins: determination of intrinsic membrane absorption parameters in the rat intestine in situ." Pharm Res **5**(10): 645-650.

Smith, D. E., B. Clemencon, et al. (2013). "Proton-coupled oligopeptide transporter family SLC15: physiological, pharmacological and pathological implications." Mol Aspects Med **34**(2-3): 323-336.

Stout, D. L. and F. F. Becker (1990). "Heme synthesis in normal mouse liver and mouse liver tumors." Cancer Research **50**(8): 2337-2340.

Thwaites, D. T., G. T. McEwan, et al. (1995). "The role of the proton electrochemical gradient in the transepithelial absorption of amino acids by human intestinal Caco-2 cell monolayers." J Membr Biol **145**(3): 245-256.

van den Boogert, J., R. van Hillegersberg, et al. (1998). "5-Aminolaevulinic acid-induced protoporphyrin IX accumulation in tissues: pharmacokinetics after oral or intravenous administration." J Photochem Photobiol B **44**(1): 29-38.

Wachowska, M., A. Muchowicz, et al. (2011). "Aminolevulinic Acid (ALA) as a Prodrug in Photodynamic Therapy of Cancer." Molecules **16**(5): 4140-4164.

Wu, S. P. and D. E. Smith (2013). "Impact of intestinal PepT1 on the kinetics and dynamics of N-formyl-methionyl-leucyl-phenylalanine, a bacterially-produced chemotactic peptide." Mol Pharm **10**(2): 677-684.

Yang, B. and D. E. Smith (2013). "Significance of peptide transporter 1 in the intestinal permeability of valacyclovir in wild-type and PepT1 knockout mice." Drug Metab Dispos **41**(3): 608-614.

CHAPTER 4

ROLE OF PEPT1 ON THE IN VIVO PHARMACOKINETICS OF 5-AMINOLEVULINIC ACID IN WILD-TYPE AND PEPT1 KNOCKOUT MICE

ABSTRACT

PURPOSE: The aim of this study was to determine the contribution of oligopeptide transporter PepT1 in the absorption and disposition of the photodynamic therapy agent 5-aminolevulinic acid (5-ALA) via *in vivo* pharmacokinetic studies in wildtype and PepT1 knockout mice.

METHODS: Radiolabeled [^{14}C] 5-ALA was given to wildtype and PepT1 knockout mice via oral gavage (0.2 and 2 μmol/g body weight) or tail vein injection (0.01 μmol/g body weight). Serial blood samples were collected over 180 min and plasma concentrations of 5-ALA were measured using a dual-channel liquid scintillation counter. Tissue distribution studies were also performed in wildtype and PepT1 knockout mice after oral administration of 0.2 μmol/g 5-ALA. The pharmacokinetic data was analyzed by a non-compartmental approach using Phoenix WinNonlin (version 1.3, Certara, St. Louis, MO).

RESULTS: Following oral administration of 5-ALA for both oral doses, the C_{max} and $AUC_{0\text{-}180}$ of 5-ALA were substantially decreased approximately 2-fold in

PepT1 knockout mice, as compared to wildtype mice. However, the C_{max} and $AUC_{0\text{-}180}$ values were dose proportional for the two genotypes. After intravenous dosing, the pharmacokinetic profiles of 5-ALA were virtually superimposable between wildtype and PepT1 knockout mice. Also, tissue samples after oral dosing were measured and showed minor significant differences between the two genotypes.

CONCLUSION: These findings demonstrate that PepT1 plays an important role in facilitating the intestinal absorption of 5-ALA. Moreover, 5-ALA oral kinetics exhibits an "apparent linearity" over the dose range studied. The tissue distribution study results combined with the intravenous pharmacokinetic study of 5-ALA suggest that PepT1 deficiency does not affect the *in vivo* disposition of this substrate.

INTRODUCTION

Proton coupled oligopeptide transporters (POTs) are an integral plasma membrane protein family that transport a broad spectrum of di-/tri-peptides and a variety of peptidomimetic substrates across biological membranes. To date, four mammalian members in the POT superfamily, PepT1 (SLC15A1), PepT2 (SLC15A2), PhT1 (SLC15A4), and PhT2 (SLC15A3), have been identified and characterized functionally, each with diverse yet some overlapping substrate specificities, capacities and affinities (Fei, Kanai et al. 1994; Brandsch 2009; Brandsch 2013; Smith, Clemencon et al. 2013). All of these membrane proteins transport di- and tri-peptides in the body that are driven by an inwardly directed proton gradient and negative membrane potential. Whereas PepT1 and PepT2 can transport di-/tri-peptides, PhT1 and PhT2 can also transport the amino acid L-histidine. PepT1 is the most widely studied and best characterized transporter among the POT family due to its physiological and pharmacological importance (Daniel and Kottra 2004; Rubio-Aliaga and Daniel 2008; Brandsch 2013; Smith, Clemencon et al. 2013). Compared to PepT2, PepT1 is considered a high-capacity low-affinity influx transporter with primary expression on the brush border membrane of epithelial cells in the small intestine. PepT1 is believed to play an essential physiological role in protein assimilation since approximately 80% of digested proteins are absorbed in the form of di-/tri-peptides that can enter the epithelial cells via PepT1-mediated active transport (Daniel 2004). Besides di/tripeptides, PepT1 can transport and influence the pharmacokinetics of a variety of therapeutic drugs with different structural and chemical characteristics,

including some β-lactam antibiotics (e.g., cefadroxil), angiotensin converting enzyme inhibitors (e.g., enalapril) and antiviral prodrugs (e.g., valacyclovir). Many studies have focused on understanding the mechanism and relative contribution of PepT1 towards the absorption and disposition of these drugs.

5-Aminolevulinic acid (5-ALA), a naturally occurring intermediate in the heme biosynthesis pathway, has been widely used in photodynamic therapy and fluorescence detection for the last twenty years (Peng, Berg et al. 1997; Peng, Warloe et al. 1997; Kelty, Brown et al. 2002; Krammer and Plaetzer 2008). Currently, 5-ALA and its esters have been approved by the FDA as a promising treatment of several malignant and premalignant conditions such as actinic keratosis, basal cell carcinoma, Bowen's disease, bladder cancer and others. In Europe, 5-ALA has been approved for intraoperative photodynamic diagnosis of residual malignant glioma while the methyl-ester and hexyl-ester derivatives of 5-ALA have been approved for the treatment of basal cell carcinoma and actinic keratosis, and the diagnostic application of bladder cancer, respectively (Dolmans, Fukumura et al. 2003; Fotinos, Campo et al. 2006; Krammer and Plaetzer 2008; Nokes, Apel et al. 2013).

Oral dosing is an administration route that is commonly used in the clinical application of 5-ALA. In practice, a high accumulation after of 5-ALA has been reported in normal enterocytes after oral administration (Loh, MacRobert et al. 1993; Regula, MacRobert et al. 1995). In addition, good oral bioavailability of 5-ALA was observed in several experimental and clinical studies (van den Boogert, van Hillegersberg et al. 1998; Dalton, Meyer et al. 1999;

Dalton, Yates et al. 2002) despite the fact that 5-ALA is a hydrophilic and polar molecule. Previous studies suggested that PepT1 may play an important role in facilitating 5-ALA intestinal absorption and its good oral bioavailability (Doring, Walter et al. 1998; Anderson, Jevons et al. 2010; Frolund, Marquez et al. 2010). Moreover, based on *in vitro* uptake experiments performed in Caco-2 cells, hPAT1-expressing COS-7 cells and hPAT1-expressing oocytes (Anderson, Jevons et al. 2010; Frolund, Marquez et al. 2010), 5-ALA was also indicated to be a substrate of the amino acid transporter PAT1. It was speculated that both PepT1 and PAT1 are involved in mediating 5-ALA uptake at the intestinal brush border membrane *in vivo*.

Collectively, the transport mechanism of 5-ALA from the gastrointestinal tract lumen into the systemic circulation system is still poorly understood and the relative contribution of intestinal transporter PepT1 in the *in vivo* oral absorption of 5-ALA is unclear. To better understand the process of 5-ALA intestinal absorption and determine the contribution of transporter PepT1 quantitatively in this process, comparative pharmacokinetic and tissue distribution studies of 5-ALA were performed in wildtype and PepT1 knockout mice.

MATERIALS AND METHODS

Animals

All experiments performed on mice were carried out in accordance with the Guide for the Care and Use of Laboratory Animals as adopted by the U.S. National Institutes of Health. Gender-matched wildtype and PepT1 knockout mice (>99% C57BL/6 genetic background, 8-10 week old) were used in all experiments (Hu, Smith et al. 2008). The mice were kept under a 12-hour light/dark cycle and in an ambient temperature-controlled environment, fed with standard diet and water ad libitum (Unit for Laboratory Animal Medicine, University of Michigan, Ann Arbor, MI).

Materials

[^{14}C]5-ALA (55 mCi/mmol) and [^{3}H]dextran (MW 70000, 100 mCi/g) were purchased from American Radiolabeled Chemicals (St. Louis, MO). Hyamine hydroxide was obtained from ICN Pharmaceuticals (Costa Mesa, CA). Unlabeled 5-ALA hydrochloride and other reagents were obtained from Sigma-Aldrich (St. Louis, MO).

Pharmacokinetic study of 5-ALA after oral administration

An oral pharmacokinetic (PK) study was performed on wildtype and PepT1 knockout mice according to the procedure described below. Briefly,

gender-matched wildtype and PepT1 knockout mice were fasted overnight prior to each experiment. Radiolabeled [^{14}C]5-ALA and cold 5-ALA were dissolved in normal saline (0.04 μCi/μL) to prepare the drug solution. 5-ALA drug solution (10 μL/g, 0.4 μCi per mouse) was administered orally by gavage (20-gauge needle) at single doses of 0.2 or 2 μmol/g body weight. Serial blood samples were collected (~20 μl) via tail nicks in 0.2 ml microcentrifuge tubes containing 7.5% potassium EDTA at 5, 10, 20, 30, 45, 60, 90, 120, 150 and 180 min after the initial oral dose. Plasma was obtained after centrifuging at 3000 g for 3 min and a 10-μL aliquot was transferred to a glass scintillation vial. CytoScint (MP Biomedicals, Solon, OH) scintillation fluid (6 ml) was added to each sample and radioactivity of the plasma sample was measured by a dual-channel liquid scintillation counter (Beckman LS 6000 SC; Beckman Coulter Inc., Fullerton, CA, USA). At 45 min after oral dosing, mice were given intraperitoneal injections of 0.3 ml warm saline to prevent dehydration.

Tissue distribution of 5-ALA after oral administration

Tissue distribution studies were performed in wildtype and PepT1 knockout mice after the 0.2 μmol/g oral administration of [^{14}C]5-ALA. Tissue samples were collected at the last time point (i.e., 180 min) of the oral PK study. To determine the tissue vascular space, 100 μL of [^{3}H]dextran 70,000 (0.2 μCi/mouse) was administered via a tail vein injection 5 minutes before harvesting the tissues. Several tissues including the eye, spleen, duodenum, jejunum, ileum,

colon, stomach, kidney, liver, lung, heart and skeletal muscle were harvested, blotted dry, weighed, and then solubilized in 0.33 ml of 1 M hyamine hydroxide overnight at 37°C. Whole blood samples (10 μL) were also collected at the same time. After incubation with hyamine hydroxide, a 40 μl aliquot of hydrogen peroxide (30% w/w) was added to each sample for decolorization. A 6 mL aliquot of CytoScint scintillation fluid (MP Biomedicals, Solon, OH) was then added to the tissue samples, and radioactivity of the samples was measured by a dual-channel liquid scintillation counter.

The corrected tissue concentrations of 5-ALA were calculated via the following equation (Ocheltree, Shen et al. 2005; Shen, Ocheltree et al. 2007):

$$C_{tiss.corr} = C_{tiss} - V \times C_b$$

where $C_{tiss.corr}$ and C_{tiss} are the corrected and uncorrected tissue concentration of 5-ALA (nmol/g), V is the blood vascular space as determined by dextran in the tissue (ml/g), and C_b is the 5-ALA blood concentration (nmol/mL).

Pharmacokinetics of 5-ALA after intravenous administration

An intravenous PK study was performed on wildtype and PepT1 knockout mice as described previously (Yang, Hu et al. 2013) and below. Briefly, radiolabeled [^{14}C]5-ALA and cold 5-ALA were dissolved in normal saline (0.025 μCi/μL, 2 nmol/μL) to prepare the drug solution. Following sodium pentobarbital anesthesia (~40-60 mg/kg i.p.), wildtype and PepT1 knockout mice received

[^{14}C]5-ALA (10 nmol/g body weight) through a tail vein injection. Serial blood samples were collected (~20 μL/sample) via tail nicks in 0.2 mL microcentrifuge tubes containing 7.5% potassium EDTA at 0.25, 1, 2, 5, 10, 15, 20, 30, 45, and 60 min after the intravenous bolus dose. For each sample, a 10 uL aliquot of plasma was obtained after centrifugation at 3000 g for 3 min and then transferred to a glass scintillation vial. A 6 mL aliquot of scintillation fluid (CytoScint®, MP Biomedicals, Solon, OH) was added to each sample and radioactivity was measured by a dual-channel liquid scintillation counter (Beckman LS 6000 SC; Beckman Coulter Inc., Fullerton, CA, USA).

Data analysis

The pharmacokinetics of 5-ALA plasma concentration versus time profiles, after oral and intravenous administration, was performed by non-compartmental and compartmental approaches (Phoenix WinNonlin version 1.3; Certara, St. Louis, MO). For compartmental analysis, 5-ALA plasma concentration-time profiles were best fitted to a two-compartment disposition model with or without first-order absorption. Model selection was based on visual inspection of the individual fits and diagnostic plots, the Akaike Information Criterion (AIC) and coefficient of determination (r^2).

Two-compartment models for disposition after oral and intravenous dosing are shown below as:

$$C(t) = A \cdot e^{-\alpha t} + B \cdot e^{-\beta t} + C \cdot e^{-K_a t} \qquad \text{(oral)}$$

$$C(t) = A \cdot e^{-\alpha t} + B \cdot e^{-\beta t}$$ (intravenous)

Data are reported as mean ± standard error (S.E.). An unpaired two-tail Student's t test was used to compare statistical differences between the two genotypes of mice (Prism version 5.0; GraphPad Software Inc., La Jolla, CA). P-values < 0.05 were considered statistically significant.

RESULTS

Pharmacokinetic studies following oral 5-ALA

The average plasma concentration-time curves following 5-ALA oral administration of 0.2 μmol/g and 2 μmol/g doses in both wildtype and PepT1 knockout mice were depicted in Figure 4.1 and Figure 4.2, respectively. As shown in both linear and logarithmic scales, the systemic exposure of 5-ALA at both oral doses was significantly different wildtype and knockout mice. Generally, in wildtype mice, the 5-ALA plasma concentrations increased rapidly and reached maximum values (C_{max}) at around 10 minutes. The plasma concentrations then decreased quickly until around 60 minutes, followed by a slower terminal phase. In PepT1 knockout mice, the maximum plasma concentrations (C_{max}) of 5-ALA were substantially lower than wildtype mice. However, no significant differences in the time to reach maximum concentration (T_{max}) were observed between the two genotypes.

Pharmacokinetic parameters were determined for the 0.2 and 2 μmol/g oral doses by non-compartmental analysis (Phoenix WinNonlin) and summarized in Table 4.1 and 4.3, respectively. The systemic exposure $AUC_{0\text{-}180}$ values were reduced by approximately 55% in PepT1 knockout mice compared with wildtype animals ($p<0.01$), suggesting reduced extent of 5-ALA oral absorption and systemic exposure due to PEPT1 ablation. The T_{max} values, an indicator of oral absorption rate, were not statistically different between wildtype and PepT1 knockout mice.

Dose-proportionality of 5-ALA C_{max} and AUC_{0-180} following oral 5-ALA in both genotypes was evaluated over the two oral doses of 0.2 and 2 μmol/g. The dose-normalized values of C_{max} and AUC_{0-180} were close and showed no statistical difference, indicating an "apparent linearity" over the dose range in both genotypes.

5-ALA tissue distribution after oral administration

Given the broad expression profiles of 5-ALA across different tissues, investigating the role of PepT1 on the *in vivo* distribution of 5-ALA was of interest. Tissue distribution studies were performed 180 minutes after oral administration of 0.2 μmol/g 5-ALA. As shown in Figure 4.3, there were no statistically significant differences of 5-ALA tissue concentrations in almost all the tissues sampled between the two genotypes. However, for heart and ileum, significantly higher tissue concentrations of 5-ALA were found in wildtype mice than that in PepT1 knockout mice. No significant differences of 5-ALA concentrations were observed in other non-gastrointestinal (GI) tissues and GI segments including stomach, duodenum, jejunum and colon between the two genotypes. In order to rule out the differences in tissue concentrations caused by the differences in systemic exposure, 5-ALA tissue concentrations were normalized by its blood concentration. The results in Figure 4.4 demonstrated a similar pattern as observed in Figure 4.3. Only 5-ALA in wildtype ileum was higher than that in Pept1 knockout mice. These results indicated that PepT1 does not play an important role in affecting the *in vivo* disposition of 5-ALA.

Pharmacokinetic studies following intravenous 5-ALA

In addition to tissue distribution studies after oral dosing, the systemic exposure of 5-ALA was examined in wildtype and PepT1 knockout mice after 0.01 μmol/g intravenous bolus administration. As depicted in the Figure 4.5, mean 5-ALA plasma concentration versus time curves were nearly superimposable between the two genotypes. Pharmacokinetic parameters derived from non-compartmental and compartmental analyses were summarized in Table 4.5 and Table 4.6, without showing any statistical difference between the two genotypes. These results supported the contention that the role of PepT1 on the *in vivo* disposition of 5-ALA in mice was minimal at best.

DISCUSSION

In vitro uptake studies have demonstrated the PepT1-mediated transport of 5-ALA in various cell systems expressing PepT1 (Doring, Walter et al. 1998; Neumann and Brandsch 2003; Anderson, Jevons et al. 2010; Frolund, Marquez et al. 2010; Hagiya, Endo et al. 2012; Chung, Kim et al. 2013; Hagiya, Fukuhara et al. 2013). By performing *in situ* intestinal perfusion studies of 5-ALA in wildtype and PepT1 knockout mice, we have shown that PepT1-mediated active transport is the main route of 5-ALA uptake in mouse small intestine, accounting for approximately 90% of 5-ALA permeability in various small intestinal segments of wildtype mice. In contrast, the potential contribution of other transporters (e.g., PAT1) in the intestinal absorption of 5-ALA was extremely low. These findings from intestinal permeability assessments of 5-ALA provided the first quantitative measure for the relative importance of PepT1 in intestinal absorption of 5-ALA. The current pharmacokinetic and tissue distribution studies, aimed at examining the *in vivo* contribution of PepT1 on 5-ALA pharmacokinetics at clinically relevant doses, were performed in wildtype and PepT1 knockout mice after oral and intravenous dosing.

New findings obtained from this study included the following: 1) the systemic exposure of 5-ALA was reduced by 55% after oral administration of drug in PepT1 knockout versus wildtype mice; 2) PepT1 deletion reduced the C_{max} of 5-ALA to ~46-63% of that in wildtype mice; 3) there was an "apparent dose linearity" in the C_{max} and $AUC_{0\text{-}180}$ of 5-ALA for both genotypes over the two oral doses 0.2 and 2 μmol/g; 4) the systemic disposition of 5-ALA was

unchanged in both genotypes after intravenous administration; and 5) PepT1 had, at best, a minor effect on the peripheral tissue distribution of 5-ALA after oral dosing.

After oral administration of 5-ALA, significant differences were observed in 5-ALA plasma concentration versus time profiles between two genotypes. As shown in Figure 4.1 and 4.2, for each dose, 5-ALA plasma levels in wildtype were always significantly higher than that in PepT1 knockout mice at the same time point after oral dosing, indicating a different absorption profile between two genotypes. The non-compartmental analysis for oral pharmacokinetic study revealed PepT1 deficiency leads to 2-fold differences in AUC and C_{max}, corroborating the quantitative importance of PepT1 in the intestinal absorption of 5-ALA. These results confirmed our previous *in situ* perfusion findings that PepT1 plays a pivotal role in the intestinal uptake of 5-ALA, accounting for 90% of its intestinal permeability. However, the magnitude of the contribution of PepT1 was found to be less pronounced *in vivo* than *in situ*, with only 2-fold as opposed to 10-fold differences between the two genotypes. A similar discrepancy was observed for other PepT1 substrates (e.g., GlySar, valacyclovir) in the same experimental platform (Jappar, Hu et al. 2011; Yang, Hu et al. 2013). One possible explanation for the discrepancy is that other passive transport mechanisms (e.g., passive perfusion, paracellular transport) may play a bigger role in the *in vivo* absorption of 5-ALA than previously believed, given that the molecular weight of 5-ALA is only 131. In addition, the *in vivo* transit of 5-ALA from proximal small intestine to distal large intestine may affect the overall extent

of intestinal absorption of 5-ALA, which reduces the gap between *in situ* and *in vivo* results. For example, 5-ALA might undergo more absorption in the distal regions of small intestine and the entire large intestine in PepT1 knockout mice given the long residence times in these regions and the greater residual concentrations of drug and, therefore, driving force for absorption.

Another interesting finding is that the time to reach maximum plasma concentration (T_{max}) is around 10 min after oral dosing with no significant difference between the two genotypes. This result indicates that the *in vivo* intestinal absorption of 5-ALA in mice is a rapid process and a large portion of the 5-ALA dose is absorbed in the upper GI tract. Compared to the T_{max} value of other PEPT1 substrates such as cefadroxil and valacyclovir (i.e., ~20 min in wildtype mice), the T_{max} of 5-ALA is somewhat smaller. Although speculative, the smaller molecular weight, and presumably greater paracellular absorption, might explain the similar T_{max} values in both wildtype and PepT1 knockout mice. To further assess the rate and extent of 5-ALA absorption in wildtype and PepT1 knockout mice, compartmental model analyses were performed (Table 4.2 and 4.4). Consistent with the noncompartmental analyses, no differences were observed between the genotypes in both T_{max} as well as the absorption rate constant (K_a).

Dose proportionality of $AUC_{0\text{-}180}$ and C_{max} of 5-ALA were observed in both genotypes of mice at oral doses of 0.2 and 2 μmol/g. These two oral doses were selected by allometric scaling of clinical doses based on body surface area. The dose-normalized values of C_{max} and $AUC_{0\text{-}180}$ were close and showed no statistical

differences. Although it is possible that changes in bioavailability (F) and systemic clearance (CL), if these changes were of the same magnitude and direction, can result in no change in the dose-normalized value of AUC (AUC/Dose=F/CL), this possibility is highly unlikely since the T_{max} and terminal half-life values were not different between the lower and higher doses for each genotype.

Tissue distribution studies, performed 180 minutes after oral administration of 0.2 μmol/g 5-ALA, showed no statistical differences in the peripheral tissue concentration of 5-ALA except for heart, which was not statistically different when normalized for blood concentrations between the two genotypes (Figure 4.3 and 4.4). These findings, combined with previous tissue distribution studies of PepT1 substrates (e.g., GlySar, cefadroxil, valacyclovir), demonstrated that PepT1 expression in the peripheral tissues had a minor to no effect on the extent of drug distribution in the body (Jappar, Hu et al. 2011; Posada and Smith 2013; Yang, Hu et al. 2013). Our intravenous pharmacokinetic study of 5-ALA supported this conclusion since the drug disposition profiles were virtually identical between genotypes (Figure 4.5). Again, this result was consistent with other pharmacokinetic studies from our laboratory for GlySar, cefadroxil, and valacyclovir in wildtype and PepT1 knockout mice.

In conclusion, results from this study characterize, for the first time, the *in vivo* pharmacokinetics of the photodynamic therapy agent 5-ALA in wildtype and PepT1 knockout mice after two clinically relevant oral doses. In particular, PepT1 ablation significantly reduced the extent of intestinal absorption of 5-ALA in

PepT1 knockout mice while PepT1 only marginally affected, at best, the *in vivo* tissue distribution and disposition of 5-ALA.

FIGURES AND TABLES

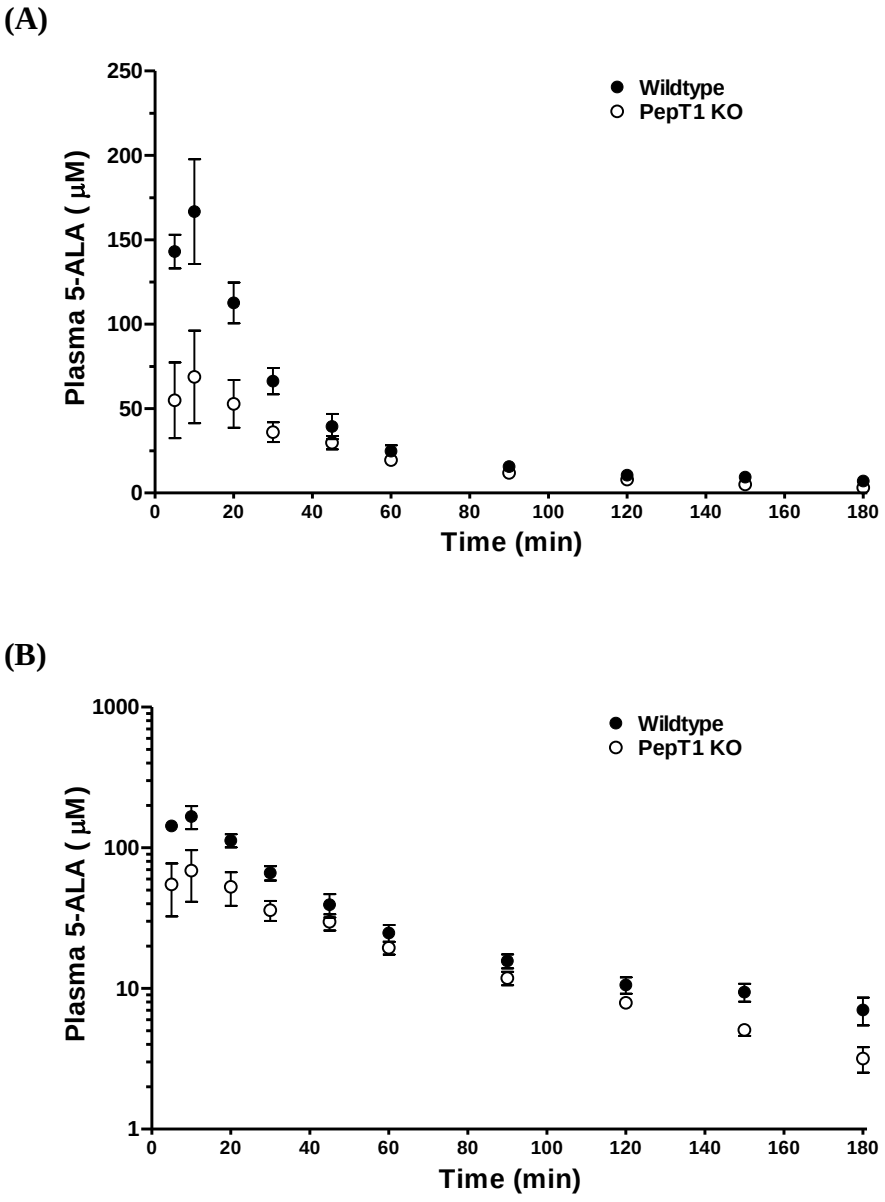

Figure 4.1 Plasma concentration-time curves of 5-ALA in wildtype and PepT1 knockout (KO) mice after oral administration of 0.2 μmol/g [^{14}C]5-ALA. The y-axis is displayed as a linear scale (A) or a logarithmic scale (B). Data are presented as mean ± SE (n=4-5).

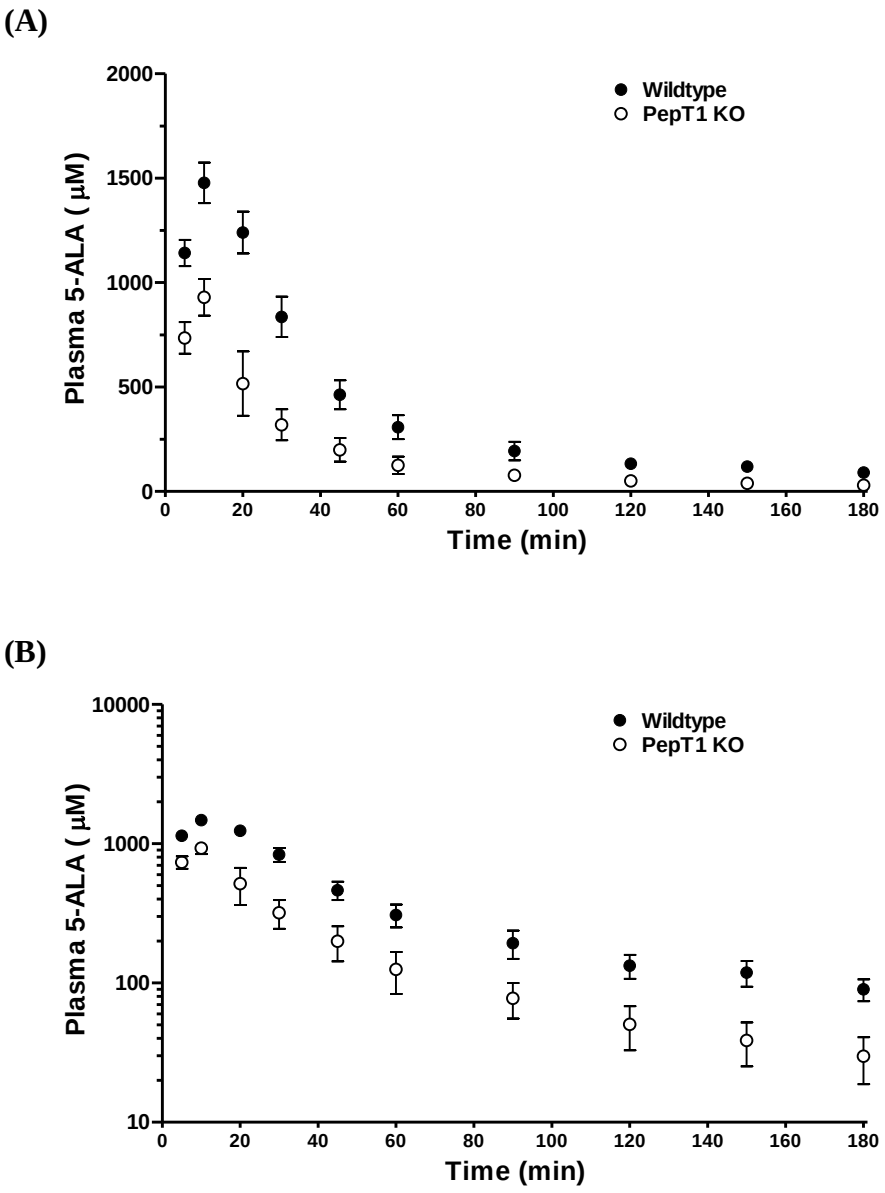

Figure 4.2 Plasma concentration-time curves of 5-ALA in wildtype and PepT1 knockout (KO) mice after oral administration of 2 μmol/g [^{14}C]5-ALA. The y-axis is displayed as a linear scale (A) or a logarithmic scale (B). Data are presented as mean ± SE (n=4).

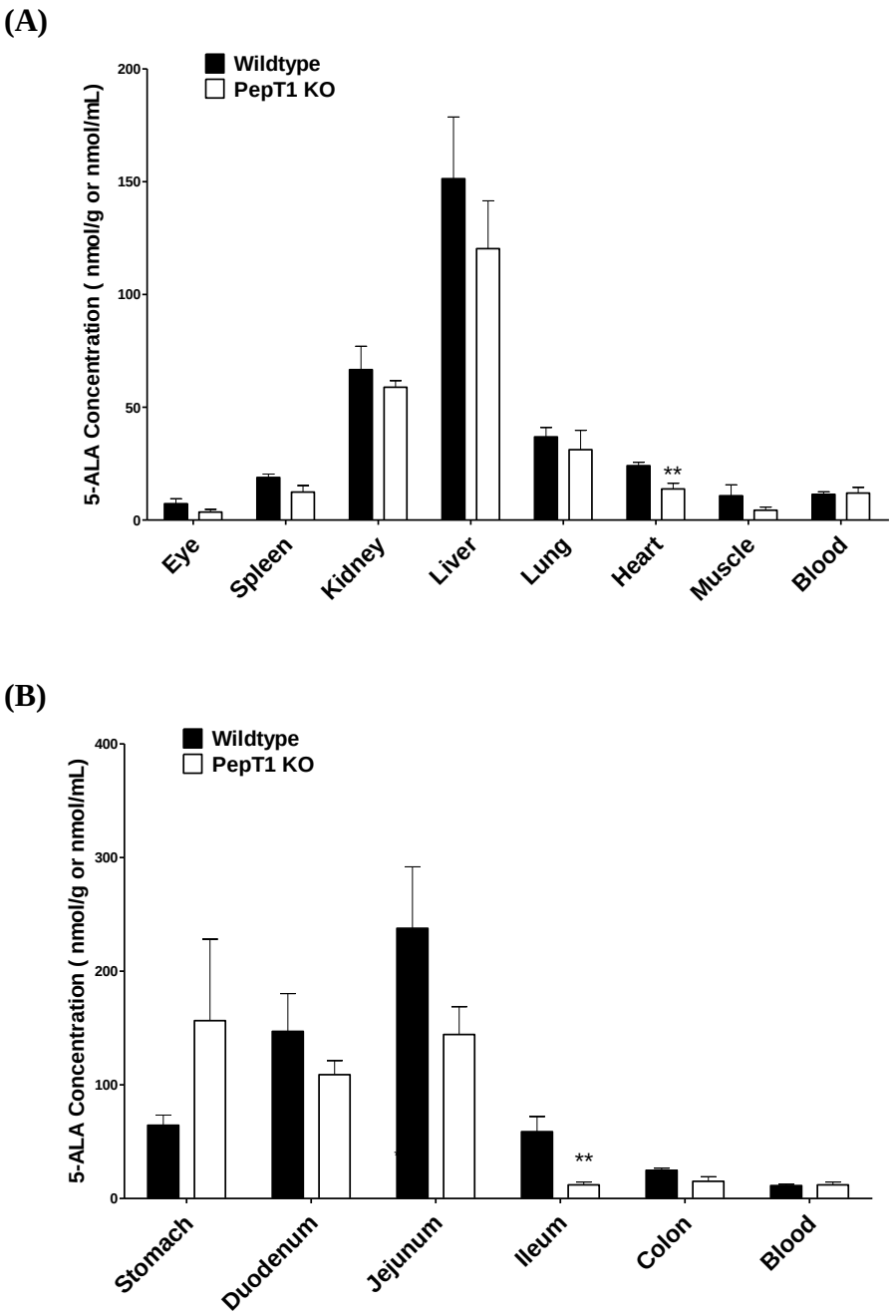

Figure 4.3 Tissue concentrations of 5-ALA 180 min after oral administration of 0.2 μmol/g [^{14}C] 5-ALA in wildtype and PepT1 knockout (KO) mice: (A) non-gastrointestinal tissues; (B) gastrointestinal segments. Data are expressed as mean ± SE (n= 4-5). ** $p<0.01$, compared with wildtype mice.

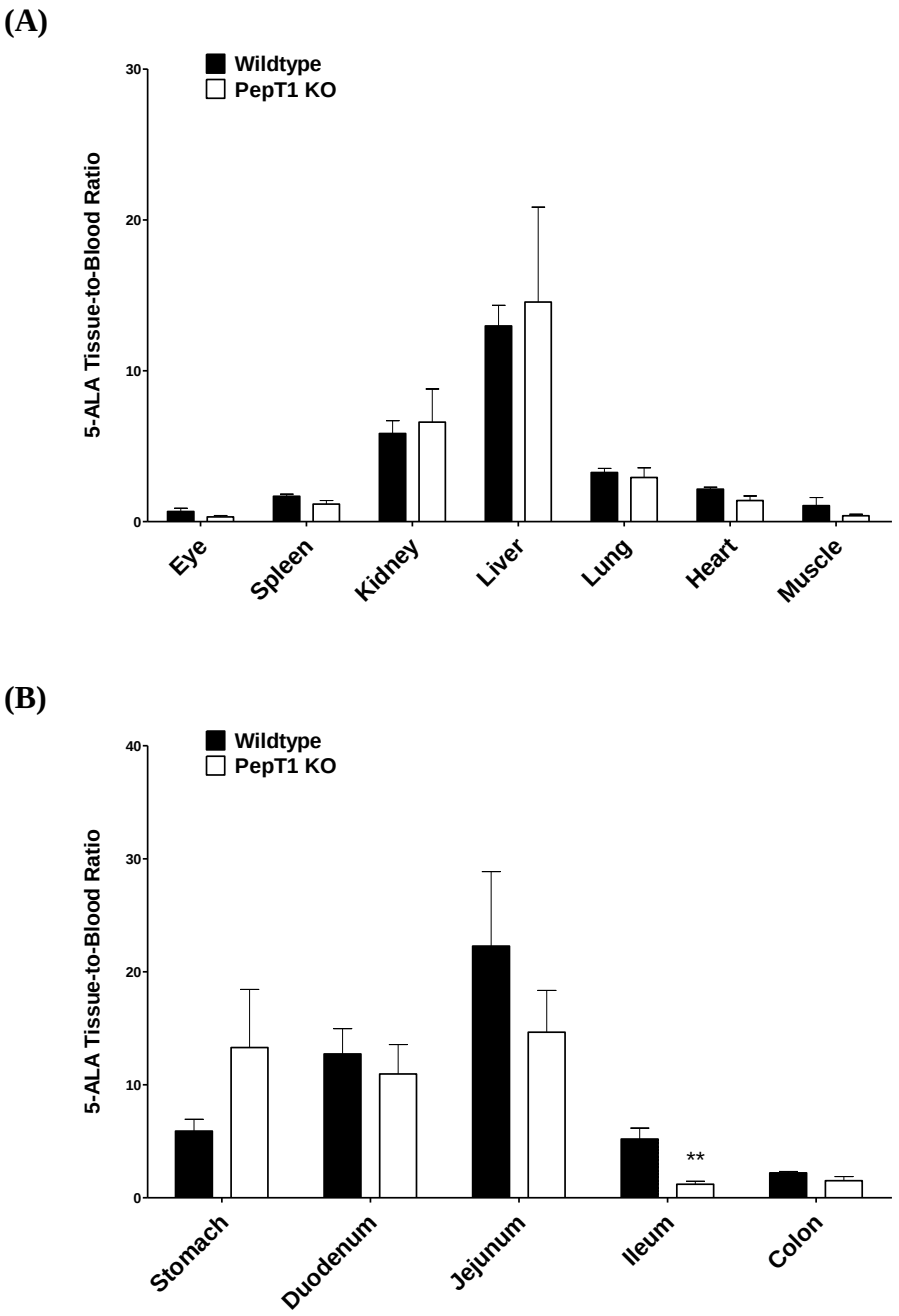

Figure 4.4 Tissue-to-blood concentration ratios of 5-ALA 180 min after oral administration of 0.2 μmol/g [^{14}C] 5-ALA in wildtype and PepT1 knockout (KO) mice: (A) non-gastrointestinal tissues; (B) gastrointestinal segments. Data are expressed as mean ± SE (n= 4-5). ** $p<0.01$, compared with wildtype mice.

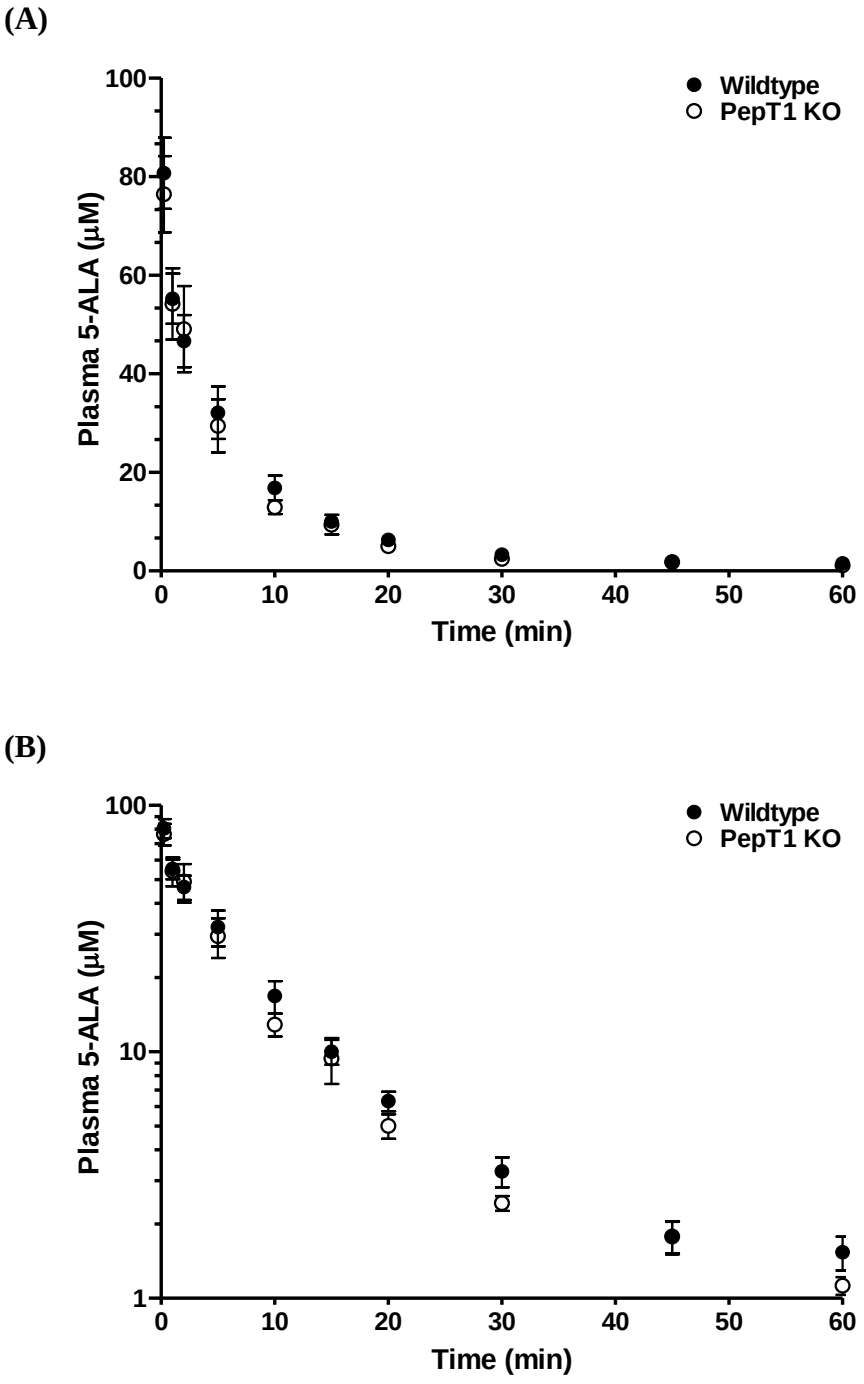

Figure 4.5 Plasma concentration-time curves of 5-ALA in wildtype and PepT1 knockout (KO) mice after intravenous dosing of 0.01 μmol/g [^{14}C] 5-ALA. The y-axis is displayed as a linear scale (A) or a logarithmic scale (B). Data are presented as mean ± SE (n=7).

Table 4.1 Noncompartmental analysis of 5-ALA after oral administration of 0.2 μmol/g [^{14}C] 5-ALA in wildtype (WT) and PepT1 knockout (KO) mice

Parameter (unit)	Wildtype	PepT1 KO	Ratio (KO/WT)
C_{max} (μM)	187.5 (18.0)	81.0 (21.8) **	0.46
T_{max} (min)	8.8 (1.3)	22.0 (9.4)	2.51
$AUC_{0\text{-}180}$ (μM•min)	7659 (1127)	3444 (466) *	0.45
$AUC_{0\text{-}\infty}$ (μM•min)	8883 (1400)	3696 (498) *	0.42
CL/F (ml/min)	0.486 (0.077)	1.152 (0.134) **	2.37
V/F (ml)	57.9 (9.3)	79.0 (16.5)	1.36
$t_{1/2}$ (min)	83.3 (10.1)	48.3 (8.4)	0.58
λ_Z (min^{-1})	0.0086 (0.0009)	0.0163 (0.0029)	1.89

Data are expressed as mean (SE) (n=4-5). * $p<0.05$, ** $p<0.01$, compared with wildtype mice.

Table 4.2 Compartmental analysis of 5-ALA after oral administration of 0.2 μmol/g [^{14}C] 5-ALA in wildtype (WT) and PepT1 knockout (KO) mice

Parameter (unit)	Wildtype	PepT1 KO	Ratio (KO/WT)
C_{max} (μM)	177 (11)	75 (21) **	0.43
T_{max} (min)	9.2 (0.8)	21.8 (8.5)	2.37
$AUC_{0-\infty}$ (μM•min)	8788 (1210)	3850 (514) **	0.44
CL/F (ml/min)	0.485 (0.074)	1.109 (0.136) **	2.29
α $t_{1/2}$ (min)	6.8 (1.1)	6.7 (1.8)	0.99
β $t_{1/2}$ (min)	98.5 (44.2)	54.9 (12.1)	0.56
K_a $t_{1/2}$ (min)	5.1 (1.0)	13.9 (6.2)	2.73
K_a (min^{-1})	0.159 (0.041)	0.140 (0.058)	0.88
V_1/F (ml)	11.1 (2.3)	36.8 (10.8)	3.32
V_2/F (ml)	27.0 (12.6)	18.3 (7.4)	0.68
r^2	0.984 (0.012)	0.951 (0.051)	-

Data are expressed as mean (SE) (n=4-5). * $p<0.05$, ** $p<0.01$ compared with wildtype mice.

Table 4.3 Noncompartmental analysis of 5-ALA after oral administration of 2 μmol/g [^{14}C] 5-ALA in wildtype (WT) and PepT1 knockout (KO) mice

Parameter (unit)	Wildtype	PepT1 KO	Ratio (KO/WT)
C_{max} (μM)	1478 (97)	930 (88) **	0.63
T_{max} (min)	10 (0)	10 (0)	1.00
$AUC_{0\text{-}180}$ (μM•min)	68212 (6884)	31056 (6338) **	0.46
$AUC_{0\text{-}\infty}$ (μM•min)	82207 (7925)	33807 (7689) **	0.41
CL/F (ml/min)	0.501 (0.052)	1.357 (0.262) *	2.71
V/F (ml)	79.8 (16.0)	107.5 (24.4)	1.35
$t_{1/2}$ (min)	108.8 (18.4)	56.8 (10.2)	0.52
λ_Z (min^{-1})	0.0072 (0.0017)	0.0135 (0.0025)	1.87

Data are expressed as mean (SE) (n=4). * $p<0.05$, ** $p<0.01$, compared with wildtype mice.

Table 4.4 Compartmental analysis of 5-ALA after oral administration of 2 μmol/g [^{14}C] 5-ALA in wildtype (WT) and PepT1 knockout (KO) mice

Parameter (unit)	Wildtype	PepT1 KO	Ratio (KO/WT)
C_{max} (μM)	1483 (61)	874 (90) **	0.59
T_{max} (min)	11.4 (1.0)	8.1 (0.9)	071
$AUC_{0-\infty}$ (μM•min)	82511 (8116)	33961 (7504) **	0.41
CL/F (ml/min)	0.500 (0.053)	1.345 (0.259) **	2.69
α $t_{1/2}$ (min)	8.2 (0.9)	6.1 (1.5)	0.74
β $t_{1/2}$ (min)	109.3 (14.2)	60.7 (5.2) *	0.56
K_a $t_{1/2}$ (min)	6.9 (1.1)	5.4 (1.4)	0.78
K_a (min^{-1})	0.109 (0.018)	0.150 (0.029)	1.38
V_1/F (ml)	11.6 (1.2)	20.0 (4.0)	1.72
V_2/F (ml)	31.3 (4.5)	40.6 (8.3)	1.30
r^2	0.989 (0.007)	0.963 (0.031)	-

Data are expressed as mean (SE) (n=4). * $p<0.05$, ** $p<0.01$ compared with wildtype mice.

Table 4.5 Noncompartmental analysis of 5-ALA after intravenous bolus administration of 0.01 μmol/g [^{14}C] 5-ALA in wildtype (WT) and PepT1 knockout (KO) mice

Parameter (unit)	Wildtype	PepT1 KO	Ratio (KO/WT)
Vd_{ss} (ml)	6.68 (0.94)	7.62 (1.07)	1.14
$AUC_{0\text{-}60}$ (μM•min)	583 (61)	527 (71)	0.90
$AUC_{0\text{-}\infty}$ (μM•min)	647 (65)	579 (71)	0.89
CL (ml/min)	0.338 (0.049)	0.377 (0.045)	1.12
$t_{1/2}$ (min)	27.8 (2.0)	30.4 (4.6)	1.11
MRT_{iv} (min)	20.2 (2.4)	20.2 (2.4)	1.00

Data are expressed as mean (SE) (n=7). No statistical differences were observed between wildtype and PepT1 KO mice.

Table 4.6 Compartmental analysis of 5-ALA after intravenous bolus administration of 0.01 μmol/g [^{14}C] 5-ALA in wildtype (WT) and PepT1 knockout (KO) mice

Parameter (unit)	Wildtype	PepT1 KO	Ratio (KO/WT)
$AUC_{0-\infty}$ (μM•min)	717 (94)	584 (75)	0.81
CL (ml/min)	0.322 (0.058)	0.377 (0.047)	1.17
α $t_{1/2}$ (min)	4.2 (0.6)	3.6 (0.4)	0.86
β $t_{1/2}$ (min)	65.0 (18.6)	36.5 (10.1)	0.56
K_{10} $t_{1/2}$ (min)	6.9 (0.8)	5.8 (0.4)	0.84
K_{10} (min^{-1})	0.109 (0.018)	0.150 (0.029)	1.38
V_1 (ml)	2.9 (0.4)	3.1 (0.4)	1.07
V_2 (ml)	7.7 (1.6)	5.5 (1.2)	0.71
V_{ss} (ml)	10.6 (1.5)	8.5 (1.3)	0.80
MRT_{iv} (min)	40.5 (9.7)	23.8 (4.8)	0.59
r^2	0.963 (0.007)	0.962 (0.013)	-

Data are expressed as mean (SE) (n=7). No statistical differences were observed between wildtype and PepT1 KO mice.

REFERENCES

Anderson, C. M., M. Jevons, et al. (2010). "Transport of the photodynamic therapy agent 5-aminolevulinic acid by distinct H+-coupled nutrient carriers coexpressed in the small intestine." J Pharmacol Exp Ther **332**(1): 220-228.

Brandsch, M. (2009). "Transport of drugs by proton-coupled peptide transporters: pearls and pitfalls." Expert Opin Drug Metab Toxicol **5**(8): 887-905.

Brandsch, M. (2013). "Drug transport via the intestinal peptide transporter PepT1." Curr Opin Pharmacol **13**(6): 881-887.

Chung, C. W., C. H. Kim, et al. (2013). "Aminolevulinic acid derivatives-based photodynamic therapy in human intra- and extrahepatic cholangiocarcinoma cells." Eur J Pharm Biopharm **85**(3 Pt A): 503-510.

Dalton, J. T., M. C. Meyer, et al. (1999). "Pharmacokinetics of aminolevulinic acid after oral and intravenous administration in dogs." Drug Metab Dispos **27**(4): 432-435.

Dalton, J. T., C. R. Yates, et al. (2002). "Clinical pharmacokinetics of 5-aminolevulinic acid in healthy volunteers and patients at high risk for recurrent bladder cancer." J Pharmacol Exp Ther **301**(2): 507-512.

Daniel, H. (2004). "Molecular and integrative physiology of intestinal peptide transport." Annu Rev Physiol **66**: 361-384.

Daniel, H. and G. Kottra (2004). "The proton oligopeptide cotransporter family SLC15 in physiology and pharmacology." Pflugers Arch **447**(5): 610-618.

Dolmans, D. E., D. Fukumura, et al. (2003). "Photodynamic therapy for cancer." Nat Rev Cancer **3**(5): 380-387.

Doring, F., J. Walter, et al. (1998). "Delta-aminolevulinic acid transport by intestinal and renal peptide transporters and its physiological and clinical implications." J Clin Invest **101**(12): 2761-2767.

Fei, Y. J., Y. Kanai, et al. (1994). "Expression cloning of a mammalian proton-coupled oligopeptide transporter." Nature **368**(6471): 563-566.

Fotinos, N., M. A. Campo, et al. (2006). "5-Aminolevulinic acid derivatives in photomedicine: Characteristics, application and perspectives." Photochemistry and Photobiology **82**(4): 994-1015.

Frolund, S., O. C. Marquez, et al. (2010). "Delta-aminolevulinic acid is a substrate for the amino acid transporter SLC36A1 (hPAT1)." Br J Pharmacol **159**(6): 1339-1353.

Hagiya, Y., Y. Endo, et al. (2012). "Pivotal roles of peptide transporter PEPT1 and ATP-binding cassette (ABC) transporter ABCG2 in 5-aminolevulinic acid (ALA)-based photocytotoxicity of gastric cancer cells in vitro." Photodiagnosis Photodyn Ther **9**(3): 204-214.

Hagiya, Y., H. Fukuhara, et al. (2013). "Expression levels of PEPT1 and ABCG2 play key roles in 5-aminolevulinic acid (ALA)-induced tumor-specific protoporphyrin IX (PpIX) accumulation in bladder cancer." Photodiagnosis Photodyn Ther **10**(3): 288-295.

Hu, Y., D. E. Smith, et al. (2008). "Targeted disruption of peptide transporter Pept1 gene in mice significantly reduces dipeptide absorption in intestine." Mol Pharm **5**(6): 1122-1130.

Jappar, D., Y. Hu, et al. (2011). "Effect of dose escalation on the in vivo oral absorption and disposition of glycylsarcosine in wild-type and Pept1 knockout mice." Drug Metab Dispos **39**(12): 2250-2257.

Kelty, C. J., N. J. Brown, et al. (2002). "The use of 5-aminolaevulinic acid as a photosensitiser in photodynamic therapy and photodiagnosis." Photochem Photobiol Sci **1**(3): 158-168.

Krammer, B. and K. Plaetzer (2008). "ALA and its clinical impact, from bench to bedside." Photochem Photobiol Sci **7**(3): 283-289.

Krammer, B. and K. Plaetzer (2008). "ALA and its clinical impact, from bench to bedside." Photochemical & Photobiological Sciences **7**(3): 283-289.

Loh, C. S., A. J. MacRobert, et al. (1993). "Oral versus intravenous administration of 5-aminolaevulinic acid for photodynamic therapy." Br J Cancer **68**(1): 41-51.

Neumann, J. and M. Brandsch (2003). "Delta-aminolevulinic acid transport in cancer cells of the human extrahepatic biliary duct." J Pharmacol Exp Ther **305**(1): 219-224.

Nokes, B., M. Apel, et al. (2013). "Aminolevulinic acid (ALA): photodynamic detection and potential therapeutic applications." J Surg Res **181**(2): 262-271.

Ocheltree, S. M., H. Shen, et al. (2005). "Role and relevance of peptide transporter 2 (PEPT2) in the kidney and choroid plexus: in vivo studies with

glycylsarcosine in wild-type and PEPT2 knockout mice." J Pharmacol Exp Ther **315**(1): 240-247.

Peng, Q., K. Berg, et al. (1997). "5-Aminolevulinic acid-based photodynamic therapy: principles and experimental research." Photochem Photobiol **65**(2): 235-251.

Peng, Q., T. Warloe, et al. (1997). "5-aminolevulinic acid-based photodynamic therapy - Clinical research and future challenges." Cancer **79**(12): 2282-2308.

Posada, M. M. and D. E. Smith (2013). "In vivo absorption and disposition of cefadroxil after escalating oral doses in wild-type and PepT1 knockout mice." Pharm Res **30**(11): 2931-2939.

Regula, J., A. J. MacRobert, et al. (1995). "Photosensitisation and photodynamic therapy of oesophageal, duodenal, and colorectal tumours using 5 aminolaevulinic acid induced protoporphyrin IX--a pilot study." Gut **36**(1): 67-75.

Rubio-Aliaga, I. and H. Daniel (2008). "Peptide transporters and their roles in physiological processes and drug disposition." Xenobiotica **38**(7-8): 1022-1042.

Shen, H., S. M. Ocheltree, et al. (2007). "Impact of genetic knockout of PEPT2 on cefadroxil pharmacokinetics, renal tubular reabsorption, and brain penetration in mice." Drug Metab Dispos **35**(7): 1209-1216.

Smith, D. E., B. Clemencon, et al. (2013). "Proton-coupled oligopeptide transporter family SLC15: physiological, pharmacological and pathological implications." Mol Aspects Med **34**(2-3): 323-336.

van den Boogert, J., R. van Hillegersberg, et al. (1998). "5-Aminolaevulinic acid-induced protoporphyrin IX accumulation in tissues: pharmacokinetics after oral or intravenous administration." J Photochem Photobiol B **44**(1): 29-38.

Yang, B., Y. Hu, et al. (2013). "Impact of peptide transporter 1 on the intestinal absorption and pharmacokinetics of valacyclovir after oral dose escalation in wild-type and PepT1 knockout mice." Drug Metab Dispos **41**(10): 1867-1874.

CHAPTER 5

FUTURE DIRECTION

Peptide transporter PepT1 has been considered to play an important pharmacological role in transporting a wide spectrum of therapeutic compounds with di-/tri-peptide structure similarity. The prodrug strategy for targeting PepT1 is under intense investigation to improve the oral absorption of certain drugs with relatively poor bioavailability. The role of PepT1 in facilitating 5-ALA intestinal absorption and improving oral bioavailability is worth characterizing, given the fact that 5-ALA is a polar and hydrophilic molecule and other intestinal transporters (e.g., PAT1) showed potential in mediating the active transport of 5-ALA. In this dissertation, I have demonstrated the significant role of PepT1 in the intestinal permeability of 5-ALA via *in situ* single-pass perfusions and quantified the effect of PepT1 on intestinal absorption and systemic exposure of 5-ALA after clinically relevant oral doses. The relative contribution of intestinal transporter PepT1 in this process, as compared to other potential intestinal transporters such as PAT1, was also assessed and discussed in this dissertation. The clinical significance and importance of this project could be further elaborated and summarized in the following aspects. First, both PepT1 and PAT1 have been demonstrated to be pharmacologically important in the intestinal absorption of numerous therapeutic compounds and may share some common substrates (e.g. 5-ALA in this case). The findings in this dissertation could provide useful

information in guiding future clinical studies on transporter related drug-drug interactions, which could affect the intestinal absorption of certain drugs (i.e., co-administration of 5-ALA with other drugs which are also PepT1 or PAT1 substrates). Second, results of PepT1-mediated uptake of 5-ALA create a better understanding of the structure-transport relationship of PepT1, which improve our understanding of drug ADME properties and eventually benefit drug development. Finally, pharmacogenetic studies of the human PEPT1 gene have shown genetic polymorphisms. Although current knowledge regarding the pharmaceutical and pharmacokinetic relevance of PEPT1 genetic variants is limited, we believe that genetic polymorphisms of PEPT1 may adversely influence the intestinal absorption of many drugs and this will become apparent with more research. Therefore, it is valuable to conduct the present study on 5-ALA oral absorption since our PepT1 knockout mice could be considered a unique animal model to mimic possible loss-of-function/activity genetic variants in human.

As discussed in Chapters 3 and 4, direct evidence to rule out a potential role of PAT1 in the *in vivo* oral absorption of 5-ALA is still lacking. Our *in situ* experimental results suggested that PepT1 accounted for approximately 90% of 5-ALA permeability in various small intestinal segments of wildtype mice while the potential contribution of other transporters (e.g., PAT1) was extremely low. However, as observed in our *in vivo* pharmacokinetic studies, the influence of PepT1 on the intestinal absorption and overall pharmacokinetic profiles of 5-ALA cannot be extrapolated from our permeability studies (i.e., approximate 2-fold change in systemic exposure versus 10-fold change in permeability). In this

regard, it would be worthwhile to directly investigate the potential contribution of PAT1 on the *in vivo* intestinal absorption and pharmacokinetics of 5-ALA in wildtype and PepT1 knockout mice after oral co-administration of 5-ALA and PAT1 inhibitors (e.g., 5-hydroxytryptophan). This could provide solid evidence whether or not PAT1 is involved in the oral absorption of 5-ALA *in vivo* and its relative contribution as compared to PepT1, if any.

To better understand the mechanisms of 5-ALA intestinal absorption and further bridge the discrepancy between *in situ* and *in vivo* experimental results, future studies could be focused on developing an "advanced compartmental absorption and transit" (ACAT) model. In this context, GastroPlus® might be used to describe the pharmacokinetic profiles of 5-ALA after oral dosing and to delineate the contribution of PepT1 in the oral absorption process. Through this modeling and simulation approach, we should be able to fit and predict 5-ALA plasma concentration-time profiles in wildtype and PepT1 knockout mice after oral administration, to examine segmental contribution to the absorption of 5-ALA, and to predict the relative contribution of PepT1-mediated active transport versus paracellular and transcellular passive diffusion of 5-ALA. In addition, this mechanism-based model could potentially be leveraged to predict the intestinal absorption and *in vivo* pharmacokinetics of 5-ALA in human by extrapolating from our animal data.

APPENDICES

APPENDIX A

INDIVIDUAL DATA FROM CHAPTER 4

Table A.1 Individual PK parameters of 5-ALA after 0.2 μmol/g oral dose in wildtype (WT) and PepT1 knockout (P1) mice (two-compartmental model)

ID	Unit	1	2	3	4	5	Mean	SE	6	7	8	9	10	Mean	SE
Geno		WT	WT	WT	WT	WT			P1	P1	P1	P1	P1		
Cmax	μM	186	168	151	139	202	169	12	32	20	99	101	124	75	21
Tmax	min	10.0	10.8	7.1	2.1	8.9	7.8	1.5	36.2	48.0	7.3	6.7	10.7	21.8	8.5
AUC	min*μM	8935	11692	5768	6527	8756	8336	1041	3200	2630	4136	3633	5651	3850	514
CL_F	ml/min	0.448	0.342	0.693	0.613	0.457	0.511	0.063	1.250	1.521	0.967	1.101	0.708	1.109	0.136
Alpha_HL	min	6.53	5.28	9.92	18.14	5.44	9.06	2.42	3.61	2.92	13.29	6.72	7.03	6.72	1.83
Beta_HL	min	231.0	53.1	58.3	171.4	51.5	113.1	37.2	25.6	33.9	82.8	49.4	83.1	54.9	12.1
K01_HL	min	7.05	5.32	2.48	0.36	5.45	4.13	1.20	24.65	32.67	2.26	2.82	6.92	13.86	6.22
K01	1/min	0.098	0.130	0.279	1.924	0.127	0.512	0.354	0.028	0.021	0.306	0.246	0.100	0.140	0.058
Alpha	1/min	0.106	0.131	0.070	0.038	0.127	0.095	0.018	0.192	0.237	0.052	0.103	0.099	0.137	0.034
Beta	1/min	0.0030	0.0130	0.0119	0.0040	0.0134	0.0091	0.0023	0.0271	0.0205	0.0084	0.0140	0.0083	0.0157	0.0036
V1_F	ml	7.8	11.2	17.5	26.8	8.0	14.2	3.6	46.0	74.1	28.8	22.6	12.4	36.8	10.8
V2_F	ml	64.6	11.5	17.7	50.1	14.3	31.6	10.8	0.1	0.2	30.8	29.5	30.7	18.3	7.4

WT #4, an outlier, was removed from the final analysis in Tables 4.1 and 4.2.

K01=Ka

Table A.2 Individual PK parameters of 5-ALA after 0.2 μmol/g oral dose in wildtype (WT) and PepT1 knockout (P1) mice (non-compartmental analysis)

ID		1	2	3	4	5	Mean	SE	6	7	8	9	10	Mean	SE
Geno	Unit	WT	WT	WT	WT	WT			P1	P1	P1	P1	P1		
Cmax	μM	221	172	144	135	213	177	17	41.7	24.1	94.9	98.1	146	81	22
Tmax	min	10	10	5	5	10	8.0	1.2	45	45	5	5	10	22.0	9.4
AUC 0-180	min*μM	6587	10578	5343	4920	8128	7111	1031	2848	2233	3731	3405	5006	3444	466
AUC 0-∞	min*μM	7337	12245	5955	5301	9997	8167	1299	2974	2652	3799	3540	5517	3696	498
CL/F	ml/min	0.545	0.327	0.672	0.755	0.400	0.540	0.080	1.347	1.550	1.046	1.127	0.725	1.152	0.134
V/F	ml	60.2	31.5	74.9	65.8	65.0	59.5	7.4	66.5	120.2	56.9	74.3	74.3	79.0	16.5
Lambda_z	1/min	0.0091	0.0104	0.0090	0.0115	0.0062	0.0092	0.0009	0.0194	0.0107	0.0254	0.0163	0.0098	0.0163	0.0029
$t_{1/2}$	min	76.6	66.8	77.3	60.4	112.6	78.7	9.0	35.7	64.8	27.3	42.5	71.1	48.3	8.4
AUC 0-30	min*μM	3946	3940	3006	2529	4211	3526	323	551	258	2062	1907	2714	1498	469
AUC 0-45	min*μM	4708	5418	3672	3147	5333	4455	452	1126	587	2561	2291	3394	1992	505
AUC 0-60	min*μM	5107	6546	4090	3549	6040	5066	565	1621	936	2852	2567	3827	2361	501
AUC 0-90	min*μM	5596	8249	4648	4130	6842	5893	748	2206	1496	3204	2922	4322	2830	477
AUC 0-120	min*μM	6009	9315	4954	4466	7363	6421	878	2555	1846	3457	3148	4625	3126	465
AUC 0-150	min*μM	6331	10013	5169	4724	7766	6801	960	2747	2070	3640	3306	4840	3321	464

Table A.3 Individual PK parameters of 5-ALA after 2 μmol/g oral dose in wildtype (WT) and PepT1 knockout (P1) mice (two-compartmental model)

ID		1	2	3	4	Mean	SE	5	6	7	8	Mean	SE
Geno		WT	WT	WT	WT			P1	P1	P1	P1		
Cmax	μM	1348	1455	1485	1643	1483	61	1054	678	768	995	874	90
Tmax	min	14.1	10.0	10.1	11.5	11.4	1.0	8.4	6.9	6.6	10.6	8.1	0.9
AUC	min*μM	77105	62101	93030	97807	82511	8116	36482	23340	21827	54193	33961	7504
CL_F	ml/min	0.519	0.644	0.430	0.409	0.500	0.053	1.096	1.714	1.833	0.738	1.345	0.259
Alpha_HL	min	9.2	6.7	10.3	6.9	8.2	0.9	3.6	4.3	6.0	10.4	6.1	1.5
Beta_HL	min	128.8	107.3	131.3	70.0	109.3	14.2	62.5	57.6	48.9	73.8	60.7	5.2
K01_HL	min	9.58	6.68	4.36	6.92	6.88	1.07	9.37	4.44	3.18	4.51	5.38	1.37
K01	1/min	0.072	0.104	0.159	0.100	0.109	0.018	0.074	0.156	0.218	0.154	0.150	0.029
Alpha	1/min	0.076	0.104	0.068	0.100	0.087	0.009	0.195	0.161	0.116	0.066	0.135	0.028
Beta	1/min	0.005	0.006	0.005	0.010	0.007	0.001	0.011	0.012	0.014	0.009	0.012	0.001
V1_F	ml	11.0	10.4	15.0	9.9	11.6	1.2	8.2	22.7	26.5	22.7	20.0	4.0
V2_F	ml	32.2	36.2	38.3	18.5	31.3	4.5	28.4	63.7	41.7	28.5	40.6	8.3

K01=Ka

Table A.4 Individual PK parameters of 5-ALA after 2 μmol/g oral dose in wildtype (WT) and PepT1 knockout (P1) mice (non-compartmental analysis)

ID		1	2	3	4	Mean	SE	5	6	7	8	Mean	SE
Geno	Unit	WT	WT	WT	WT			P1	P1	P1	P1		
Cmax	μM	1260	1380	1580	1690	1478	97	1180	810	805	924	930	88
Tmax	min	10	10	10	10	10	0	10	10	10	10	10	0
AUC 0-180	min*μM	64334	52949	69493	86073	68212	6884	34204	21741	20606	47676	31056	6338
AUC 0-∞	min*μM	75653	62845	95140	95189	82207	7925	35564	22828	21936	54900	33807	7689
CL/F	ml/min	0.529	0.636	0.420	0.420	0.501	0.052	1.125	1.752	1.823	0.729	1.357	0.262
V/F	ml	87.8	109.9	87.0	34.5	79.8	16.0	56.9	116.9	170.9	85.3	107.5	24.4
Lambda_z	1/min	0.0060	0.0058	0.0048	0.0122	0.0072	0.0017	0.0198	0.0150	0.0107	0.0085	0.0135	0.0025
$t_{1/2}$	min	115.0	119.7	143.4	56.9	108.8	18.4	35.1	46.2	65.0	81.2	56.8	10.2
AUC 0-30	min*μM	31235	31140	32825	38275	33369	1680	21395	12275	13338	22630	17409	2678
AUC 0-45	min*μM	43138	38198	41810	49300	43111	2312	25903	14458	15820	29013	21298	3623
AUC 0-60	min*μM	49055	41565	47653	57303	48894	3240	28505	15951	17052	33415	23731	4298
AUC 0-90	min*μM	55745	45795	55333	68763	56409	4716	31010	18438	18435	39205	26772	5095
AUC 0-120	min*μM	59374	48752	60703	76383	61303	5694	32419	20109	19398	42850	28694	5586
AUC 0-150	min*μM	62077	51029	65383	81828	65079	6371	33371	21078	20100	45573	30030	5996

Table A.5 Individual PK parameters of 5-ALA after 0.01 μmol/g intravenous dose in wildtype (WT) and PepT1 knockout (P1) mice (two-compartmental model)

ID		1	2	3	4	5	6	7	Mean	SE	8	9	10	11	12	13	14	Mean	SE
Geno	Unit	WT	WT	WT	WT	WT	WT	WT			P1	P1	P1	P1	P1	P1	P1		
AUC	min*μM	515	1079	676	736	876	828	313	717	94	728	520	569	591	934	402	346	584	75
CL	ml/min	0.389	0.185	0.296	0.272	0.228	0.242	0.639	0.322	0.058	0.275	0.385	0.352	0.338	0.214	0.498	0.578	0.377	0.047
Alpha_HL	min	1.5	5.2	4.6	5.2	4.9	5.1	2.6	4.2	0.6	4.7	4.5	2.8	4.1	3.8	3.4	2.0	3.6	0.4
Beta_HL	min	19.6	110.8	34.5	52.6	147.7	73.0	16.9	65.0	18.6	94.3	30.1	36.3	33.9	16.6	27.6	17.0	36.5	10.1
K10_HL	min	4.3	8.8	7.7	9.4	7.4	6.6	4.2	6.9	0.8	7.1	6.6	4.4	6.2	5.7	4.9	5.5	5.8	0.4
K10	1/min	0.162	0.079	0.090	0.074	0.094	0.105	0.166	0.110	0.015	0.098	0.106	0.159	0.111	0.123	0.143	0.125	0.123	0.008
Alpha	1/min	0.455	0.133	0.152	0.133	0.142	0.135	0.268	0.202	0.046	0.147	0.154	0.244	0.170	0.182	0.206	0.353	0.208	0.027
Beta	1/min	0.035	0.006	0.020	0.013	0.005	0.009	0.041	0.019	0.005	0.007	0.023	0.019	0.020	0.042	0.025	0.041	0.025	0.005
V1	ml	2.4	2.4	3.3	3.7	2.4	2.3	3.8	2.9	0.3	2.8	3.6	2.2	3.0	1.7	3.5	4.6	3.1	0.4
V2	ml	5.5	11.1	4.7	7.6	15.6	5.1	4.5	7.7	1.6	11.4	4.1	5.7	4.7	1.1	5.0	6.2	5.5	1.2
Vss	ml	7.9	13.4	8.0	11.3	18.0	7.4	8.3	10.6	1.5	14.2	7.7	7.9	7.7	2.8	8.5	10.8	8.5	1.3
MRT	min	20.4	72.4	27.0	41.5	78.7	30.6	13.0	40.5	9.7	51.8	20.1	22.4	22.8	13.3	17.1	18.6	23.7	4.8

Table A.6 Individual PK parameters of 5-ALA after 0.01 μmol/g intravenous dose in wildtype (WT) and PepT1 knockout (P1) mice (non-compartmental analysis)

ID		1	2	3	4	5	6	7	Mean	SE	8	9	10	11	12	13	14	Mean	SE
Geno		WT	WT	WT	WT	WT	WT	WT			P1	P1	P1	P1	P1	P1	P1		
AUC 0-60	min*μM	478	802	574	577	617	727	304	583	61	578	470	516	521	906	367	330	527	71
AUC 0-∞	min*μM	555	872	670	684	664	759	323	647	65	631	512	628	595	929	402	356	579	71
Vdss	ml	9.24	4.01	7.95	8.32	4.89	3.37	8.95	6.68	0.94	5.65	7.21	10.27	8.06	2.54	8.92	10.69	7.62	1.07
CL	ml/min	0.360	0.229	0.298	0.292	0.301	0.264	0.620	0.338	0.049	0.317	0.391	0.318	0.336	0.215	0.498	0.561	0.377	0.045
$t_{1/2}$	min	30.7	24.1	32.9	33.2	30.1	19.8	24.0	27.8	2.0	31.6	25.4	53.5	36.3	17.3	29.1	19.3	30.4	4.6
Lambda_z	1/min	0.0226	0.0288	0.0211	0.0208	0.0230	0.0351	0.0289	0.0258	0.0020	0.0220	0.0273	0.0130	0.0191	0.0401	0.0238	0.0359	0.0259	0.0036
MRT	min	25.6	17.5	26.6	28.5	16.2	12.8	14.4	20.2	2.4	17.8	18.5	32.3	24.0	11.8	17.9	19.0	20.2	2.4

Diagnostic plots of two-compartmental model analysis

Figure A.1 Individual predicted and observed plasma concentration-time profiles at 0.2 μmol/g oral dose in wildtype (WT) mcie.

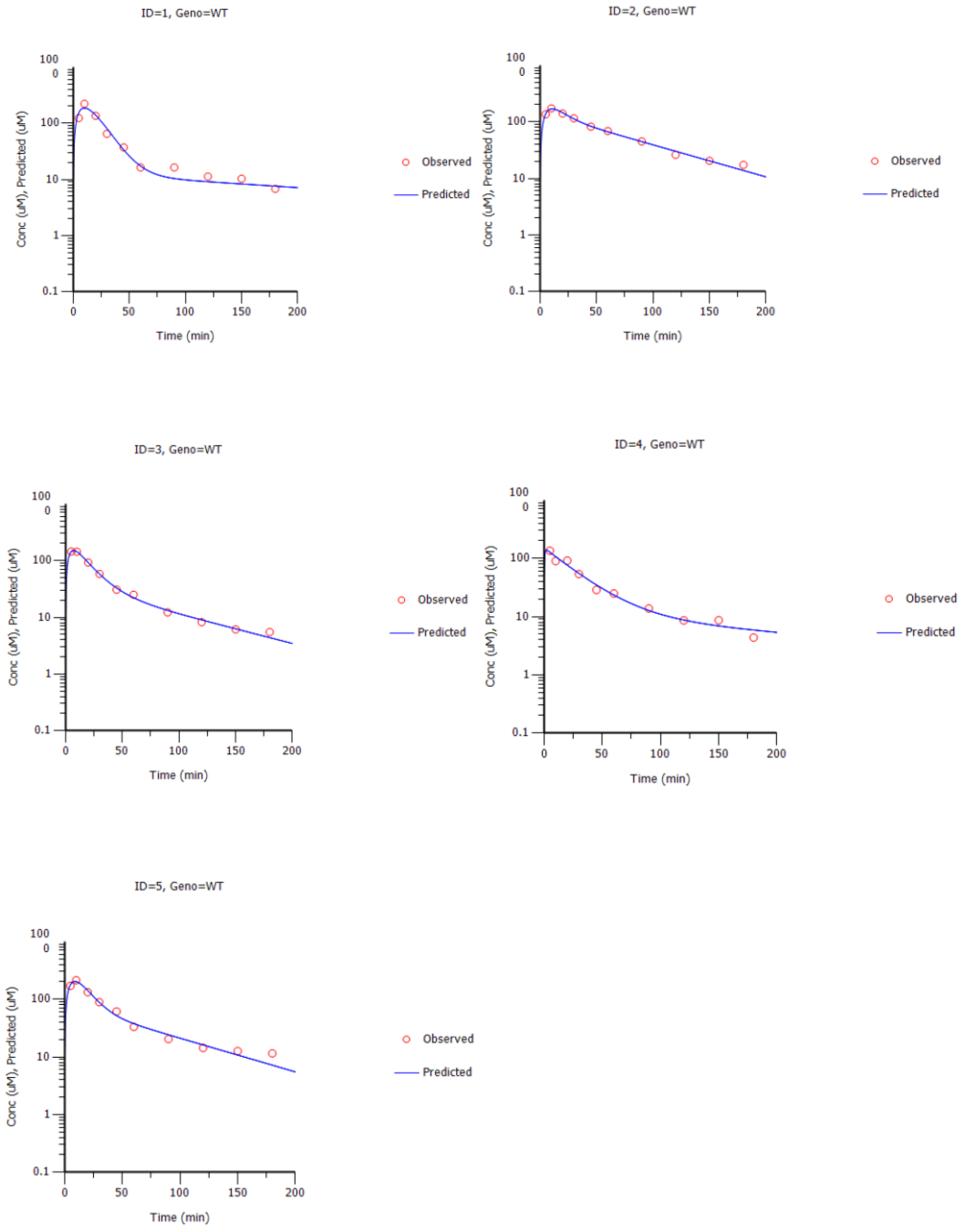

Figure A.2 Individual predicted and observed plasma concentration-time profiles at 0.2 μmol/g oral dose in PepT1 knockout (P1) mcie.

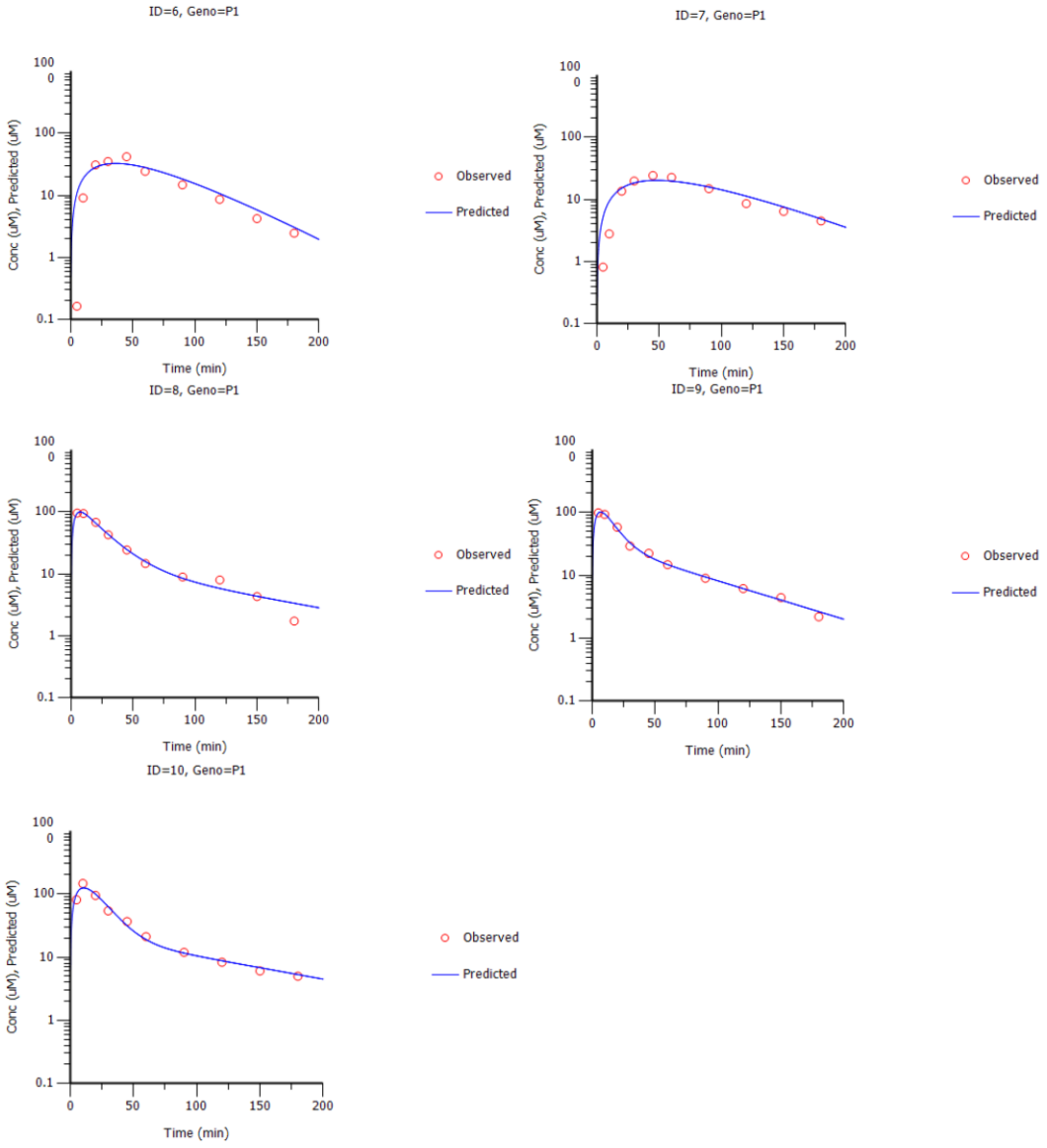

Figure A.3 Individual predicted and observed plasma concentration-time profiles at 2 μmol/g oral dose in wildtype (WT) mcie.

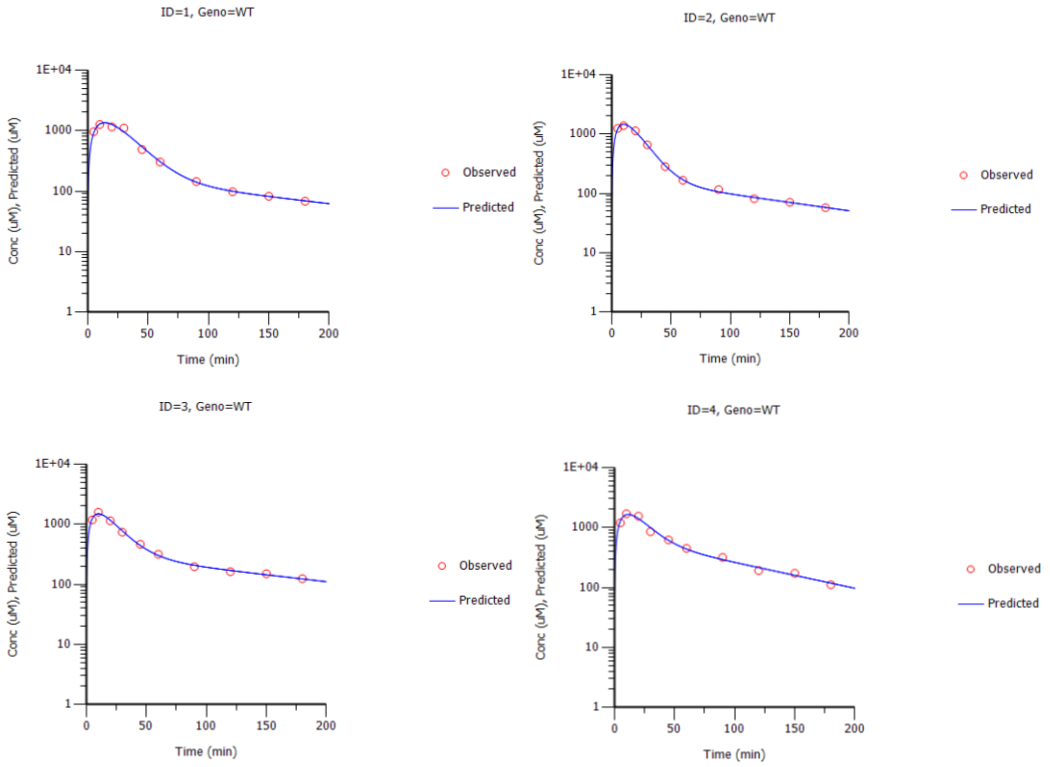

Figure A.4 Individual predicted and observed plasma concentration-time profiles at 2 μmol/g oral dose in PepT1 knockout (P1) mcie.

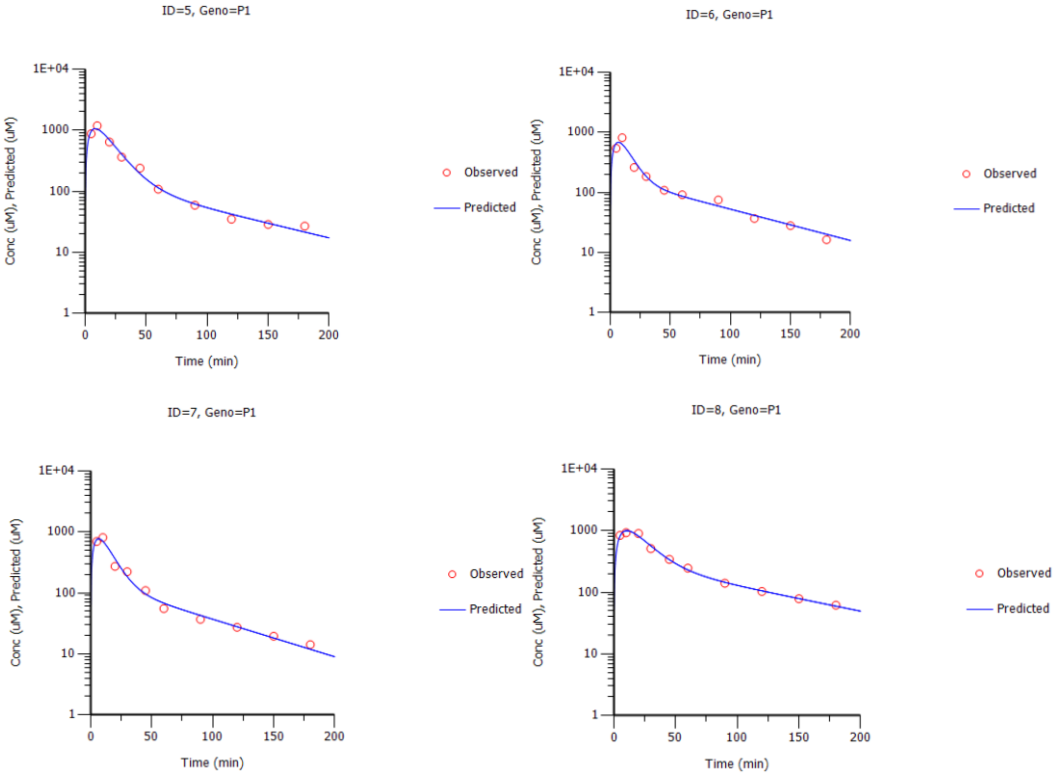

Figure A.5 Individual predicted and observed plasma concentration-time profiles at 0.01 μmol/g intravenous dose in wildtype (WT) mcie.

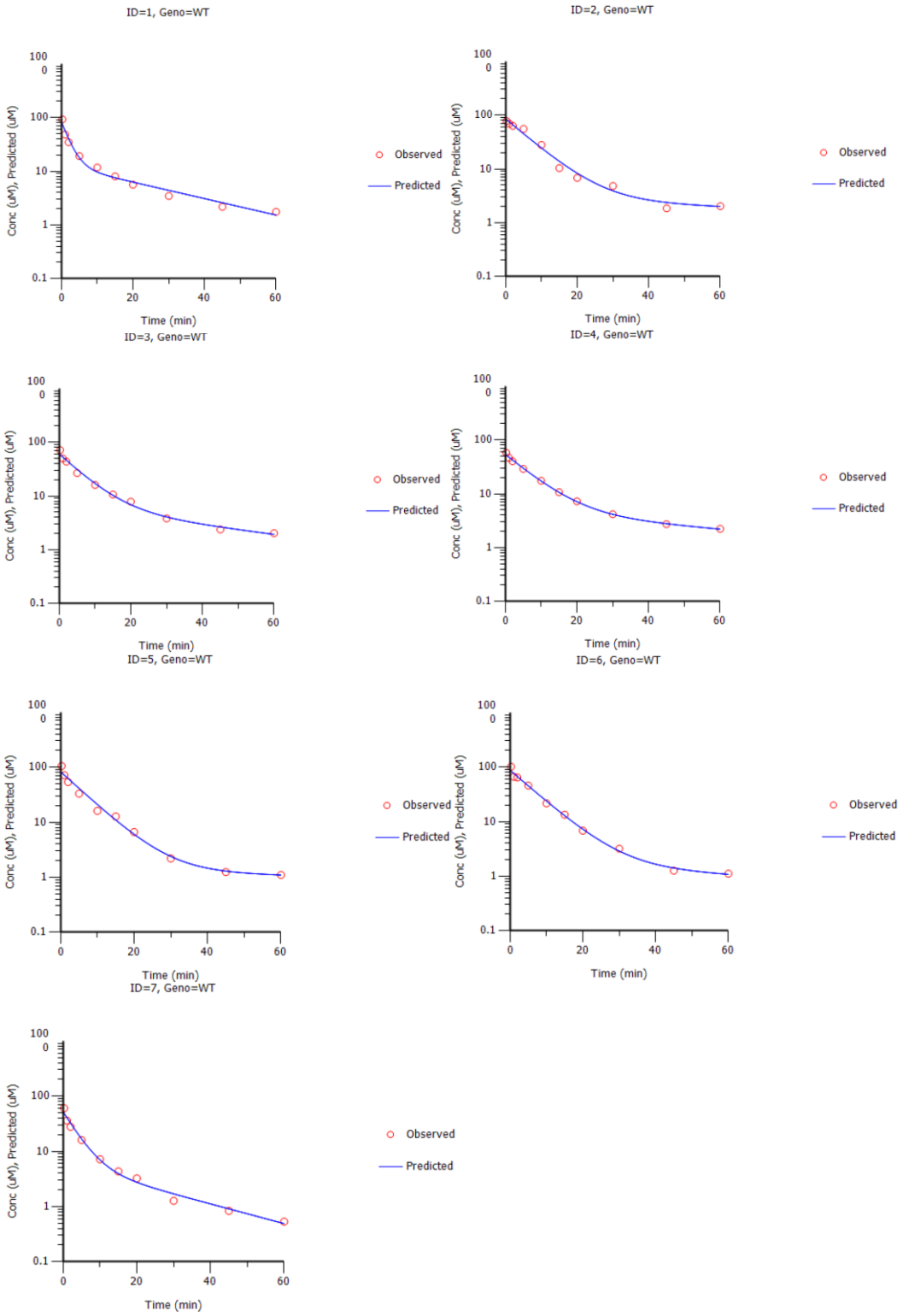

Figure A.6 Individual predicted and observed plasma concentration-time profiles at 0.01 μmol/g intravenous dose in PepT1 knockout (P1) mcie.

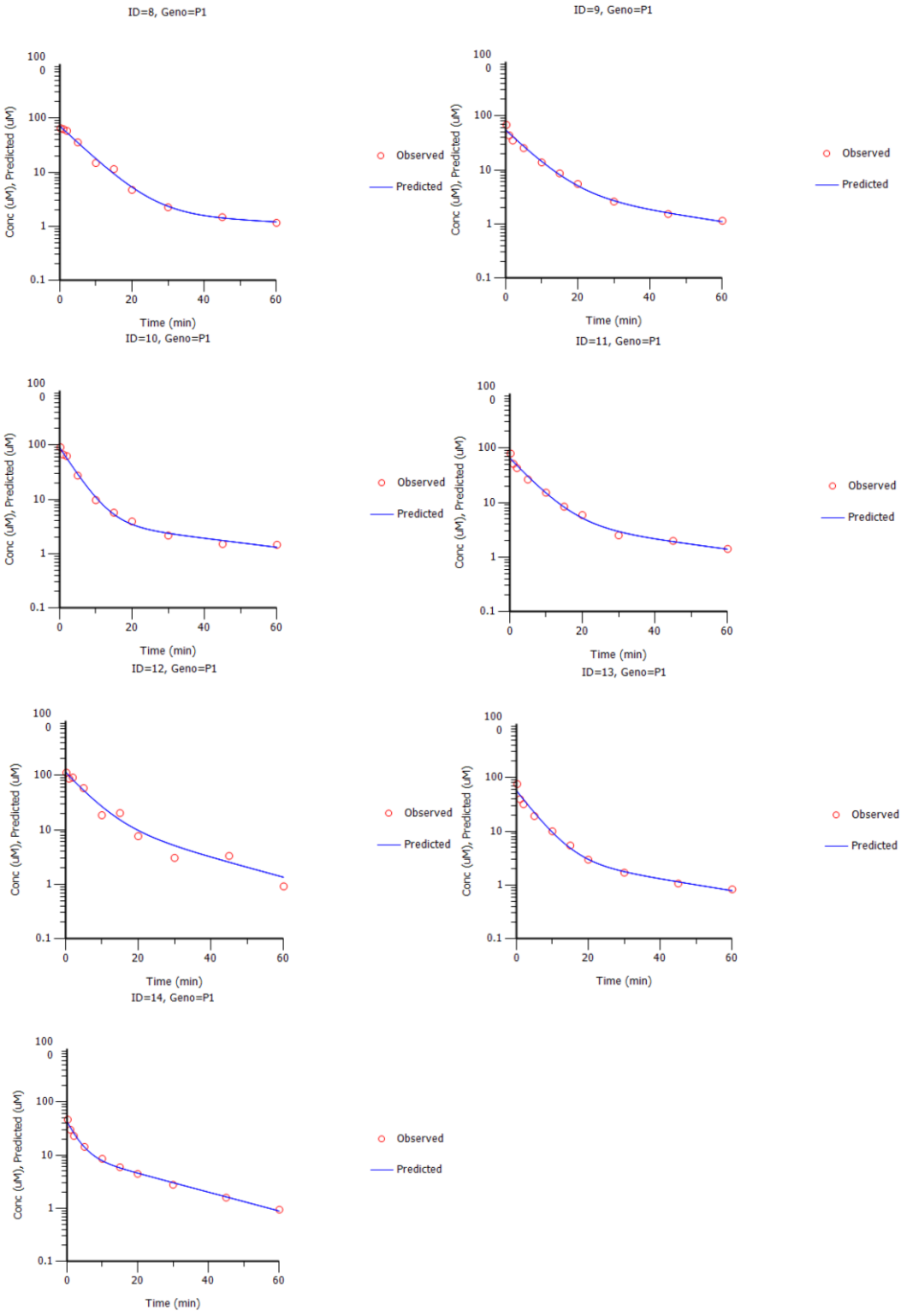

APPENDIX B

POPULATION PHARMACOKINETIC MODELING OF CEFADROXIL RENAL TRANSPORT IN WILDTYPE AND PEPT2 KNOCKOUT MICE

ABSTRACT

Cefadroxil is a broad-spectrum β-lactam antibiotic that is widely used in the treatment of various infectious diseases. Currently, poor understanding of the drug's pharmacokinetic profiles and disposition mechanism(s) prevents determining optimal dosage regimens and achieving ideal antibacterial responses in patients. In the present study, we developed a population pharmacokinetic model of cefadroxil in wildtype and PepT2 knockout mice using the NONMEM approach. Cefadroxil pharmacokinetics were best described by a two-compartment model, with both saturable and nonsaturable transport processes to/from the central compartment. Through this modeling approach, pharmacokinetic parameters in wildtype and PepT2 knockout mice were well estimated, respectively, as: volume of central compartment V_1 (3.43 vs 4.23 ml), volume of peripheral compartment V_2 (5.98 vs 8.61 ml), inter-compartment clearance Q (0.599 vs 0.586 ml/min), and linear elimination rate constant K_{10} (0.111 vs 0.070 min^{-1}). Moreover, the secretion kinetics (i.e., V_{m1} = 17.6 nmol/min and K_{m1} = 37.1 μM) and reabsorption kinetics (i.e., V_{m2} = 15.0

nmol/min and K_{m2} = 27.1 μM) of cefadroxil were quantified in kidney, for the first time, under *in vivo* conditions. Our model provides a unique tool to quantitatively predict the transporter-mediated nonlinear disposition of cefadroxil as well as optimize dose-response relationships.

INTRODUCTION

Cefadroxil is a β-lactam compound with a broad spectrum of antibacterial activity (Buck and Price 1977). This semisynthetic and first-generation aminocephalosporin was shown more effective and resistant to β-lactamases than cephalexin against certain bacteria (Ripa and Prenna 1979). It has been commonly used in the treatment of different kinds of infections including skin, respiratory and urinary tract infections (Tanrisever and Santella 1986). Due to its wide application for infectious diseases, a better understanding of cefadroxil pharmacokinetics would be of significant value for appropriate dose adjustment in patient subpopulations. Clinical studies showed that, after oral administration, cefadroxil is rapidly and almost completely absorbed in the gastrointestinal tract (Tanrisever and Santella 1986; Barbhaiya 1996). Cefadroxil is minimally metabolized, at best, in the body and excreted primarily by the kidney with over 90% of the administered dose being recovered in the urine intact within 24 hours (Lode, Stahlmann et al. 1979; Nightingale 1980). Experimental results have demonstrated that cefadroxil is a substrate of the peptide transporters PepT1 and PepT2, and several organic anion transporters (i.e., OATs) (Ganapathy, Brandsch et al. 1995; Shitara, Sato et al. 2005). The renal elimination of cefadroxil is governed by glomerular filtration, OAT-mediated renal secretion, and PEPT2-mediated renal reabsorption. The collective contributions (or balance) between these processes determine the net renal clearance of cefadroxil.

PEPT2 (SLC15A2) belongs to the proton-coupled oligopeptide transporter (POT) family in which the primary function is to translocate various

di-/tri-peptides and peptidomimetics across biological membranes (Daniel and Kottra 2004; Smith, Clemencon et al. 2013). To date, four members of the POT family have been identified in mammals (i.e., PEPT1, PEPT2, PHT1 and PHT2). Among the four transporter members, PEPT2 is recognized as a high-affinity, low-capacity transporter when compared to PEPT1. PEPT2 is predominantly localized at the apical membrane of proximal tubule epithelial cells and is the major peptide transporter involved in the renal tubular reabsorption of many peptide-like drugs (e.g., bestatin, valacyclovir, 5-amino-levulinic acid) (Inui, Tomita et al. 1992; Ganapathy, Huang et al. 1998; Rodriguez, Batlle et al. 2006; Hu, Shen et al. 2007). Previous findings by our laboratory (Shen, Ocheltree et al. 2007) showed that deletion of the PepT2 gene in mice caused a dramatic increase in the *in vivo* renal and total clearances of cefadroxil, with concomitant decreases in systemic exposure. Moreover, significant dose-dependent pharmacokinetics was observed in PepT2 knockout mice whereas a more modest dose-dependency was observed in wildtype mice. In this analysis, the authors (Shen, Ocheltree et al. 2007) proposed that wildtype mice were more influenced by capacity-limited tubular reabsorption and that PepT2 knockout mice were more influenced by capacity-limited secretion. In reality, the analysis is more complex in which varying degrees of saturation occurred for each carrier-mediated process (i.e., Oat(s) for secretion and PepT2 for reabsorption), depending upon the plasma (and tubular) concentrations achieved relative to transport affinity. Thus, a model that could accommodate the contributions of glomerular filtration and transporter-mediated secretory/reabsorptive processes, along with their *in vivo* Km values,

would provide a powerful tool in predicting cefadroxil drug levels over a wide dose range.

Characterization of transporter-mediated nonlinear pharmacokinetics is of importance in understanding and predicting pharmacologic actions of drugs, and sometimes difficult to achieve via traditional pharmacokinetic analyses. Thus, a nonlinear mixed effect modeling (NONMEM) approach can be utilized to address different sources of variability and allow the estimation of all the kinetic parameters of interest (i.e., nonlinear and/or linear pharmacokinetic parameters) (Beal and Sheiner 1984). This method has been employed to analyze transporter-mediated nonlinear pharmacokinetics of several compounds including cefuroxime, glycylsarcosine and levofloxacin (Ruiz-Carretero, Merino-Sanjuan et al. 2004; Huh, Hynes et al. 2013; Hurtado, Weber et al. 2014). Hence, the purpose of this study was to develop a population pharmacokinetic model of cefadroxil in wildtype and PepT2 knockout mice using the NONMEM approach. With this pharmacokinetic model, we were able to describe the nonlinear pharmacokinetics of cefadroxil with emphasis on quantifying the importance and contribution of transporters during *in vivo* saturable renal tubular secretion and reabsorption processes.

MATERIALS AND METHODS

Animals

All animal studies were performed in accordance with the Guide for the Care and Use of laboratory Animals as adopted and promulgated by the U.S. National Institutes of Health.

Experimental Design

The pharmacokinetic profiles of cefadroxil were assessed in wildtype and PepT2 knockout mice using NONMEM, based on data generated previously by our laboratory (Shen, Ocheltree et al. 2007). In brief, gender-matched mice (6-8 weeks) were fasted overnight before the onset of each experiment. After anesthesia with sodium pentobarbital, mice were administered [^{3}H]cefadroxil (5 μL/g and 0.5 Ci/g body weight) intravenously by tail vein injection. Blood samples (approximately 15 μL) were collected into heparinized tubes via tail nicks at pre-determined times (i.e., 0.25, 1, 2, 5, 15, 30, 45, 60, 90 and 120 min) after drug administration. Plasma samples were harvested immediately after centrifuging the blood at 2000 g for 10 min. The radioactivity of plasma samples was measured by a dual-channel liquid scintillation counter (Beckman LS 3801; Beckman Coulter, Inc., Fullerton, CA). To investigate the dose dependency of cefadroxil pharmacokinetics, ascending doses of [^{3}H]cefadroxil were administered separately to both genotypes (1, 12.5, 50 and 100 nmol/g body weight).

Noncompartmental Analysis of Cefadroxil Pharmacokinetics

Noncompartmental analysis (NCA) of the individual profiles was performed using Phoenix WinNonlin version 1.3 (Pharsight Corp., St. Louis, MO). Pharmacokinetic parameters, such as total clearance (CL), volume of distribution steady-state (Vd_{ss}), terminal half-life ($T_{1/2}$), mean residence time (MRT), and area under the plasma concentration-time curve (AUC), were calculated using standard methods.

Population Pharmacokinetic Modeling of Cefadroxil

Population pharmacokinetic analyses were conducted using NONMEM software (Version 7.2, Icon Development Solutions, MD, USA). The first-order conditional estimates (FOCE) method, with an interaction option implemented in NONMEM, was used for estimation. All models were parameterized as a system of differential equations using the ADVAN 6 TRANS 1 subroutine in NONMEM. Model diagnostic plots were performed using R software (version 2.15.0) with the Xpose package.

For the modeling development strategy, a sequential compartmental model building approach was adopted. Different compartmental models, including one-, two- and three-compartments, were tested on the cefadroxil pharmacokinetic profiles after intravenous administration. The analyses revealed that a two-compartment model best described the structural model of cefadroxil. After that, different population pharmacokinetic models, with linear elimination and/or nonlinear Michaelis-Menten kinetics for renal tubular secretion from the central

compartment, were tested in PepT2 knockout mice. The final pharmacokinetic model (Fig. 5.1A) was described by the following equations:

$$dA(1)/dt = -V_{m1}*C/(K_{m1}+C) - K_{10}*A(1) - K_{12}*A(1) + K_{21}*A(2) \quad (1)$$

$$dA(2)/dt = K_{12}*A(1) - K_{21}*A(2) \quad (2)$$

where A(1) is the amount of cefadroxil in central compartment, A(2) is the amount of cefadroxil in peripheral compartment, C is the concentration of cefadroxil in central compartment, V_{m1} is the maximum rate of saturable renal elimination from central compartment, K_{m1} is the Michaelis-Menten constant for saturable renal elimination from central compartment, K_{12} and K_{21} are the inter-compartment rate constants describing cefadroxil transport between the two compartments, and K_{10} is the linear elimination rate constant from central compartment.

Once the pharmacokinetic model for PepT2 knockout mice was established, the model was extended to include nonlinear Michaelis-Menten kinetics for the renal tubular reabsorption of cefadroxil in wildtype mice. The final pharmacokinetic model for wildtype mice (Fig. 5.1B) was described by the following equations:

$$dA(1)/dt = -V_{m1}*C/(K_{m1}+C) + V_{m2}*C/(K_{m2}+C) - K_{10}*A(1) - K_{12}*A(1) + K_{21}*A(2) \quad (3)$$

$$dA(2)/dt = K_{12}*A(1) - K_{21}*A(2) \quad (4)$$

where V_{m2} is the maximum rate of saturable renal reabsorption and K_{m2} is the Michaelis-Menten constant for saturable renal reabsorption. Inter-individual variability (IIV or η) for the pharmacokinetic parameters was described by an exponential model as shown below:

$$\theta_i = \theta \times \exp(\eta_i) \qquad (5)$$

where θ_i is the pharmacokinetic parameter of the i^{th} individual, θ is the population parameter estimate, and η_i is the IIV which is assumed to follow a normal distribution with mean of zero and variance of ω^2. The residual variability was tested by different error models and best described by exponential error model.

Model selection was based upon visual inspection of diagnostic goodness-of-fit plots, precision of parameter estimates, and numerical comparison of the objective function value by decreasing at least 6.63 (log-likelihood ratio test; $p < 0.01$).

Nonparametric Bootstrap Analysis

To check stability of the final population pharmacokinetic model and obtain confidence intervals (CI) for the model parameters, nonparametric bootstrap analyses (n=1,000) were performed using Perl-speaks-NONMEM (PsN) 3.6.2 (http://psn.sourceforge.net) (Lindbom, Ribbing et al. 2004; Keizer, Karlsson et al. 2013). Specifically, 1,000 replicate bootstrap data sets using subjects as sampling units were generated by random resampling with replacement from the

original data set. Stratification by dose during the random resampling process was implemented to ensure that the bootstrap data sets adequately represented the original data. Each new sample set was fitted to the final population pharmacokinetic model to obtain parameter estimates. The empirical 90% CI were constructed by obtaining the 5^{th} and 95^{th} percentiles of parameter distributions from the successful bootstrap runs. Final model parameter estimates were compared with bootstrap median parameter estimates to evaluate the final model performance.

Visual Predictive Check

To assess predictive performance of the final population pharmacokinetic model, a prediction-corrected visual predictive check (pcVPC) (Bergstrand, Hooker et al. 2011) with 1,000 data sets simulation was performed. The median, 5^{th} and 95^{th} percentiles of the simulated concentrations were calculated at each time point, and checked by visual inspection to see how the simulated intervals overlapped with the observed data.

RESULTS

Noncompartmental Analysis of Cefadroxil Pharmacokinetics

To examine the influence of PepT2 and/or Oat(s) in affecting the disposition of cefadroxil, and potential for saturation, a pharmacokinetic study was performed in wildtype and PepT2 knockout mice after intravenous dosing of drug over a 100-fold dose range (Figure B.2). Cefadroxil pharmacokinetic parameters were estimated by a non-compartmental analysis as summarized in Table B.1. When the highest dose (100 nmol/g) was administered, only minor differences were observed between genotypes in the pharmacokinetics of drug (e.g., < 15% higher total clearance during PepT2 ablation). However, when the lowest dose (1 nmol/g) was administered, the pharmacokinetics of cefadroxil was substantially different between wildtype mice and PepT2 knockout animals (e.g., 3-fold higher total clearance during PepT2 ablation). These findings suggest that the pharmacokinetics of cefadroxil is nonlinear, primarily reflecting the saturability of PepT2-mediated tubular reabsorption in kidney at the higher dose comparison. Moreover, as the doses increase, the total clearance of cefadroxil in PepT2 knockout mice is steadily reduced, thereby, suggesting saturability of Oat(s)-mediated renal secretion of drug at the higher dose levels.

Population Pharmacokinetic Modeling

To sequentially build a population pharmacokinetic model for cefadroxil in mice, the plasma concentration versus time profiles of drug over the dose range studied were first fitted by NONMEM in PepT2 knockout mice. A two-

compartment model, comprised of both saturable and nonsaturable efflux processes from the central compartment, was selected as the final model. The system of differential equations for the final model was given in Equations 1 and 2. Estimated pharmacokinetic parameters of cefadroxil in the final model of PepT2 knockout mice are listed in Table B.2. In this model, the nonlinear kinetics of renal tubular secretion are well characterized by the Michaelis-Menten parameters V_{m1} and K_{m1} which reflect the Oat(s)-mediated vectorial secretion of cefadroxil across renal epithelial cells.

The population pharmacokinetic model for wildtype mice was developed subsequently by adding a saturable component, for the cellular influx of cefadroxil from tubular fluid into the central compartment, to describe the transporter-mediated uptake of drug in wildtype mice. The system of differential equations for this final model was shown as Equations 3 and 4. The pharmacokinetic parameter estimates of cefadroxil in this final model are shown in Table B.2 for wildtype mice. It should be noted that the values of V_{m1} and K_{m1}, as determined previously in PepT2 knockout mice, were fixed in this pharmacokinetic model of wildtype mice. All parameters were estimated with high precision. In particular, the Michaelis-Menten kinetics were well characterized, as judged by the low values of RSE (< 25%) for V_{m2} and K_{m2}, which reflect the PepT2-mediated vectorial reabsorption of cefadroxil across renal epithelial cells.

Final Model Validation

Basic goodness-of-fit plots of the final pharmacokinetic models were displayed in Figure B.3 and B.4. As observed, the individual and population predictions were in good agreement with observed plasma concentrations in both wildtype and PepT2 knockout mice. Moreover, the conditional weighted residuals (CWRES) do not deviate from zero (i.e., no significant trend) with respect to time or individual prediction. Overall, the results suggest there is no misspecification of the final pharmacokinetic models in both genotypes.

The final models were further evaluated using a nonparametric bootstrap analysis. The empirical 90% CI was constructed by obtaining the 5^{th} and 95^{th} percentiles of the parameter distributions from the successful bootstrap runs. As shown in Table B.3, pharmacokinetic parameter estimates from the original data were very similar to median values obtained from the bootstrap estimates, and were within the bootstrap confidence intervals indicating there was no significant bias in the final model parameters.

To assess predictive performance of the final pharmacokinetic model, a prediction-corrected visual predictive check of cefadroxil plasma concentration-time profiles was performed using 1,000 data set simulations (Fig. B.5). The median, 5^{th} and 95^{th} percentiles of simulated concentrations were calculated at each time point and then checked by visual inspection to compare how the simulated results overlap with the observed data. As shown, approximately 90% of observed data fall into the region covered by 5^{th} and 95^{th} percentiles of simulated data, thus, indicating that the final models adequately predict the

observed plasma concentrations of cefadroxil with respect to the average (median) and the spread of the data (prediction interval).

DISCUSSION

The pharmacodynamic response to an antibacterial agent is largely determined by the antibacterial activity of the drug, which depends on its exposure at pharmacological target sites and pharmacokinetic profiles. Therefore, in-depth understanding of the pharmacokinetic profiles and its disposition mechanism(s) is crucial to determine optimal dosage regimens for achieving ideal antibacterial effects in patients. It is of interest that several contradictory studies on cefadroxil pharmacokinetics have been reported in humans and animals (Marino and Dominguez-Gil 1980; La Rosa, Ripa et al. 1982; Santella and Henness 1982; Garrigues, Martin et al. 1991; Garcia-Carbonell, Granero et al. 1993; Posada and Smith 2013). Some studies described a dose-linearity in pharmacokinetics, whereas others found dose-dependent changes in pharmacokinetic profiles. Regardless, the molecular mechanisms that affect the pharmacokinetics and tissue distribution of cefadroxil was lacking until our recent studies in genetically modified mice (Shen, Smith et al. 2003; Shen, Ocheltree et al. 2007; Kamal, Keep et al. 2008). Due to the availability of PepT2 knockout mice, we were able to elucidate the role and relevance of this oligopeptide transporter in the renal and systemic disposition of cefadroxil in wildtype mice and during PepT2 ablation (Shen, Ocheltree et al. 2007). Our experimental data clearly demonstrated that PepT2, as opposed to PepT1, had a predominant role in the renal tubular reabsorption of cefadroxil, accounting for 95% of the drug's reabsorption in kidney. However, because the transport kinetics (i.e., Vm and Km)

of cefadroxil were not characterized, for either secretory or reabsorptive transport, predictability of dose-response relationships was not possible.

In the present report, several new findings were revealed. In particular, this was the first study to examine a semi-mechanistic population pharmacokinetic model of cefadroxil transport in kidney. Moreover, we quantified the secretion kinetics (i.e., V_{m1} = 17.6 nmol/min and K_{m1} = 37.1 μM) and reabsorption kinetics (i.e., V_{m2} = 15.0 nmol/min and K_{m2} = 27.1 μM) of cefadroxil in kidney under *in vivo* conditions. In doing so, the potential for capacity-limited transport of cefadroxil can be better predicted and, thus, result in an optimized host response to invading bacteria. For example, plasma concentrations produced at the 1 nmol/g intravenous dose of cefadroxil were approximately 0.01-10 μM, values that fall into the range of minimal inhibitory concentrations for most, but not all, bacteria (Hartstein, Patrick et al. 1977; Courtieu and Drugeon 1983). By defining the entire pharmacokinetic profile of cefadroxil, relevant concentrations in plasma (and urine) can now be determined across a wide range of doses, *a priori*, and compared to bacterial susceptibility for a more favorable drug response.

The renal clearance of cefadroxil is governed by three processes, which are glomerular filtration, renal tubular secretion, and renal tubular reabsorption. Since renal clearance, glomerular filtration and fraction unbound in plasma can be determined, and given the (almost) exclusive reabsorption of drug by PepT2 in kidney (Shen, Ocheltree et al. 2007), it was possible to estimate the Oat(s)-mediated nonlinear and linear contributions (i.e., 62% and 38%, respectively) to

cefadroxil renal excretion in PepT2 knockout mice. In the present study, we found the K_{m1} for Oat(s) vectorial secretion to equal 37.1 μM, a value much lower than the millimolar values of IC50 and/or Ki reported previously for cefadroxil in renal proximal tubule cells expressing rat Oat1-3 (Jung, Takeda et al. 2002; Khamdang, Takeda et al. 2003) and human OAT1-4 (Takeda, Babu et al. 2002; Khamdang, Takeda et al. 2003). Although speculative, this disparity may result from the different species and experimental systems being employed. Moreover, IC50 and Ki values obtained from the *in vitro* inhibition of a model substrate by cefadroxil do not necessarily represent the Km values of cefadroxil obtained under *in vivo* physiological conditions. On the other hand, the K_{m2} value of 27.1 μM for vectorial reabsorption of cefadroxil is in good agreement with other investigators, who reported Km values for cefadroxil of 9 μM in rat kidney brush border membrane vesicles (Ries, Wenzel et al. 1994), 17 μM (Shen, Keep et al. 2005) and 27 μM (Ocheltree, Shen et al. 2004) in rat isolated choroid plexus, 39 μM in rat choroid plexus primary cell cultures (Shen, Keep et al. 2005) and 32 μM in rabbit PepT2-expressing Xenopus oocytes (Boll, Herget et al. 1996). It should be appreciated that cefadroxil is reabsorbed from luminal fluid by PepT2 localized on the apical membrane of renal proximal tubule cells. Therefore, the estimated K_{m2} is an apparent value in which plasma concentrations were used as surrogate values for drug concentrations in luminal fluid at the transport membrane site in order to fit the model. Notwithstanding this uncertainty, these two biological fluids are likely close in value since cefadroxil is 80% unbound in plasma (Shen, Ocheltree et al. 2007).

Many studies have shown transporters to be major determinants of the pharmacokinetic, safety and efficacy profiles of drugs. Moreover, single nucleotide polymorphisms of drug transporters, identified by advanced sequencing technology, appear to be responsible for the variation in drug responses among individuals (Evans and Relling 1999; Evans and McLeod 2003). In this regard, the proton-coupled oligopeptide transporter PepT2 had significant effects on peptide-like drug disposition as well as drug action and toxicity (Hu, Shen et al. 2007; Kamal, Keep et al. 2008). Genetic variants of the PEPT2 gene have been reported in humans with functional polymorphisms (Pinsonneault, Nielsen et al. 2004; Terada, Irie et al. 2004; Liu, Tang et al. 2011). For example, Terada et al. (43) found that the genetic variant R57H of PEPT2 completely lost its transport activity of glycylsarcosine, a substrate of PepT2, in transfected HEK293 cells and Xenopus oocytes. Based on our results, we confirmed that PepT2 played an overwhelmingly predominant role in the tubular reabsorption of cefadroxil, an aminocephalosporin peptide-like drug. Thus, it is conceivable that patients with PEPT2 deficiency may experience a substantial reduction in the reabsorption of certain drugs in kidney, thus, influencing efficacy due to decreased renal and systemic exposure. The semi-mechanistic population pharmacokinetic model presented in this study provides a unique tool to quantitatively predict the transporter-mediated nonlinear disposition of cefadroxil. Further studies will be focused on extrapolating this model to humans once more information is gathered regarding relevant transporter expression profiles and other interspecies differences. In doing so, a physiologically based

pharmacokinetic model may provide mechanistic insight and better predictability of cefadroxil pharmacokinetics, as well as dosage optimization and response in patient subpopulations.

FIGURES

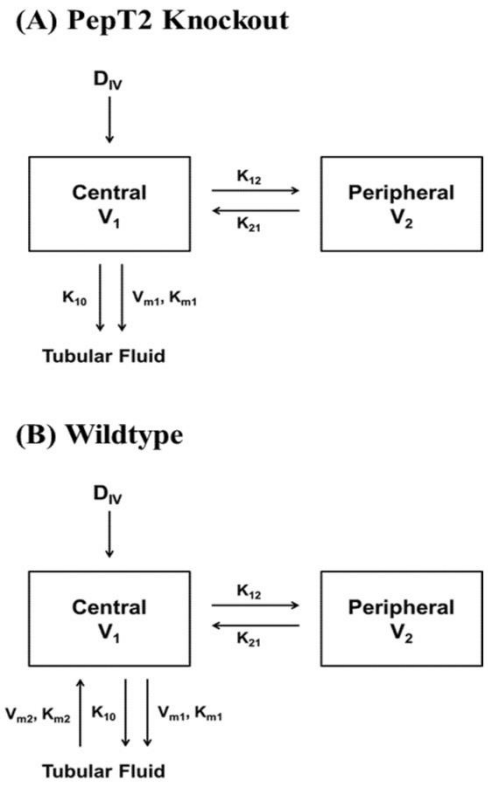

Figure B.1 Schematic two-compartment models of cefadroxil after intravenous bolus administration in PepT2 knockout (A) and wildtype (B) mice.

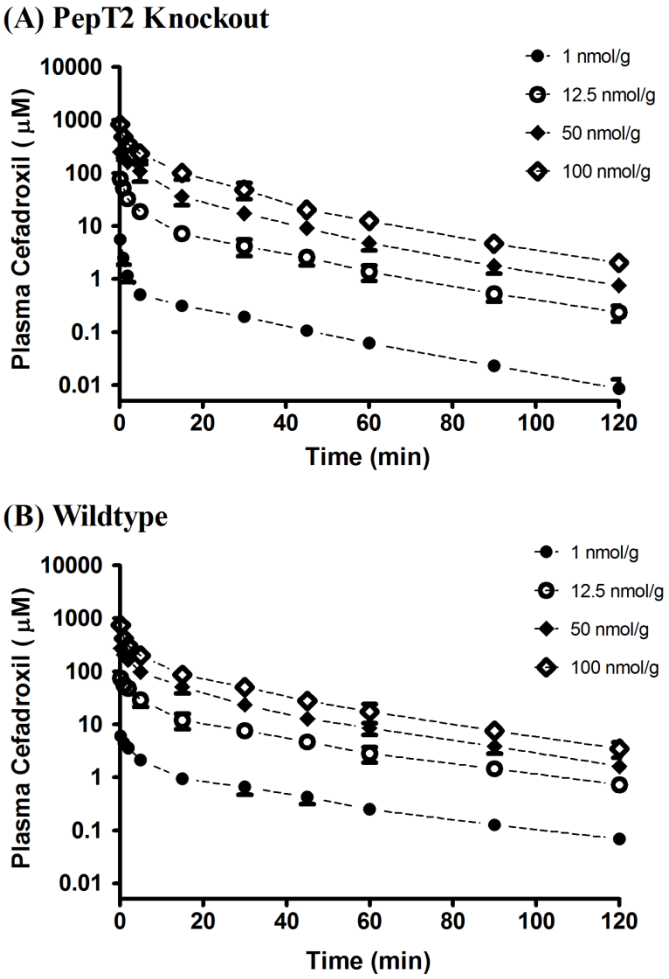

Figure B.2 Plasma concentration-time profiles of cefadroxil after intravenous bolus administrations of 1, 12.5, 50 and 100 nmol/g in PepT2 knockout (A) and wildtype (B) mice. The figures were adapted from a previous publication (Shen, Ocheltree et al. 2007).

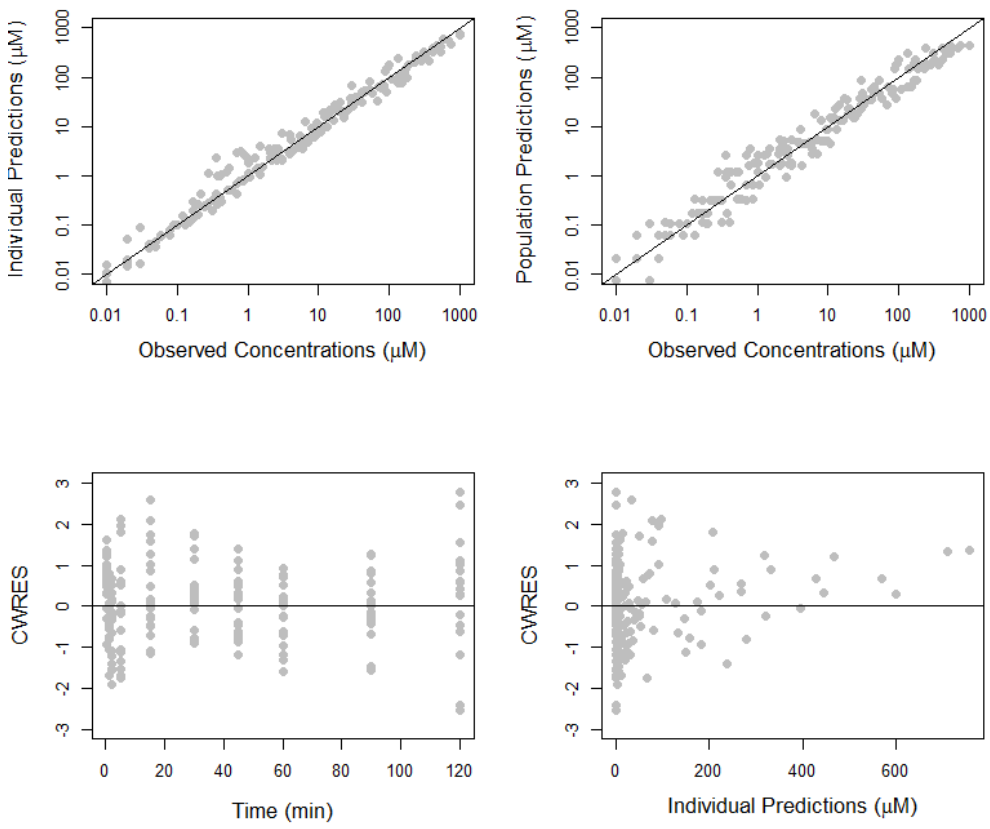

Figure B.3 Goodness-of-fit plots for the final pharmacokinetic model of cefadroxil in PepT2 knockout mice. Solid lines represent the line of identity.

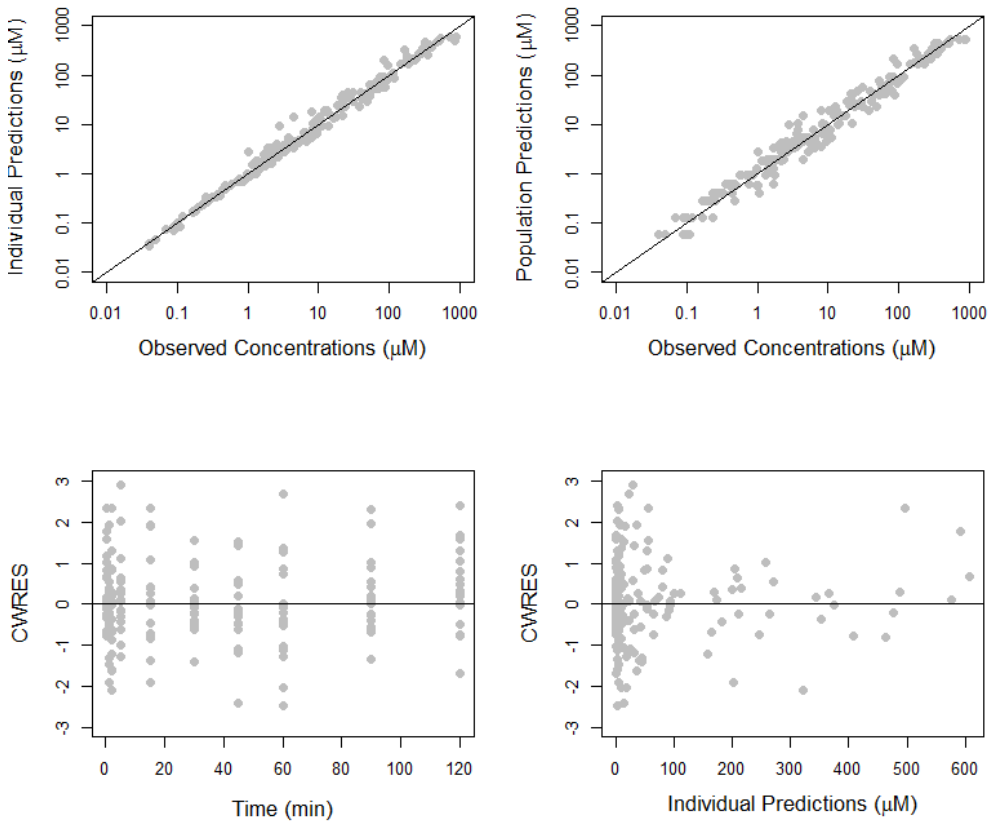

Figure B.4 Goodness-of-fit plots for the final pharmacokinetic model of cefadroxil in wildtype mice. Solid lines represent the line of identity.

(A) PepT2 Knockout

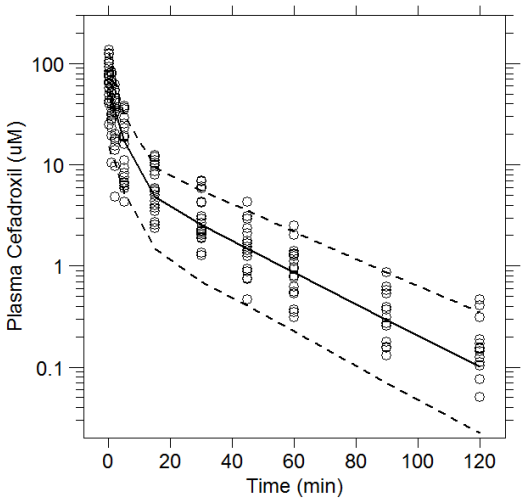

(B) Wildtype

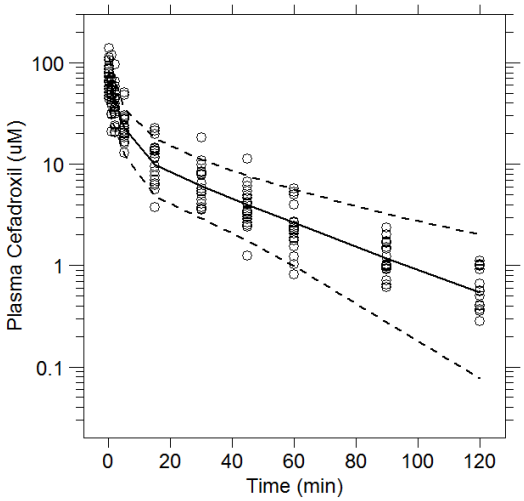

Figure B.5 Prediction corrected visual predictive check plots in PepT2 knockout (A) and wildtype (B) mice. Plasma concentration-time profiles are displayed in which the circles represent prediction corrected observed data. Dashed lines depict the 5th and 95th percentiles, and solid lines represent the median values of 1,000 simulated data sets.

Table B.1 Noncompartmental analysis of cefadroxil pharmacokinetics in PepT2 knockout (KO) and wildtype mice after intravenous bolus administration[a]

Genotype	Parameters (units)	Dose (nmol/g)			
		1	12.5	50	100
PepT2 KO	Vd_{ss} (ml)	20.9 ± 2.9	10.5 ± 2.4[b]	9.4 ± 2.8[b]	7.9 ± 2.7[b]
	$T_{1/2}$ (min)	20.9 ± 2.2	22.2 ± 1.7	19.2 ± 2.8	21.9 ± 3.1
	CL (ml/min)	1.03 ± 0.13	0.60 ± 0.20	0.50 ± 0.12[b]	0.40 ± 0.11[b]
	MRT (min)	17.7 ± 1.3	17.1 ± 1.4	16.8 ± 2.6	16.9 ± 1.0
	$AUC_{0\text{-tlast}}$ (μM·min)	22 ± 4	521 ± 117[b]	2372 ± 542[b]	5924 ± 1304[b]
Wildtype	Vd_{ss} (ml)	10.3 ± 1.3	10.9 ± 4.5	8.1 ± 1.1	8.3 ± 1.4
	$T_{1/2}$ (min)	32.0 ± 3.0	28.3 ± 5.0	17.9 ± 0.8[b]	24.0 ± 2.8
	CL (ml/min)	0.330 ± 0.041	0.322 ± 0.061	0.360 ± 0.033	0.352 ± 0.027
	MRT (min)	24.5 ± 0.7	24.0 ± 2.8	20.4 ± 1.6	20.5 ± 2.5
	$AUC_{0\text{-tlast}}$ (μM·min)	67 ± 13	828 ± 155[b]	2825 ± 314[b]	5658 ± 424[b]

[a] Data are expressed as mean ± SE (n=4-7).

[b] $p < 0.05$ compared to 1 nmol/g dose of cefadroxil, as determined by ANOVA followed by Dunnett's test.

Table B.2 Parameter estimates of the final population pharmacokinetic model of cefadroxil in PepT2 knockout (KO) and wildtype mice after intravenous bolus administration

PepT2 KO	Estimate	RSE (%)
Primary parameters (units)		
V_{m1} (nmol/min)	17.6	17.2
K_{m1} (μM)	37.1	35.8
V_1 (ml)	4.23	12.2
Q (ml/min)[a]	0.586	20.5
V_2 (ml)	8.61	16.7
K_{10} (min^{-1})	0.070	28.1
Intersubject variabiliby (% CV)		
V_{m1}	24.7	26.8
V_1	42.7	15.1
Residual variabiliby (% CV)		
Proportional error	41.1	8.3
Wildtype	**Estimate**	**RSE (%)**
Primary parameters (units)[b]		
V_{m2} (nmol/min)	15.0	23.5
K_{m2} (μM)	27.1	24.0
V_1 (ml)	3.43	7.2
Q (ml/min)[a]	0.599	21.2
V_2 (ml)	5.98	14.4
K_{10} (min^{-1})	0.111	13.0
Intersubject variabiliby (% CV)		
V_1	23.6	23.5
V_2	42.5	26.5
Residual variabiliby (% CV)		
Proportional error	26.4	8.7

[a] $Q = V_1K_{12} = V_2K_{21}$

[b] In determining the estimates in wildtype mice, V_{m1} = 17.6 nmol/min and K_{m1} = 37.1 μM, as determined previously in PepT2 knockout mice.

Table B.3 Comparison of parameter estimates of the final population pharmacokinetic model of cefadroxil in PepT2 knockout (KO) and wildtype mice based on the original data set and from 1,000 bootstrap replicates

Parameters	Estimate	Nonparametric Bootstrap	
		Median	90% Confidence Interval
PepT2 KO			
V_{m1} (nmol/min)	17.6	17.5	8.1 – 49.0
K_{m1} (μM)	37.1	40.7	21.2 - 76.2
V_1 (ml)	4.23	4.27	3.57 - 4.90
Q (ml/min)	0.586	0.589	0.394 - 0.757
V_2 (ml)	8.61	8.52	6.98 - 10.70
K_{10} (min^{-1})	0.070	0.073	0.063 - 0.100
Wildtype			
V_{m2} (nmol/min)	15.0	15.3	8.6 - 28.3
K_{m2} (μM)	27.1	28.0	16.8 - 46.9
V_1 (ml)	3.43	3.44	3.05 - 3.82
Q (ml/min)	0.599	0.608	0.429 - 0.807
V_2 (ml)	5.98	5.89	4.65 - 7.58
K_{10} (min^{-1})	0.111	0.110	0.089 - 0.163

REFERENCES

Barbhaiya, R. H. (1996). "A Pharacokinetic Comparison of cefadroxil and cephalexin after administration of 250, 500 and 1000 mg solution doses." Biopharmaceutics & Drug Disposition **17**(4): 319-330.

Beal, S. L. and L. B. Sheiner (1984). NONMEM Users Guide: users basic guide April 1980, University of California Press.

Bergstrand, M., A. C. Hooker, et al. (2011). "Prediction-corrected visual predictive checks for diagnosing nonlinear mixed-effects models." AAPS J **13**(2): 143-151.

Boll, M., M. Herget, et al. (1996). "Expression cloning and functional characterization of the kidney cortex high-affinity proton-coupled peptide transporter." Proc Natl Acad Sci U S A **93**(1): 284-289.

Buck, R. E. and K. E. Price (1977). "Cefadroxil, a new broad-spectrum cephalosporin." Antimicrob Agents Chemother **11**(2): 324-330.

Courtieu, A. L. and H. Drugeon (1983). "Compared sensitivities of 532 bacterial strains to six cephalosporins." Int J Clin Pharmacol Res **3**(3): 195-201.

Daniel, H. and G. Kottra (2004). "The proton oligopeptide cotransporter family SLC15 in physiology and pharmacology." Pflugers Arch **447**(5): 610-618.

Evans, W. E. and H. L. McLeod (2003). "Pharmacogenomics--drug disposition, drug targets, and side effects." N Engl J Med **348**(6): 538-549.

Evans, W. E. and M. V. Relling (1999). "Pharmacogenomics: translating functional genomics into rational therapeutics." Science **286**(5439): 487-491.

Ganapathy, M. E., M. Brandsch, et al. (1995). "Differential recognition of beta - lactam antibiotics by intestinal and renal peptide transporters, PEPT 1 and PEPT 2." J Biol Chem **270**(43): 25672-25677.

Ganapathy, M. E., W. Huang, et al. (1998). "Valacyclovir: a substrate for the intestinal and renal peptide transporters PEPT1 and PEPT2." Biochem Biophys Res Commun **246**(2): 470-475.

Garcia-Carbonell, M. C., L. Granero, et al. (1993). "Nonlinear pharmacokinetics of cefadroxil in the rat." Drug Metab Dispos **21**(2): 215-217.

Garrigues, T. M., U. Martin, et al. (1991). "Dose-dependent absorption and elimination of cefadroxil in man." Eur J Clin Pharmacol **41**(2): 179-183.

Hartstein, A. I., K. E. Patrick, et al. (1977). "Comparison of pharmacological and antimicrobial properties of cefadroxil and cephalexin." Antimicrob Agents Chemother **12**(1): 93-97.

Hu, Y., H. Shen, et al. (2007). "Peptide transporter 2 (PEPT2) expression in brain protects against 5-aminolevulinic acid neurotoxicity." J Neurochem **103**(5): 2058-2065.

Huh, Y., S. M. Hynes, et al. (2013). "Importance of Peptide transporter 2 on the cerebrospinal fluid efflux kinetics of glycylsarcosine characterized by nonlinear mixed effects modeling." Pharm Res **30**(5): 1423-1434.

Hurtado, F. K., B. Weber, et al. (2014). "Population pharmacokinetic modeling of the unbound levofloxacin concentrations in rat plasma and prostate tissue measured by microdialysis." Antimicrob Agents Chemother **58**(2): 678-686.

Inui, K., Y. Tomita, et al. (1992). "H+ coupled active transport of bestatin via the dipeptide transport system in rabbit intestinal brush-border membranes." J Pharmacol Exp Ther **260**(2): 482-486.

Jung, K. Y., M. Takeda, et al. (2002). "Involvement of rat organic anion transporter 3 (rOAT3) in cephaloridine-induced nephrotoxicity: in comparison with rOAT1." Life Sci **70**(16): 1861-1874.

Kamal, M. A., R. F. Keep, et al. (2008). "Role and relevance of PEPT2 in drug disposition, dynamics, and toxicity." Drug Metab Pharmacokinet **23**(4): 236-242.

Keizer, R. J., M. O. Karlsson, et al. (2013). "Modeling and Simulation Workbench for NONMEM: Tutorial on Pirana, PsN, and Xpose." CPT Pharmacometrics Syst Pharmacol **2**: e50.

Khamdang, S., M. Takeda, et al. (2003). "Interaction of human and rat organic anion transporter 2 with various cephalosporin antibiotics." Eur J Pharmacol **465**(1-2): 1-7.

La Rosa, F., S. Ripa, et al. (1982). "Pharmacokinetics of cefadroxil after oral administration in humans." Antimicrob Agents Chemother **21**(2): 320-322.

Lindbom, L., J. Ribbing, et al. (2004). "Perl-speaks-NONMEM (PsN)--a Perl module for NONMEM related programming." Comput Methods Programs Biomed **75**(2): 85-94.

Liu, R., A. M. Tang, et al. (2011). "Effects of sodium bicarbonate and ammonium chloride pre-treatments on PEPT2 (SLC15A2) mediated renal clearance of cephalexin in healthy subjects." Drug Metab Pharmacokinet **26**(1): 87-93.

Lode, H., R. Stahlmann, et al. (1979). "Comparative pharmacokinetics of cephalexin, cefaclor, cefadroxil, and CGP 9000." Antimicrob Agents Chemother **16**(1): 1-6.

Marino, E. L. and A. Dominguez-Gil (1980). "Influence of dose on the pharmacokinetics of cefadroxil." Eur J Clin Pharmacol **18**(6): 505-509.

Nightingale, C. (1980). "Pharmacokinetics of the oral cephalosporins in adults." J Int Med Res **8**(Suppl 1): 2-8.

Ocheltree, S. M., H. Shen, et al. (2004). "Mechanisms of cefadroxil uptake in the choroid plexus: studies in wild-type and PEPT2 knockout mice." J Pharmacol Exp Ther **308**(2): 462-467.

Pinsonneault, J., C. U. Nielsen, et al. (2004). "Genetic variants of the human H+/dipeptide transporter PEPT2: analysis of haplotype functions." J Pharmacol Exp Ther **311**(3): 1088-1096.

Posada, M. M. and D. E. Smith (2013). "In vivo absorption and disposition of cefadroxil after escalating oral doses in wild-type and PepT1 knockout mice." Pharm Res **30**(11): 2931-2939.

Ries, M., U. Wenzel, et al. (1994). "Transport of cefadroxil in rat kidney brush-border membranes is mediated by two electrogenic H+-coupled systems." J Pharmacol Exp Ther **271**(3): 1327-1333.

Ripa, S. and M. Prenna (1979). "Laboratory studies with BL-S 578 (Cefadroxil) a new broad-spectrum orally active cephalosporin." Chemotherapy **25**(1): 9-13.

Rodriguez, L., A. Batlle, et al. (2006). "Study of the mechanisms of uptake of 5-aminolevulinic acid derivatives by PEPT1 and PEPT2 transporters as a tool to improve photodynamic therapy of tumours." Int J Biochem Cell Biol **38**(9): 1530-1539.

Ruiz-Carretero, P., M. Merino-Sanjuan, et al. (2004). "Pharmacokinetic models for the saturable absorption of cefuroxime axetil and saturable elimination of cefuroxime." Eur J Pharm Sci **21**(2-3): 217-223.

Santella, P. J. and D. Henness (1982). "A review of the bioavailability of cefadroxil." J Antimicrob Chemother **10 Suppl B**: 17-25.

Shen, H., R. F. Keep, et al. (2005). "PEPT2 (Slc15a2)-mediated unidirectional transport of cefadroxil from cerebrospinal fluid into choroid plexus." J Pharmacol Exp Ther **315**(3): 1101-1108.

Shen, H., S. M. Ocheltree, et al. (2007). "Impact of genetic knockout of PEPT2 on cefadroxil pharmacokinetics, renal tubular reabsorption, and brain penetration in mice." Drug Metab Dispos **35**(7): 1209-1216.

Shen, H., D. E. Smith, et al. (2003). "Targeted disruption of the PEPT2 gene markedly reduces dipeptide uptake in choroid plexus." J Biol Chem **278**(7): 4786-4791.

Shitara, Y., H. Sato, et al. (2005). "Evaluation of drug-drug interaction in the hepatobiliary and renal transport of drugs." Annu Rev Pharmacol Toxicol **45**: 689-723.

Smith, D. E., B. Clemencon, et al. (2013). "Proton-coupled oligopeptide transporter family SLC15: physiological, pharmacological and pathological implications." Mol Aspects Med **34**(2-3): 323-336.

Takeda, M., E. Babu, et al. (2002). "Interaction of human organic anion transporters with various cephalosporin antibiotics." Eur J Pharmacol **438**(3): 137-142.

Tanrisever, B. and P. J. Santella (1986). "Cefadroxil. A review of its antibacterial, pharmacokinetic and therapeutic properties in comparison with cephalexin and cephradine." Drugs **32 Suppl 3**: 1-16.

Terada, T., M. Irie, et al. (2004). "Genetic variant Arg57His in human H+/peptide cotransporter 2 causes a complete loss of transport function." Biochem Biophys Res Commun **316**(2): 416-420.